DYNAMICS OF BLOWOUT AND THERMOACOUSTIC INSTABILITY IN A BLUFF BODY STABILIZED TURBULENT COMBUSTOR

A THESIS

submitted by

VISHNU R UNNI

for the award of the degree

of

DOCTOR OF PHILOSOPHY

DEPARTMENT OF AEROSPACE ENGINEERING

INDIAN INSTITUTE OF TECHNOLOGY MADRAS.

APRIL 2017

THESIS CERTIFICATE

This is to certify that the thesis titled **DYNAMICS OF BLOWOUT AND THERMOACOUSTIC INSTABILITY IN A BLUFF BODY STABILIZED TURBULENT COMBUSTOR SUBMITTED TO IITM**, submitted by **Vishnu R Unni**, to the Indian Institute of Technology Madras, Chennai for the award of the degree of **Doctor of Philosophy**, is a bona fide record of the research work done by him under our supervision. The contents of this thesis, in full or in parts, have not been submitted to any other Institute or University for the award of any degree or diploma.

Prof. R. I. Sujith
Research Guide
Professor
Dept. of Aerospace Engineering
IIT-Madras, 600 036

Place: Chennai

Date: 21st April 2017

to my grandfather

ACKNOWLEDGEMENTS

First and foremost I would like to express my sincere gratitude to Prof. R. I. Sujith for the invaluable guidance and mentoring throughout my research work. He has helped me in innumerable ways beyond his role as a research guide. He has been a constant source of inspiration and motivation for me in both technical and non-technical aspects. He has, from day one, given his relentless and consistent support for the metamorphosis of this work and was available even at the oddest of hours for discussions regarding any research problem. He always insisted on collaboration amongst my peers and mentored us to be a 'team' rather than a 'group'. I will always be indebted to him for teaching me the importance of honest and active discussions and the formidable significance of 'writing' in doing research. His dedication to research and hardworking nature has and always will be an inspiration for me to be a better researcher.

My interest to pursue research was first kindled by Prof. S. R. Chakravarthy, early on in my under graduate days. His lectures have always been amazing, leaving one curious to know more, thus igniting the desire to learn. I would like to thank him for patiently answering each of my questions even when they were mundane and for all the support he gave me throughout my stay at IIT Madras.

I also wish to thank my doctoral committee - Dr. Sunetra Sarkar, Prof. Arul Lakshminarayan, Dr. Amit Kumar and Prof. K. Srinivasan. I am grateful to them for raising key questions which helped me pose my research problem better. I would like to

thank Prof. V. Bhaskar, the Head of the Department of Aerospace for all the little discussions that I had with him which instilled renewed confidence in me.

I wish to thank Dr. Swetaprovo Chaudhuri and Prof. Achintiya Mukhopadhyay for their valuable contribution to the research work presented in this thesis. Discussions with Dr. Swetaprovo Chaudhuri gave me deeper understanding regarding flame dynamics close to blowout and helped me construct the cellular automata model based model for flame dynamics close to blowout described in Chapter 6 of this thesis. Prof. Achintiya Mukhopadhyay introduced me to symbolic time series analysis which we were able to use to study the onset of thermoacoustic instability (Appendix A of this thesis). I would like to thank Prof. G. Ambika and Dr. K. P. Harikrishnan for teaching me concepts in fractal analysis. I am indebted to them for providing the code for multifractal analysis of phase space that is used for the work presented in Chapter 3 of this thesis. I would like to acknowledge the fruitful discussions I have had with Prof. M. Lakshmanan, Dr. D. V. Senthilkumar, Dr. V. K. Chandrasekhar, Dr. Sayan Gupta and Dr. Partha Sharathi Dutta regarding various concepts in nonlinear dynamics. I am extremely grateful to Prof. Rama Govindarajan for patiently answering to my questions related to fluid dynamics.

I thank Prof. W. Polifke for inviting me to TU Munich for an exciting research visit and to attend n3l conference. I thank Institute for Advanced Studies, TUM for funding this visit. I would like to thank Ralf, Sebastian and Stephan for all the help during the visit.

I would like to thank Prof Jürgen Kurths for hosting me at Potsdam Institute of Climate Impact Research (PIK) for a month long research visit. I thank Humboldt University for funding me for this visit. I am grateful to Prof. Elena Surovyatkina and Dr. Norbert

Marwan for extending their support during this time with detailed discussions on nonlinear dynamics. I thank them for introducing me to a new perspective on complex systems that I aspire to use in the future.

I feel great pride in having been a part of Sujith's team and thank each of my colleagues for their invaluable support and the impact they have had on my life during these years. I thank Lipika for mentoring me at the beginning years of my association with the lab. I thank Gireesh sir and Vineeth for introducing me to the experimental setup and procedure. I profusely thank Gopalji for being there as a pillar of strength in the most difficult of times. I am grateful to Vineeth and Gopalji for raising the right questions about my research which enabled me to get improved clarity and for their immense help with preparation of comprehensive examination.

I have been really fortunate to have an amazing team who has greatly helped me with the experiments for this research work. They have helped in enriching me both academically and personally. I thank Dileesh and Tilak in their meticulous help in fabricating the experimental setup. I would like to especially thank Swati, Dileep, Nitin, Shyam, Mani and Luca for their help in performing the experiments. I thank Shyam and Dileep for all the help in purchasing equipment for experiments. I am very grateful to Sirshendu, Samadhan and Nitin for their immense help in meticulously correcting my papers and providing their valuable comments on the research, and moral support in times of need. I acknowledge Abin, Manikandan (GTRE), Meena, Mrudula, Vishnu (Agni), Vinu, Diego, Priya, Sateesh, Prabhod, Rana sir, Mukund for all the help they have provided. I have no words to thank Sreelekha, Akshay, Vedasri and Tony for helping me with insightful

discussions in dynamical systems theory. I wish to thank Rama, Induja and Hashir for helping me with my work whenever I needed, even at a moment's notice.

I would like to acknowledge the funding provided by Ministry of Human Resources and Development (MHRD), Govt. of India during my Ph. D and also the generous funding by IIT Madras for attending the Combustion Symposium, 2016 held in South Korea. I wish to thank the Office of Naval Research Global (ONRG) for funding. I would like to specially thank Dr. Ramesh Kolar (ONRG) who encouraged and inspired me during the project review meetings.

I would like thank the staff of IIT Madras for all the support they have provided me during my research. I have been constantly supported by Mrs. Mekhala, Mrs. Aruna, Mrs. Nirmala, Mrs. Savitri, Mrs. Regina, Kennedy, Mr. Manikandan, Mr. Sankar Kumaraswamy, Mr. John George, Mr. Stephen, Mr. Biju Kumar and Mr. Dayalan during my Ph.D.

Most of all, I would like to thank IIT Madras for having been my home away from home for the last nine years, starting from my undergraduate course. I thank all the people with whom I have become acquainted with in the institute during this period, especially Dr. Porchelvi and Dr. Saraswathi of the Institute Hospital who has provided help whenever I have been ill.

Finally, I would like to thank my family without whose support this Ph.D would not have been possible. Especially, I thank my parents for helping me during times of duress, constantly providing motivation and moral support. I thank my sisters Veena and Vrinda for being there whenever I needed them. I also thank Rewanth, for all his help during tmy

my stay at IIT. No words can describe the sacrifices they've made and the patience and understanding with which they ensured my quirks and vices throughout these years. I owe the completion of my research to their efforts in providing me with mental and spiritual support. And for this, I'm forever grateful to them.

ABSTRACT

KEYWORDS: Blowout; Thermoacoustic instability; Multifractality; Recurrence Quantification Analysis; Flame dynamics; Population dynamics; Absorbing state.

Many gas turbine combustors are operated in fuel lean conditions in order to ensure reduced emissions. However, combustors operating in lean conditions are susceptible to flame blowout and thermoacoustic instability. Traditionally, flame blowout is described as loss of static stability of the combustion system whereas thermoacoustic instability is seen as loss of dynamic stability of the system. At blowout, the system transitions from a stable reacting state to a non-reacting state indicating a loss of static stability of the reaction. However, this simple description of stability margin is inadequate since recent studies have shown that combustors exhibit complex nonlinear behavior prior to blow out. Recently, it was also shown that combustion noise that characterizes the regime of stable operation, itself is dynamically complex and exhibit multifractal characteristics. Researchers have already described the transition from combustion noise to combustion instability as a loss of multifractality. In this work, we characterize the complexity of dynamics prior to blowout and provide a multifractal description for lean blowout in combustors with turbulent flow. Thus, we bring in a unified framework within which both thermoacoustic instability and blowout can be described. Further, we introduce a method for predicting an impending blowout based on a multifractal description of blowout.

It is known that combustion systems with turbulent reactive flow exhibit intermittency prior to flame blowout. We characterize the variation of this intermittent behavior as lean blowout is approached using recurrence quantification analysis and thereby provide viable precursors to an impending blowout. We observe that as blowout is approached, the system exhibits increased aperiodicity in oscillations. We show that statistical quantities estimated from recurrence plots such as recurrence rate, trapping time and entropy of diagonal lines can act as precursor to blowout. Further, we suggest a method of recurrence quantification analysis that is computationally less expensive and hence more suitable for online prognosis of dynamic transitions in a turbulent combustor.

We observe that, on the reduction of equivalence ratio from stoichiometry to lean conditions, turbulent combustors exhibit intermittency before the occurrence of thermoacoustic instability and before flame blowout. We compare the dynamic characteristics of intermittency prior to thermoacoustic instability and that prior to blowout. The analysis of the unsteady pressure fluctuations within the combustor suggests that both intermittencies are of type II. We also compare the flame dynamics during either state using high speed Mie scattering images acquired simultaneously with unsteady pressure. We observe that during both regimes of intermittency, the flame switches between two distinct patterns of oscillations; one where the flame oscillates in an aperiodic manner due to the inherent turbulent fluctuations, and another where the flame exhibits periodic roll-up as a consequence of the periodic vortex shedding at the dump plane. Nevertheless, it is observed that the flame dynamics during intermittency prior to thermoacoustic instability and prior to flame blowout are different. During intermittency before the occurrence of thermoacoustic instability, the flame along the

inner shear layer is stabilized by the stagnation point flow behind the bluff body. In contrast, during intermittency prior to blowout, the flame along the inner shear layer is stabilized by the recirculation zone created by the bluff body. We also observe that very close to blowout, the flame dynamics is aperiodic and is largely governed by the intermittent formation of flame holes.

We introduce a low order model that can capture the complex dynamics of the combustor close to blowout. We consider the turbulent flame as a collection of flamelets. The model approaches the problem of flame stabilization in a turbulent combustor as a problem of population dynamics these flamelets. It is assumed that, the birth process of flamelet is analogues to the process of ignition of the reactants and the process of extinction of flamelet corresponds to the death of flamelet. A cellular automata model that captures the population dynamics of the flamelets is constructed. We show that the model is able to capture various characteristics of flame dynamics observed close to blowout. As we approach blowout, the modeled flame gets stretched, the number of flame holes in the flame increases and there is reduction of average concentration of free radicals. Finally, we show that the cellular automata model that represents the dynamics of the turbulent combustor undergoes an absorbing transition to an extinct phase imitating flame blowout in the turbulent combustor

TABLE OF CONTENTS

LIST OF FIGURES

ABBREVIATIONS

RP	Recurrence Plot
RQA	Recurrence Quantification Analysis
CA	Cellular Automaton
LPG	Liquefied Petroleum Gas
NOx	Nitrogen Oxides
PFSA	Probabilistic Finite State Automata

NOTATIONS

I_τ	Average mutual information
D_1	Characteristic dimension for the computations of *Re*
D_0	Diameter of the burner
T	Dominant time period during combustion instability
μ	Dynamic viscosity
Eq. Ratio	Equivalence ratio
D	Fractal dimension
d	Height of the backward facing step
H	Hurst exponent
N	Length of the time signal
$\dot{m}$	Mass flow rate
$\bar{p}$	Mean pressure
d_0	Optimum embedding dimension
τ_{opt}	Optimum time delay for embedding
P_i	Position of i^{th} point in the phase space
P	Probability of flame propagation
H_q	q^{th} order Hurst exponent
p'_{rms}	R.m.s. value of pressure fluctuations
R	Recurrence matrix
Re	Reynolds number
F_s	Sampling frequency
ENTR	Shannon entropy
α	Singularity
λ	Size of the attractor in phase space
σ	Standard deviation
$f(\alpha)$	Strength of singularity

St	Strouhal number
F_q^w	Structure function
ε	Threshold measure for recurrence plot
τ	Trapping time
$\dot{Q}'$	Unsteady heat release
$p'(t)$	Unsteady pressure

CHAPTER 1

Introduction

Gas turbine engines are widely used in power generation and aviation industries. While they help us produce the ever needed mechanical and electrical energy from the stored chemical energy in the fossil fuels, they also produce a significant amount of pollutants. A major concern is the production of harmful oxides of nitrogen otherwise known as NOx. NOx are produced when the nitrogen present in the air reacts with oxygen in the high-temperature environment inside the combustor of a gas turbine engine. One of the techniques used in many combustors to reduce emissions is to employ ultra-lean premixed combustion which ensures low combustion temperature and consequently, reduced NOx emission.

However, the operation of combustors at fuel-lean conditions is faced with challenges of flame blowout and thermoacoustic instability. Blowout is a state when the flame ceases to exist inside the combustor. Blowout can happen either through flame blow-off or flame extinction. On the other hand, thermoacoustic instability refers to the large amplitude acoustic oscillations that are established inside a combustor when the unsteady heat release rate from the combustor has a positive feedback with the acoustic perturbations. Near fuel-lean limits, combustors are susceptible to blowout and thermoacoustic instability due to the increased sensitivity of the flame to the flow perturbations.

The flow velocities inside the combustors are usually much greater than the speed at which the flame can propagate into the flow. Hence, to stabilize or anchor the flame, a flame holding mechanism is incorporated in the combustor. Bluff-bodies, backward

facing step, swirlers and porous beds are a few among the different flame holding mechanisms that are used. Flame holders create regions of low velocity inside the combustor where the flame can be stabilized. Thus, they ensure that the unburned fuel-air mixture entering the combustor comes in contact with the hot gasses and free radicals produced during combustion, warranting its ignition and a sustained reaction inside the combustor. At lower equivalence ratios, due to the presence of excess air in reactants, the chemical time scale of the reaction increases and consequently, the flame speed reduces. Under these conditions, the flame is more susceptible to various perturbations in the flow and eventually loses its ability to anchor itself within the combustor and blows out. Various mechanisms have been proposed to explain blowout in terms of reaction kinetics, interaction between the flow field and the flame and the diffusion characteristics of the reactants (Glassman, 1996; Cheng & Kovitz 1957; Peters & Williams, 1983). Even though there are differences in the details, all of these studies unanimously point to the significance of competing mechanisms of the heat release and the heat loss from the reactive flow field in determining the blowout characteristics.

Understanding flame blowout is essential since it can be very detrimental for a gas turbine engine. In military aircraft, rapid combat manures could induce transient fluctuations in the reactive flow which can induce flame blowout. An engine is prone to blowout during a rapid deceleration (throttle reduction), since the fuel flow rates tend to vary much faster than the airflow rates whose reduction rate is determined by the rotational inertia of the compressor. Further, in gas turbine engines, the combustor dynamics gets coupled with the dynamics of compressors and turbines. Hence, a failure to rapidly ignite the combustor post a blowout event would induce a compressor stall

causing its rotational speeds reduce to its windmilling value. Furthermore, the narrow stability margin for a relight at high altitudes would demand a descent of the aircraft to lower altitudes to relight combustor and thus recover from blowout. Traditionally, a flame stabilized inside a combustor is considered to be “statically stable”. Thus, flame blowout is regarded as the loss of static stability of the combustor (Lieuwen, 2007).

In contrast, thermoacoustic instability is considered as loss of dynamic stability of the combustor and is caused due to the positive feedback between the unsteady heat release rate from combustion and the acoustic field of the confinement (Lieuwen, 2007). Unsteadiness is inherent to the flame inside a gas turbine engine thanks to the turbulence in the reactive flow. This irregular flame fluctuations produce aperiodic pressure fluctuations (acoustic waves) inside the combustor known as combustion noise. Combustion noise has low amplitude and has a broadband frequency spectrum. However, at particular operating conditions, the flame has increased sensitivity to perturbations due to the complex interplay of various mechanisms that determine the stability of the flame. This increased sensitivity enhances the positive feedback between the acoustic field of the combustor and the flame fluctuations causing the growth of periodic oscillations inside the combustor. The amplitude of pressure fluctuations inside the combustor during thermoacoustic instability can be very high and can induce structural damage to the combustor. The periodic oscillations also cause increased heat transfer to the combustor walls causing thermal damage.

There have been extensive studies regarding the dynamics of blowout and thermoacoustic instability. Initial studies focused on finding the stability margins for flame blowout and thermoacoustic instability for various combustor configurations. Further, as described

before, the loss of stability of flames at the lean blowout limit is described as a loss of static stability of the combustor; in contrast, thermoacoustic instability is considered as a loss of dynamic stability of the combustor (Lieuwen 2007). However, recent findings have suggested that both transition to thermoacoustic instability and transition to blowout occur through dynamic regimes that exhibit complex behavior (Gotoda *et al.*, 2012; Domen *et al.*, 2015). Further, some of the recent studies (Nair & Sujith, 2014; Nair *et al.*, 2014) focused on the characterization of the complex dynamics observed during transition from combustion noise to thermoacoustic instability. The primary objective of this thesis is to characterize the complex dynamics of a combustor during transition from stable combustion blowout and provide an alternative description for the transition to blowout. We will also provide a unified framework to describe both transition to blowout and transition to thermoacoustic instability.

1.1 Historic overview: Lean blowout

1.1.1 Stability of the flame

Most of the early studies in flame blowout focused on global flame stabilization characteristics. One of the early studies by Lewis and Von elbe (1938) suggested that flame blowout is caused due to the increased velocity gradients at the burner tip. In 1950's various studies ventured to give better descriptions and explanations to blowout phenomenology for various different flame holder configuration (Zukoski & Marble 1954, 1955; Williams *et al.*, 1951). They were able to provide correlations based on different continuity criteria (mass and energy balance) to describe blowout. Zukoski & Marble (1956) suggested that the fresh air-fuel mixture in the shear layer ignites when it

interacts with the hot combustion products within the recirculation zone and a flame blowout happens when the ignition time delay is more than the resident time of the fresh reactants in the shear layer. A critical time delay of ignition for blowout was defined as, $t_b = l_r/V_b$. Here, l_r is the length of the recirculation zone and V_b is the blowout velocity. l_r is found to be a function of the equivalence ratio.

Longwell (1953) considered the recirculation zone to be a well-stirred reactor (WSR). He suggested that blowout happens when the reaction zone fails to generate enough heat to ignite the fresh reactants. Since the recirculation zone in practical combustors can seldom be compared to a perfectly homogeneous WSR, a correlation based on this assumption proves to be inaccurate for practical combustors. Splading (1953) and proposed that LBO is influenced by the ratio between the resident time of the reactants in the combustor and the reaction timescale represented by Damkhöler number, *Da*. Here, the chemical time scale associated with combustion is calculated from laminar flame speeds and thermal diffusivity.

Another approach is to look at blowout as a collective flamelet extinction event (Plee & Mellor, 1979; Radhakrishnan *et al.*, 1981). The effect of strain rates and flow characteristics on flamelet extinction was discussed by Yamagachi *et al.* (1985) and Pan *et al.* (1991). When blowout is considered as a collective flamelet extinction event, the ratio of the flow speed to the flame speed could also be used to characterize blowout. Blowout happens when this ratio exceeds one at critical locations in the combustor (Chaudhuri *et al.* 2010). In summary, all these studies indicate that the stability of the flame inside the combustor depends largely on the ability of hot products of the reaction to induce reaction of the incoming reactants.

This was further substantiated in a very detailed review of blowout of bluff body stabilized flames by Shanbhogue *et al.* (2009). Compiling the blowout data from over fifty previous studies, they developed correlations between the extinction stretch rates and extinction time scales. Further, they pointed out that recent research (Nair & Lieuwen 2007) indicates that blowout happens through multiple stages, the local extinction along the flame sheet, large scale wake disruption, and the final flame blowout. They argued that simple correlations based on *Da* number be largely successful in predicting blowout limits since they contain essential physics to capture the first stage of the blowout. During the first stage of the blowout, flame holes form at various locations of the flame where the local strain rate exceeds the extinction strain rate which can be correlated with the local Damköhler number. However, they also noted that such correlations do not describe the second stage of the blowout which is governed by much more complex chemistry and flow dynamics.

1.1.2 Flame dynamics prior to flame blowout

In practical applications, the flame exhibits highly unsteady behavior prior to blowout. A detailed study of this behavior was performed by De Zilwa *et al.*, (2000) using high-speed flame images and pressure fluctuation signals from a turbulent combustor with a backward facing step to stabilize the flame. They observed that as lean blowout was approached, the flame exhibited transverse flapping, asymmetric flame dynamics and eventual extinction. The frequencies of these oscillations were found to be much less than the acoustic frequencies of the combustor.

Further, Nair and Lieuwen (2007) identified the two stages of blowout in bluff body stabilized flames. In the first stage, momentary strain levels exceed the flames extinction

strain rates creating flame holes. However, the flame is observed to be rather symmetric during this state. In the second stage, the life of the flame holes increases due to enhance strain levels of the flow. This leads to large-scale wake disruption and vigorous flapping of the flame which induces acoustic oscillations with timescales as that of von Karman vortex shedding (Chaudhuri *et al.* 2010). They also observed that these acoustic oscillations had increased amplitude for the frequency spectrum ranging from 40 to100 Hz. They also observed that as blowout was approached, the number and the frequency of extinction and reignition events increased and by characterizing these extinction and reignition events one could predict lean blowout. A similar study on blowout in swirl-stabilized combustor was performed by Muruganandam (2006) which identified comparable dynamics close to flame blowout.

Chaudhuri *et al.* (2010) used time-resolved chemiluminescence imaging along with simultaneous particle image velocimetry (PIV) and OH planar laser-induced fluorescence (PLIF) to investigate the interaction between flame fronts and shear layer vortices prior to blow out in a turbulent combustor with a bluff body stabilized flame. Based on the experimental observations, they were able to hypothesize a mechanism for flame blowout. As the equivalence ratio of the incoming reactants is reduced, the flame speed decreases. This causes the flame to shift into the shear layer vortices. The enhanced interaction between the shear layer vortices and the flame cause local strain rates along the flame to increase more than the extinction strain rates causing partial flame extinction. Further, due to the partial flame extinction, the unburned mixture enters the recirculation zone and burn inside the recirculation zone created by the bluff body due to favorable time scales. This causes chemiluminescence inside the recirculation zone. The

reaction inside the recirculation zone either reignites the shear layers and relates the flame or fails to reignite the shear layer. This corresponds to stage one of blowout as described by Nair & Lieuwen (2007). In case the reaction in the recirculation zone fails to reignite the shear layer, more of the flame along the shear layer extinguishes. This induces absolute instability in the shear layer and the associated asymmetric mode oscillations cause flame flapping (Chaudhuri *et al.* 2010). This corresponds to stage 2 of blowout. Finally, the flame blowout happen, when the flame kernel inside the recirculation zone extinguishes. In some cases where the flame - acoustic coupling is very strong, the thermoacoustic oscillations themselves can induce flame blowout which is called a thermoacoustically induced blowout (Kabiraj & Sujith, 2012). However, such cases are not considered in this thesis.

The flame dynamics in specific combustor configurations and a more general review of the work on blowout in bluff body stabilized flame are given by Shanbogue *et al.* (2009). Blowout in swirl-stabilized flames were studied in detail by Stöher *et al.* (2011). They identified the significance of flame root in stabilizing the flame. Further, they showed that blowout happens when the flame root extinguishes for more than the time period of the precision of the precessing vortex core of the swirling flow field.

1.1.3 Precursors to flame blowout

Nair (2006) and Muruganandam (2006) studied the dynamics of flame near blowout by using signatures of acoustic perturbations and chemiluminescence measurements. They observed burst like behavior prior to blowout in both signals. This corresponded to the extinction and reignition events of flame within the combustor at low equivalence ratios. As blowout is approached they observed that the frequency of such events increased.

They used wavelet and statistical techniques on the acoustic pressure and *OH** chemiluminescence signals to extract indicators to an impending blowout.

Gotoda *et al.* (2011, 2012, 2014) used nonlinear time series analysis to study the onset of thermoacoustic oscillations as the equivalence ratio is reduced. Gotoda *et al.* (2012) established that the phase space corresponding to combustion oscillations prior to blowout exhibits multifractal characteristics. They also evaluated the degree of multifractality in terms of the equivalence ratio. They further emphasized that a multifractal analysis is indeed necessary to understand the nonlinear dynamics associated with these oscillations and that simple measures such as the divergence of phase space trajectories could not capture the rich dynamics at the blowout limit. In another recent study, Gotoda *et al.* (2014) described that the translation error, which quantifies the degree of parallelism of trajectories in the phase space, can be used as a precursor to detect LBO. Further, Domen *et al.* (2015) suggested that permutation entropy, quantifying the rank order pattern of components in phase space vectors constructed from the short time-series data of the acoustic pressure fluctuations, can also be used as an indicator to forewarn of LBO.

Further, Mukhopadhyay *et al.* (2013) described the dynamics of blowout from its acoustic and chemiluminescence signature using symbolic time series analysis and suggested a precursor (an indicative measure) to detect the proximity of a combustor to blowout. By using anomaly detection symbolic time series analysis, they were able to extract the nonlinear characteristics of the acoustic and *CH** chemiluminescence time series. A more generalized form of this technique was introduced by Sarkar *et al.* (2012).

In summary, all the above studies indicate oscillations observed on approaching blowout has complex dynamics and simple descriptions based on loss of static stability and Damköhler correlations may not be adequate to describe this phenomenon. However, there have been only very few studies that explored these nonlinear dynamics leading to lean blowout and characterized them.

1.2 Historic overview: Thermoacoustic instability

1.2.1 Traditional approaches

The occurrence of self-sustained large amplitude pressure oscillations in a combustor produced due to the coupling between the unsteady flame and the acoustic field of the confindment is known as thermoacoustic instability (McManus *et al.* 1993). When the unsteady heat release fluctuation is in phase with the acoustic pressure fluctuation, acoustic energy is produced inside the combustor (Rayleigh 1857). This cause growth of pressure oscillations which saturates into a limit cycle oscillation as the nonlinearities of the system becomes significant (Dowling 1997).

At the onset of thermoacoustic instability, the otherwise ‘stable’ combustion system becomes unstable exhibiting periodic oscillations. In this context, the onset of thermoacoustic instability was seen as loss of dynamic stability of the combustor. A significant amount of past research is directed towards establishing models for the thermoacoustic system based on linear flame transfer functions coupled with the acoustic field of the combustor and determining the growth rates by calculating the eigenvalues through a linear stability analysis (Huber & Polifke 2009a, b). The eigenvalues of the system are considered to indicate the stability of the system. However, it is observed that

a finite amplitude disturbance can cause a linearly stable thermoacoustic system to undergo ‘triggering’ and exhibit limit cycle behavior. Such a behavior indicates the necessity to model the nonlinear nature of the combustion process (Zinn & Lieuwen 2005).

Early research on thermoacoustic instability considered that it is the nonlinearities in the gas dynamic process that lead to thermoacoustic instability (Culick 1970,1976a, b, 1988, 1994). Culick and coworkers considered the acoustic field of a combustor to be nonlinear and derived models for thermoacoustic instability based on this assumption. However, the research by Sterling (1993) suggested that acoustic oscillations need not be nonlinear and that it is the nonlinearities in the flame response that cause triggering of thermoacoustic instabilities. This was further substantiated by Dowling (1997), Peracchio & Proscia (1999) and Lieuwen (2002) who pointed out that in most of the studies involving combustors that exhibit thermoacoustic instability, the acoustic pressure is less than 5% of the mean pressure and hence the nonlinearities in acoustic waves are not significant. Further, it was shown that for lean premixed combustors, the nonlinearities in flame response is very significant (Lieuwen, 2004; Preetham and Lieuwen, 2004, 2005; Hosseini and Lawn, 2005).

The response of a turbulent flame to perturbations and its tendency to cause thermoacoustic instability in a combustor depends upon various factors that influence the combustion. In a gas turbine engine, combustion process is characterized by various time scales such as the atomization and evaporation time scale of the fuel, convection time scales, mixing time scales, chemical time scales and the acoustic time scales. In a simplified sense, parity between these timescales can induce thermoacoustic instability

(Polifke 2004). Further, the coherent structures in the reactive flow formed due to the characteristics of the flame holding devices or the geometry of the combustor can interact with the flame causing heat release rate fluctuations resulting in thermoacoustic instability (Zinn & Lieuwen 2005). Unsteady combustion usually produces entropy waves in the flow field. These entropy waves when accelerated through the combustor exit or the turbine entrance can generate acoustic waves (otherwise known as indirect combustion noise) that travel upstream and affect the flame dynamics. Such interaction coupled with the acoustic field of the combustor is known to effect thermoacoustic instability (Marble & Candel, 1977; Bake *et al.* 2009; Goh & Morgans, 2013). Equivalence ratio fluctuations are also known to cause thermoacoustic instability (Lieuwen *et al.* 2001). Thus, thermoacoustic instability can originate as a result of interaction between various flow features with the flame characteristics and the acoustic field. In almost all cases, this interaction is highly complicated and nonlinear due to the interplay of turbulence, the chemistry of the reaction and the non-uniform spatial distribution of reacting species within the combustor. The nonlinearities in combustion response are consequently an unavoidable aspect that we need to consider while studying thermoacoustic instability in gas turbine engines.

In many experimental and theoretical studies concerning thermoacoustic instabilities, in order to avoid the complexities of the combustion process, a Rijke tube (Rijke 1859) with a heated wire mesh (heater) is adopted as a prototypical thermoacoustic system. A horizontal Rijke tube consists of a heated wire mesh positioned inside a horizontal duct through which a flow of air is established (Matveev 2003). At an appropriate position of the wire mesh and the air flow rate, the Rijke tube exhibits thermoacoustic instability

beyond a critical value of heater power. Rayleigh (1878) gave the most appropriate explanation for the thermoacoustic oscillations in a Rijke tube. Heckl (1985, 1988, 1990), through a series of papers applied nonlinear theory to understand the oscillations in a Rijke tube. She was able to use a modified version of King's law to model the heat release rate from the heated wire mesh, and provide a model to predict the limiting amplitude in Rijke tube. She also experimentally studied the nonlinear effects of heat release rate in Rijke tube and implemented active control strategies to suppress the thermoacoustic oscillations in Rijke tube. Nonlinear nature of oscillations in a Rijke tube was further characterized by Matveev and Culick (2003) who observed hysteresis in the onset of thermoacoustic instability when heater power was used as a bifurcation parameter. It was also observed that the hysteresis width varied with the mass flow rate of air.

In a pioneering study, the non-normal nature of the thermoacoustic system was identified by Sujith & co-workers (Balasubramanian & Sujith 2008 a, b). The effect of this nonnormal nature on the stability was also investigated (Nagaraja *et al.* 2009; Mariappan & Sujith 2010; Mariappan, Sujith & Schmid 2015; Subramanian & Sujith 2011). It was observed that non-normality causes the system to have transient growth in disturbance energy which when clubbed with the nonlinearities of the system can introduce thermoacoustic instability at those parameter locations which under a classical stability analysis is linearly stable. Further, studies by Juniper and co-workers (Juniper, 2011; Juniper, 2012; Waugh & Juniper, 2011) focused on the effect of non-normality on triggering in thermoacoustic systems.

The effect of noise on the stability of a horizontal Rijke tube was investigated by Waugh & Juniper (2011). They observed that under the influence of noise, a thermoacoustic system could become unstable even in the linearly stable regime. This predictionwas validated through experiments by Jagadeesan and Sujith (2013) who showed that transition to thermoacoustic instability is possible even when the noise level is significantly lower than the triggering amplitude. The effect of noise on the hysteresis characteristics of a horizontal Rijke tube was studied by Gopalakrishnan and Sujith (2015), both experimentally and theoretically. They observed that the width of the bistable region reduced as the noise intensity was increased. In the presence of high-intensity noise, the bistable region was completely suppressed.

The presence of such nonlinear characteristics of thermoacoustic oscillations even in a prototypical system indicates the need for nonlinear analysis to understand thermoacoustic instability. Even though a significant portion of the past research focused on linear stability analysis and identifying flame transfer functions to characterize thermoacoustic instability in different combustors, recently there has been an increased focus on the nonlinear dynamics of thermoacoustic oscillations.

1.2.2 Recent Advances: Dynamical systems approach

Any system that changes with time is called a dynamical system. Usually, such a system can be described through a set of differential equations. Dynamical systems theory is the branch of mathematics that describes the behavior of a dynamical system. Especially, the tools from dynamical systems theory help characterize the long-term qualitative behavior of the dynamical system even when you do not have access to all the state variables of a system. This is especially useful when we have to characterize the dynamics of a

thermoacoustic system since in almost all practical scenarios, during experiments, we can only measure the pressure fluctuations inside the combustor. In this section we will see a brief overview of various studies that used dynamical systems approach to study the nonlinear characteristics of thermoacoustic instability.

Using numerical continuation methods, Jahnke and Culick (1993) suggested that a thermoacoustic system can not only exhibit simple limit cycle oscillations but also could undergo a pitchfork and torus bifurcation and exhibit quasiperiodic oscillations. The quasiperiodic oscillation is characterized by the presence of two incommensurate dominant frequencies and their multiples and thus is not periodic. The possibility of chaotic oscillations was identified by Sterling (1993) and Lei & Turan (2009) by using numerical bifurcation analysis on models for premixed combustors. In experiments with lean gas turbine combustors, the chaotic dynamics of heat release rate oscillation was observed by Fichera *et al.* (2001).

Recently, numerical continuation was used to investigate the bifurcation to thermoacoustic instability for a horizontal Rijke tube (Subramanian, 2011). They observed interesting dynamical behavior such as co-existing multiple attractors, quasiperiodic behavior and period doubling route to chaos. They further employed similar analysis for a model for a ducted laminar premixed flame and obtained analogous results (Subramanian & Sujith, 2011).

In experiments, Kabiraj *et al.* (2012a, b, c,) and Kabiraj & Sujith (2012) established routes to chaos in thermoacoustic system through bifurcation studies. In a ducted laminar premixed laminar combustor, they observed that apart from limit cycle oscillations

thermoacoustic systems exhibited various complex dynamic states such as intermittency, frequency locked and chaotic states. The different dynamic states were characterized using phase space reconstruction, recurrence plots and bifurcation diagrams. The role of flame dynamics in generation of such dynamic states was investigated by Vishnu *et al.* (2015). Kabiraj *et al.* (2012a, b, c,) and Kabiraj & Sujith (2012) also observed both the Ruelle-Takens and the frequency locking quasi-periodic route to chaos in their experiments. Later, detailed numerical investigations confirmed these findings (Kashinath *et al.*, 2013; Kashinath & Juniper 2013; Orchini *et al.*, 2015; Kashinath *et al.*, 2015).

Studying the dynamics of the onset of thermoacoustic instability, Nair *et al.* (2013) suggested that the low amplitude aperiodic combustion noise from a turbulent combustor is chaotic and described the transition from combustion noise to thermoacoustic oscillations as a transition from chaos to order. Tony *et al.* (2015) through surrogate analysis confirmed that combustion noise is deterministic and hence chaotic. Nair *et al.* (2014) also observed that the transition region is characterized by intermittent oscillations where the system switches from low amplitude chaotic oscillations to high amplitude periodic oscillations. Nair *et al.* (2014) was able to quantitatively characterize the intermittency in the time series of acoustic pressure and was able to device a precursor to an impending thermoacoustic instability using recurrence quantification analysis (RQA). A detailed description of RQA is given in Chapter 3. Later, Pawar *et al.* (2015) used RQA to characterize the dynamics of a laboratory spray combustor. They observed that transition to thermoacoustic instability happened through a regime of intermittency and

that the intermittency is possibly of type II suggesting that the underlying bifurcation responsible for the intermittency is subcritical Hopf bifurcation.

The above observations exhibit the complex nature of oscillations in a combustor during different dynamic regimes. Especially, the chaotic nature of the oscillations during combustion noise is the result of underlying turbulent fluctuations in the flow field of the combustor. Already, it is established that turbulent flows have a multifractal scaling behavior (Sreenivasan & Meneveau 1986) arising from the underlying multiplicative process of Richardson's energy cascade (Richardson 1922). Systems that exhibit multifractal behavior are better studied in the framework of complex systems theory.

1.2.3 Recent advances: Complex system approach

Systems composing of large number of interacting units are called a complex systems. The interaction between the units result in an aggregate behavior that is nonlinear. Further, the system self-organizes under the influence of external force to exhibit a collective behavior and such a collective behavior cannot be inferred from the behavior of the individual elements of the complex system. A turbulent combustor could be considered as a complex system. It composes of various interacting units, the collection of reactive fluid parcels confined within the combustor, whose interaction is governed by various factors such as molecular mixing, turbulent transport (which has a wide range of scales), the complex chemistry of the reactions and the acoustic and hydrodynamics fields. At different dynamic conditions, the combustors exhibit various nonlinear behavior ranging from chaotic oscillations during combustion noise to ordered limit cycle oscillations during thermoacoustic instability and intermittency during the transition regime from combustion noise to thermoacoustic instability. These dynamics are the

result of the reactive flow self-organizing itself into various dynamic behavior as the flow conditions (equivalence ratio in our case) are varied.

Adopting a complex system framework, and performing fluctuation analysis of the time series of acoustic pressure from the combustor, Nair and Sujith (2014) showed that the "combustion noise" generated by a flame in a confined environment has multifractal characteristics and is not mere stochastic fluctuations. Thus, they showed that the 'noise', which in general is either filtered out or treated as stochastic background in traditional analysis and modeling of combustion dynamics, does contain important information about the dynamical state of the system. Further, they also suggested that the 'noise' might be a direct consequence of inherent complexity of turbulent combustion dynamics and hence the separation of the measurements into a signal and noise may lead to loss of valuable information.

They observed that as the system transitioned from combustion noise to thermoacoustic instability the multifractal spectrum width reduced and at thermoacoustic instability, the multifractal spectrum shrunk to a single point. Considering this, Nair and Sujith (2014) described onset of thermoacoustic instability as loss of multifractality. They were also able to suggest Hurst exponent, a measure of fractal dimension of the time series as a precursor to an impending thermoacoustic instability. They reported that Hurst exponent was able to predict the impending instability much before compared to P_{rms} which is traditionally used as an indicator to the onset of thermoacoustic instability.

Another approach to study a complex system is by constructing the corresponding complex network and studying its topological charecteristics. Using visibility algorithm,

Murugesan & Sujith (2015) constructed complex networks corresponding to the pressure fluctuations inside the combustor. They were able to show that combustion noise can be topologically represented as a scale-free network. Thus, they suggested that the transition to combustion instability is a transition from a scale-free network to a regular network. They were also able to show that network parameters such a clustering coefficient and characteristic path length could be used as viable precursors to onset of thermoacoustic instability.

It is observed that despite the differences in the components that constitute the complex systems, they often exhibit similar dynamic behavior. This is an interesting aspect since we see that the transition to various oscillatory instabilities involving turbulent flow have similar dynamic characteristics. Systems that exhibit aero-elastic instability, aero-acoustic instability, surge etc., exhibit intermittency en route to the corresponding oscillatory instabilitiy. It is also observed that all the precursors that are useful for predicting thermoacoustic instability are viable precursors to predict any one of these oscillatory instabilities.

1.3 Dynamics of oscillation prior to blowout: Lacuna

Even though, recently there have been many detailed studies of complex dynamics during transition from combustion noise to thermoacoustic instability, there have been very few studies that studied the complex nature of oscillations prior to lean blowout. Recent studies focusing on nonlinear dynamics of combustors show that transition to both thermoacoustic oscillations and blowout exhibit dynamically rich behavior. Kabiraj and Sujith (2012), discovered intermittent dynamics in a thermoacoustic system with laminar

premixed combustion. They identified that prior to blowout, the thermoacoustic system exhibited intermittency, where the system switched from low amplitude periodic fluctuations to high amplitude chaotic fluctuations. From the analysis of pressure fluctuations in a combustor with turbulent flame, Gotoda *et al.* (2012) established that the phase space corresponding to combustion oscillations prior to blowout exhibited multifractal characteristics. They also evaluated the degree of multifractality in terms of the equivalence ratio of combustion. They further emphasized that a multifractal analysis is indeed necessary to understand the nonlinear dynamics associated with these oscillations and that simple measures such as the divergence of the phase space trajectories could not capture the rich dynamics at the blowout limit. In another recent study, Gotoda *et al.* (2014) described that the translation error, which quantifies the degree of parallelism of trajectories in the phase space, can be used as a control variable to detect lean blowout. Further, Domen *et al.* (2015) suggested that permutation entropy, quantifying the rank order pattern of components in phase space vectors constructed from the short time-series data of pressure fluctuations, can also be used as a control variable to prevent LBO. All these studies, point to the nonlinear nature and complexity of combustion dynamics prior to blowout.

Traditionally, blowout is described as loss of static stability of the combustor. Considering the complex nature of dynamics at the transition to blowout, it seems that the mere description of blowout as loss of static stability of the flame is inadequate. Further, it is evident from prior research (Nair & Sujith, 2014) that even the so-called stable dynamics in the context of stability analysis (i.e., combustion noise) is highly complex. In the context of onset of thermoacoustic oscillations, Nair *et al.* (2014) addressed this

problem by adopting a multifractal description of combustion noise and describing the onset of thermoacoustic instability as a loss of multifractality. This description gives a clearer definition to the stability margin for the onset of thermoacoustic instability in turbulent combustor while being able to accommodate the complex dynamics seen prior to the onset of thermoacoustic instability. Further, they were able to provide a novel precursor, the Hurst exponent (a measure indicative of the fractal nature of a time series) to detect the onset of an impending thermoacoustic instability. Considering these aspects, we attempt to address following four issues in this thesis.

1. The complexity in scaling characteristics of the pressure oscillations from combustion noise to thermoacoustic instability was studied by Nair & Sujith (2014). Further, the phase space corresponding to the pressure oscillations prior to blowout is found to exhibit multifractal scaling behavior (Gotoda 2012). A detailed characterization of the scaling behavior of the oscillations during the transition from stable combustion to blowout needs to be performed.
2. Thermoacoustic system exhibits intermittency prior to lean blowout (Nair & Sujith 2015). A detailed characterization of this intermittency needs to be performed. Recurrence quantification analysis of intermittent oscillations in the transition regime from combustion noise to thermoacoustic instability provided viable precursors to onset of thermoacoustic instability. Similar precursors can be sought out for lean blowout.
3. Even though there is difference in the underlying physics of two complex systems, they can have similar collective behavior. For example, intermittency is observed prior to the onset of various oscillatory instabilities that involve turbulent flow

such as thermoacoustic instability in a combustor, aeroacoustic instability in a whistle, aero elastic instability of a structural component etc. Clearly, the underlying physics that governs the interaction between the different subsystems in each case is vastly different. However, the emergent or collective behavior is similar. We observe that the combustor exhibits intermittency both prior to thermoacoustic instability and prior to blowout. However, it is clear that flame dynamics in both cases cannot be similar since the flame becomes more and more unstable as we approach blowout. Hence, the intermittency prior to thermoacoustic instability and that prior to blowout needs to be compared and contrasted.

4. There have been various models that describe blowout in a combustor. Even though many of these models are successful in identifying the stability margins for blowout, there are no low order models that can capture the dynamics of the oscillations prior to lean blowout. A model that considers the turbulent flame as a collection of flamlets interacting with each other embodies the philosophy of complex nature of the combustor in its core and may be able to capture the dynamics close to blowout.

1.4 Objectives of this thesis

The primary objective of the present work is to understand the complex dynamics that a bluff body stabilized turbulent combustor exhibits prior to lean blowout and compare the transition to blowout with the transition to thermoacoustic instability. Further the study also aims to provide precursors to an impending blowout in a combustor. The specific objectives are:

1. To provide a unified framework that describes both transitions to blowout and thermoacoustic instability.
2. Characterize the intermittency prior to blowout to obtain viable precursors to an impending blowout.
3. Compare and contrast the intermittency prior to thermoacoustic instability and blowout.
4. Develop a low-order model that can capture the dynamics of a turbulent combustor prior to lean blowout.

1.5 Overview of the thesis

We conducted experiments on a laboratory scale dump combustor with a bluff body as flame stabilizing mechanism to pursue the objectives detailed in §1.2. Measurements of pressure and chemiluminescence intensity were used to characterize the dynamics of the combustor. This was to ensure that the precursors to blowout that we may obtain from this study will be useful in practical combustors where the types of obtainable measurements useful for diagnosing the dynamic stability are mostly restricted to the pressure fluctuations inside the combustor. We further use tools from dynamical systems theory and complex systems theory to characterize these oscillations and to obtain precursors to an impending blowout. We further compare the dynamics during the transition to blowout with the dynamics during the transition to thermoacoustic instability using recurrence plots. Further, the corresponding flame dynamics were compared using high-speed Mie scattering images. Finally, a low order model that can mimic the complex characteristics of the chemiluminescence fluctuations close to blowout is suggested.

The rest of the thesis is laid out as follows. **Chapter 2** gives a detailed description of the experimental setup and the measurement techniques used for this study. In **Chapter 3**, the scaling characteristics of the pressure and chemiluminesence fluctuation are investigated. We use multifractal detrended fluctuation analysis (MFDFA) to achieve this. We show that while we approach thermoacoustic instability, the multifractal spectrum width reduces to zero and as blowout is approached, multifractal spectrum width increases. This indicates that we can have a unifying description to both blowout and thermoacoustic instability where the onset of thermoacoustic instability can be considered as loss of multifractality and the approach to blowout as an increase in multifractal spectrum width. Further, we also show that Hurst exponent can be used as a precursor to an impending blowout.

In **Chapter 4**, we study the dynamic characteristics of oscillations during the transition from stable combustion to lean blowout using recurrence quantification analysis (RQA). We show that various recurrence parameters such as trapping time, Shannon entropy of the lines parallel to the diagonal and recurrence rate increases as we approach an impending blowout owing to the increased aperiodicity of the oscillations close to blowout and hence can serve as precursors to an impending blowout. We will further show that a method of recurrence quantification analysis that does not involve phase space reconstruction and analyzes the recurrence of the value of the state variable in time is effective at prognosis of dynamic transitions in a turbulent combustor. Since such a method is computationally less expensive, it can be adopted for online diagnostics of thermoacoustic instability and blowout in a turbulent combustor.

Chapter 5 gives a comparison of intermittent states that are observed prior to the occurrence of thermoacoustic instability and that is observed prior to lean blowout. Using recurrence plots, we observe that both intermittencies are possibly of type II and are hence dynamically very similar. However, high-speed Mie scattering experiments show that the flame dynamics corresponding to either intermittency is different due to the difference in the flame stabilization during both dynamic regimes. We also note that the flame dynamics very close to blowout is largely affected by the intermittent formation of flame holes making the pressure oscillations just before blowout to be highly aperiodic.

In **Chapter 6,** we suggest that flame dynamics close to blowout can be modeled as a problem of population dynamics of flamelets in the reaction zone. The turbulent flame is considered as a collection of flamelets interacting with each other and the unburned gas in the reaction field. A flamelet is born when a parcel of unburned gas is surrounded by a flamelet. The flamelet extinguishes or dies when all the fuel inside the parcel burns. Blowout in such a context is a situation when the flamelets become extinct in the reaction field, and the combustion ceases to continue. We introduce a model based on population dynamics of flamelets that mimic the flame dynamics at the lean limit. Finally, the conclusions derived from this thesis are summarized in **Chapter 7**.

CHAPTER 2

Experimental setup and methods

Experiments described in this thesis were conducted in a laboratory scale backward facing step combustor with a bluff body used as the flame stabilizing mechanism. Primarily, the unsteady pressure fluctuations and the chemiluminescence fluctuations inside the combustor were measured. The experimental setup had optical access to the combustion chamber which enabled performance of Mie scattering experiments to study the flame dynamics at different dynamic states of the combustor.

2.1 Experimental Setup

This test rig, christened TARA (**T**hermo**A**coustic **R**ig for **A**xial instabilities) was previously used by Nair and Sujith (2014). The combustion chamber is a square duct with a cross-section of 90 × 90 mm^2. The combustion chamber is divided into multiple sections. The first section is attached to the dump plane and has quatz window to enable optical acess. The length of the combustor can be varied by adding or removing sections from the combustor. The total length of the combustor can be 70 cm, 100cm or 140 cm. A sparkplug mounted at the dump plane, is used for ignition. The fuel used here is LPG (60% Butane and 40% Propane). The fuel is injected 120 mm upstream of the bluff body. Air is partially premixed with the fuel before the mixture enters the combustion chamber. A flame arrester is provided 50 mm upstream the dump plane which ensures that the flame does not flash back into the settling chamber.

The bluff body used for flame stabilization is a circular disc of thickness 10 mm and diameter 47 mm. Within the combustor, bluff body is positioned 50 mm from the dump plane. The first section of the combustor is equipped with quartz windows (90 mm × 140 mm) to enable optical access to the combustion zone. The tail end of the combustor is connected to a decoupler of size 1 m × 0.5 m × 0.5 m. The decoupler is provided to reduce the radiation of acoustic energy from the combustor to the surroundings.

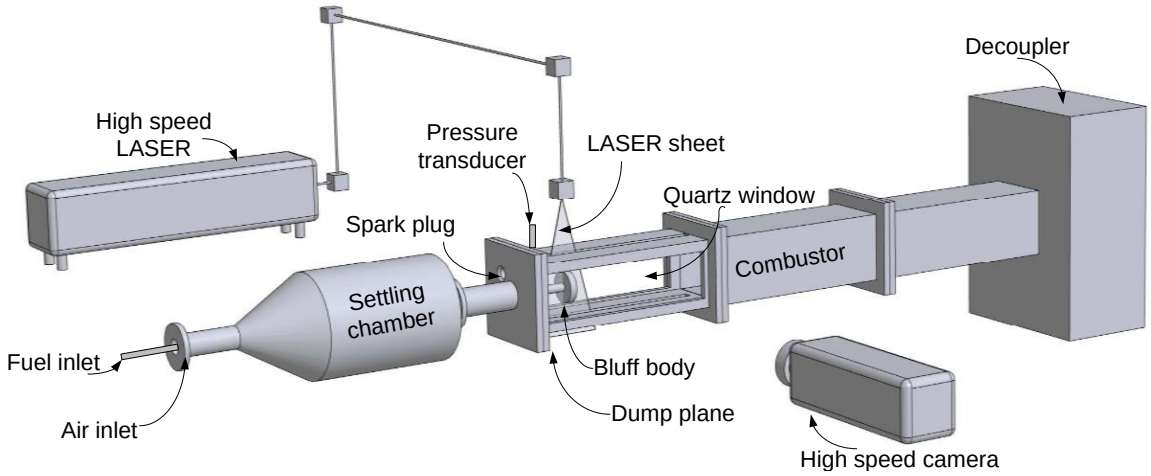

Figure 2.1: The schematic of the lab scale combustor used for this study. A pressure transducer is used to measure the pressure fluctuations in the system. The flame stabilizing mechanism is a circular bluff body. The length of the combustion chamber can be changed by adding more number of sections in the combustor. For this study, the length was fixed at 1400 mm. The design of this combustor was adapted from Komarek & Polifke (2012)

2.2 Measurements and Instrumentation

The experimental setup is equipped with various measurement units and controllers in order to conduct experiments and enable measurements. The mass flow rates of the fuel and air is controlled during experiments in order to vary the equivalence ratio at which the combustion is carried out. The acoustic pressure and CH^* chemiluminesence fluctuations inside the combustor are measured at various experimental condition. High speed Mie scattering images were used to study the flame dynamics during different dynamic regimes of the combustor.

2.2.1 Mass flow controllers

The mass flow rates of fuel and air supplied to the combustor were controlled using a mass flow controllers (Alicat Scientific, MCR Series) with solenoid valves. Air flow rate was controlled with a mass flow controller which supported a maximum flow rate of 4000 SLPM. The mass flow controller used for fuel had maximum flow rate of 100 SLPM. During Mie scattering experiments, a part of the air flow rate was bypassed through a 100 SLPM mass flow controller to a Laskin nozzle. This air is bubbled through the olive oil bath inside the Laskin nozzle to make a mixture of air and suspended olive oil droplets. This mixture is then injected back into the plenum chamber where it gets mixed with the rest of the air flow. Thus the air fuel mixture that enters the combustion chamber is seeded with olive oil droplets. The mass flow controllers have an uncertainity of ± (0.8% of reading + 0.2% of full scale). In this study, we have represented the variation of various parameters with equivalence ratio of the combustion mixture. Equivalence ratio is estimated as $Eq.\ Ratio = (\dot{m}_f/\dot{m}_a)_{actual}/(\dot{m}_f\ /\dot{m}_a)_{stoichiometry}$. The uncertainty in the estimated equivalence ratio is ± 0.02.

2.2.2 Unsteady pressure

Unsteady pressure fluctuations inside the combustor were measured using piezoelectric (PCB103B02 uncertainty ± 0.15 Pa) transducer. Even though the sensor had a metallic housing, the maximum operating temperature of the sensor was 121^{o}C. Hence specially made pressure ports were used to mount transducer on to the combustor walls. The pressure ports had Teflon adaptors on to which the pressure transducer was connected. The pressure ports were connected to semi-infinite tubes to prevent acoustic resonance within the pressure ports. It was observed that phase correction needed for this type of arrangement of pressure ports is less than 2^{0}. Even though the combustor had provision to measure pressure at various locations along its length, all the measurements reported in this thesis are from a pressure port located 5 cm away from the dump plane. This location is very close to the acoustically closed end of the combustor (dump plane) and hence is closest to a pressure antinode for all the acoustic modes of the combustor.

2.2.3 *CH** Chemiluminescence

Chemiluminescence measurements were performed using a photomultiplier tube (PMT, Hamamatsu H10722-01). The PMT module was placed 50 mm from the quartz window normal to the plane of the window (in Fig. 2.1, in the same location as that of high speed camera). This position ensured that the photomultiplier captured the dynamics of the entire flame. The PMT module measured the filtered light intensity (narrow band, peak at 432 nm, 10 nm FWHM) corresponding to *CH** chemiluminescence from the combustor. Thus at each instant of time, the PMT module was able to measure the total *CH** chemiluminesence from the combustor indicating the instantaneous rate of reaction or alternatively the heat release rate within the combustor. The collection cone angle for

the PMT, for the particular configuration that is used in our experiments is 4.65 steradians.

2.2.4 Data Acquisition

The signals from the pressure transducer and the PMT module were acquired using an A-D card (NI-6143, 16 bit) at a sampling frequency of 10 kHz, for duration of three seconds. Images taken with Phantom V 12.1 camera was directly saved to the memory of the camera during the experiments. The maximum storage space available for the camera was 32 GB. This restricted the total data accusation time to 25 seconds for a frame rate of 2000 fps of images of resolution of 1280 × 800 pixels.

2.2.5 Mie Scattering experiments

The unsteady fluctuations of the flame drives various dynamic behavior of the combustor. Hence, it is important to understand the flame dynaics during different dynamic states of the combustor to devise combustion control strategies. To that end, we performed high speed Mie scattering experiments. In order to conduct Mie scattering experiments, the incoming air was seeded with olive oil droplets of dimension 1-2 microns. A Lazkin nozzle was used to produce olive oil droplets. During combustion, the oil droplets in the air pass through the flame, evaporate and burn. When a laser sheet is shone through the combustion zone, the oil droplets present in the flow scatters light (Mie scattering). Since the oil droplets are present only before the flame, the boundary of the illuminated region in the Mie scattering image approximately represents the flame front in the plane of illumination of the laser sheet. The high-speed Mie scattering image thus reveal the dynamics of the flame front along a single plane through the combustor as

opposed to a high-speed chemiluminescence image which is the line of sight integrated image of the three dimensional flame.

The laser light required for the illumination of the image plane is produced from a high speed Nd YLF laser (DM527-50 Nd YLF laser, single cavity, double pulsed). The laser produces light of wavelength 527 nm and has a maxim pulse rate of 10 kHz. The light beam produced by the laser is then passed though series of prisms to direct it through the 8 mm slit in the first section of the combustor. Just before the beam enters the combustion chamber, it is passed through a light sheet optics module (TSI instruments, 610027) that converts the laser beam into a light sheet that illuminates a cross section of combustor as shown in the Fig. 2.1. The light sheet optics consists of a combination of cylindrical and spherical lenses whose relative position can be adjusted to vary the thickness of the light sheet. For the present study, the sheet thickness was approximately 1 mm.

The laser pulses were synchronized with a Phantom V12.1 camera in order to capture the Mie scattering images. Phantom V12.1 camera has the capability to image at a rate of 6000 fps with a resolution of 1280 × 800 pixels. However, for this study the frame rate used is 2000 fps.

CHAPTER 3

Multifractal characteristics of combustion dynamics prior to lean blowout

In classical literature, blowout is described as loss of static stability of the combustion system whereas thermoacoustic instability is seen as loss of dynamic stability of the system. The description of blowout as loss of static stability stems from the assertion that at blowout, the system transitions from a stable reacting state to a non-reacting state indicating loss of static stability of the reaction. However, this simple description of stability margin is inadequate since recent studies have identified that combustors exhibit complex nonlinear behavior prior to blowout. Recently, it was also shown that combustion noise that characterizes the regime of stable operation in itself is dynamically complex and exhibit multifractal characteristics. Researchers have already described the transition from combustion noise to combustion instability as a loss of multifractality (Nair & Sujith 2014). In this chapter, we will provide a multifractal description for lean blowout in combustors with turbulent flow and thus bring in a unified framework within which both thermoacoustic instability and blowout can be described. Further, we will introduce a method for predicting blowout based on the multifractal description of blowout. However, before venturing into the multifractal analysis, we will first study the pressure and chemiluminesence signals that represent the dynamics of the combustor at different equivalence ratios.

3.1 Route to blowout: pressure and chemiluminescence oscillations

Dynamics of the turbulent combustor can be characterized by measuring any one of the state variable that describes the dynamic state of the system. We choose to use the unsteady pressure signal and the *CH** chemiluminesence to characterize the dynamics since these measurements are also feasible in industrial combustors. We conducted experiments at different fuel flow rates (1.04 g/s, 0.93 g/s, 0.81 g/s, 0.56 g/s) each corresponding to different power levels of combustor (18.2 kW, 16.25 kW, 14.3 kW and 9.75 kW respectively). In each experiment, the airflow rate is varied such that the equivalence ratio is decreased from 0.98 in discrete steps until the flame in the combustor blows out. The range of Reynolds number for the reported experiments is from 1.03×10^4 to 3.7×10^4.

As the equivalence ratio is varied from near stoichiometry to blowout, we observe that pressure and *CH** chemiluminescence signals exhibit various different temporal modulations. In Fig. 3.1 we illustrate these oscillations present in a bluff body stabilized combustor for fuel flow rate of 1.04 g/s. Here, we can identify that the transition from stoichiometric combustion to blowout follows the path, low amplitude aperiodic oscillations → intermittency → thermoacoustic instability → intermittency → low amplitude aperiodic oscillations → blowout.

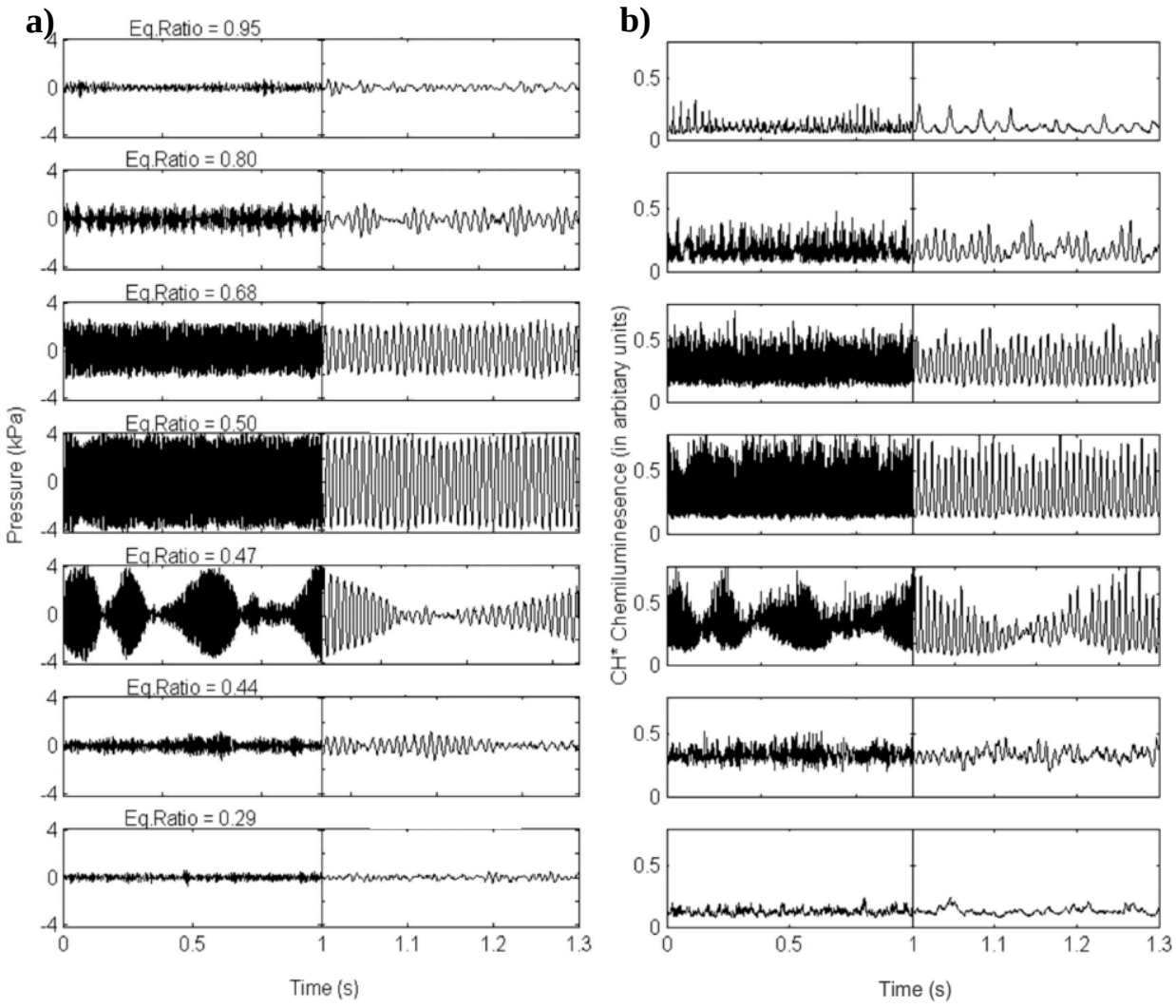

Figure 3.1: Variation of (**a**) pressure fluctuations and (**b**) *CH** chemiluminescence fluctuations at different equivalence ratio conditions for a bluff body stabilized combustor operating in turbulent regime. The fuel flow rate is 1.04 g/s. At an equivalence ratio of 0.95 ($Re = 1.13 \times 10^4$) the pressure and *CH** chemiluminescence fluctuations are aperiodic and have of low amplitude. At equivalence ratio of 0.80 ($Re = 1.34 \times 10^4$), we observed intermittency in both pressure and chemiluminescence signal. On further reduction of equivalence ratio to 0.68 ($Re = 1.57 \times 10^4$), we observe periodic behavior for both pressure and chemiluminescence signals. At equivalence ratio of 0.50 ($Re = 2.14 \times 10^4$), we still observe periodic oscillations. However, the amplitude of oscillations is higher than that at

equivalence ratio of 0.68. When the equivalence ratio is 0.47 ($Re = 2.28 \times 10^4$), we observe intermittency in both pressure and chemiluminescence signals with oscillations switching from high amplitude periodic fluctuations to low amplitude aperiodic fluctuations. When the equivalence ratio is further reduced, at equivalence ratio of 0.44 ($Re = 2.43 \times 10^4$), the amplitude of periodic content in the oscillation reduces. When the equivalence ratio is 0.29 ($Re = 3.69 \times 10^4$), the pressure and chemiluminescence oscillations are aperiodic and have very low amplitude.

At equivalence ratio of 0.95, we observe that the pressure fluctuations have low amplitude and are aperiodic. Similarly the corresponding *CH** chemiluminescence fluctuations are also aperiodic and has low amplitude. At equivalence ratio of 0.80, we observe some periodic part in the time series alternating with aperiodic oscillations. This state is referred to as intermittency in dynamical systems theory. The existence of such intermittent dynamics in the transition region from combustion noise to instability has been reported by Nair *et al.* (2014). When the equivalence ratio is reduced to 0.68, we start observing periodic fluctuations in both pressure and chemiluminescence signal. On further reduction of equivalence ratio, the amplitude of the periodic fluctuations (both chemiluminescence and pressure signals) increases. We can observe this by comparing pressure and chemiluminescence signals corresponding to equivalence ratios of 0.68 and 0.50. The amplitude of periodic fluctuations is higher for the case with lower equivalence ratio. At equivalence ratio of 0.47, we start observing intermittency again. Here, the pressure signal has bursts of high amplitude periodic fluctuations followed by low amplitude aperiodic fluctuations. A similar intermittent behavior is observed for chemiluminescence fluctuations as well. The intermittent behavior in chemiluminescence signal suggests that at this dynamic regime, the flame fluctuates periodically for a short

period of time and then oscillates in an aperiodic manner for a few acoustic cycles. This switch in dynamic behavior is repeated in an apparently random manner. On further reduction of equivalence ratio, the amplitude of the periodic part of the intermittent oscillations starts to decrease. This change can be seen comparing the signals corresponding to equivalence ratios 0.47 and 0.44. In the case of equivalence ratio of 0.44, the periodic bursts in the signal have much smaller amplitude compared to the signals corresponding to equivalence ratio of 0.47. As we reduce the equivalence ratio further, the system exhibits low amplitude aperiodic oscillations in both pressure and chemiluminescence signals.

In Fig 3.2 we can see the power spectra (FFT) corresponding to the time series of pressure and chemiluminesence fluctuations illustrated in Fig. 3.1. We observe that as the instability is approached (Fig. 3.2, *Eq. Ratio* = 0.68 and 0.50), the FFT corresponding to both chemiluminesence and pressure fluctuations show peak at a single frequency close to 120 Hz. This frequency varies slightly as the equivalence ratio is changed. This variation can be attributed to variation in the flame shape and flame dynamics at different equivalence ratios leading to variation in local acoustic impedance and speed of sound along the length of the combustor. A detailed flame analysis is required to gain thorough understanding about this observation. Such a study is out of the scope of the present work. As the equivalence ratio is further reduced, the amplitude of the peak reduces (Fig. 3.2, *Eq. Ratio* = 0.47). Close to blowout, the power spectrum does not contain any significant peaks.

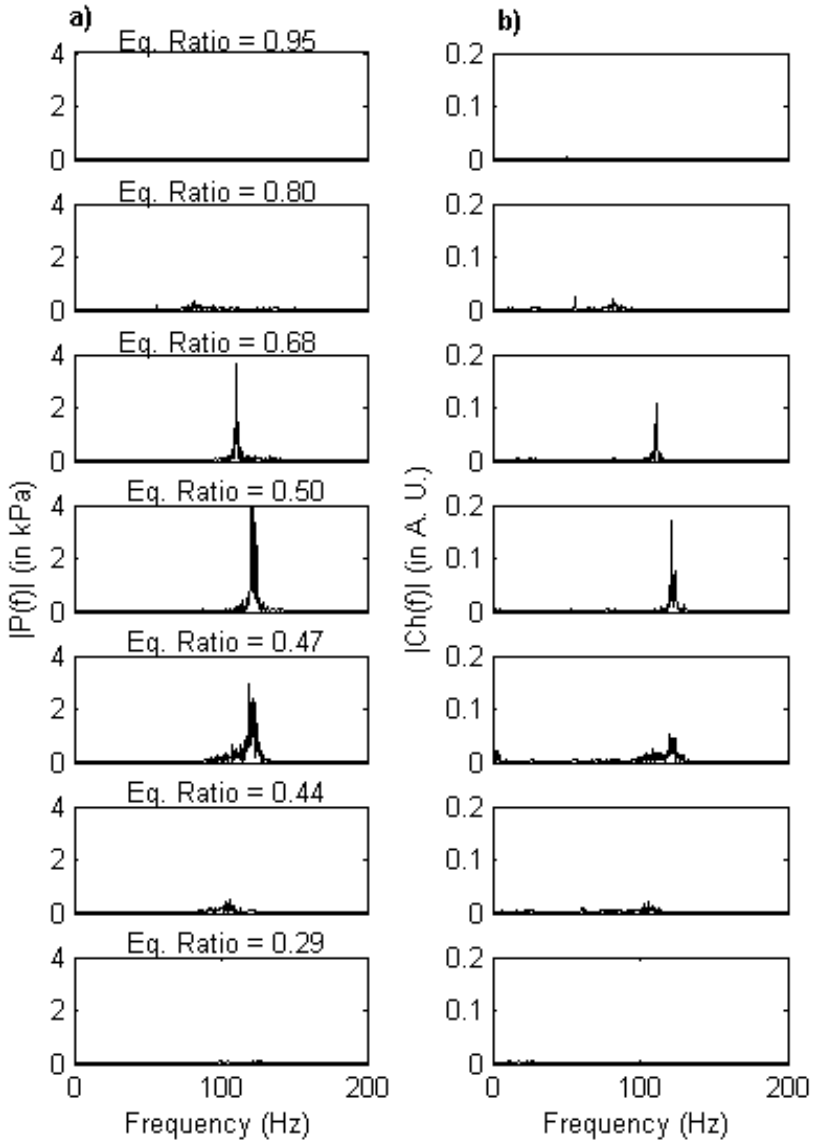

Figure 3.2: a) FFT's corresponding to that of pressure fluctuations in Fig. 3.1.a. b) FFT's corresponding to chemiluminesence fluctuations in Fig. 3.1.b. We observe that in both pressure and chemiluminesence time series, as we approach instability, there is growth of oscillations at single frequency around 120 Hz (slight variations according to equivalence ratio). However, as we approach blowout, the oscillations at the dominant frequency dies down.

Analyzing the power spectra of the pressure and chemiluminesence fluctuations, we were not able to obtain any significant understandings regarding the complex dynamics exhibited by the pressure and chemiluminesence fluctuations. In the next section, we try to understand the complex behaviors of pressure and chemiluminescence signals detailed in this section by studying the variation of the fractal characteristics of both chemiluminescence and pressure signals.

3.2 Scaling behavior of the pressure and chemiluminescence signals

In order to understand the scaling characteristic of the fluctuations in pressure and chemiluminescence signals, we analyze the fractal characteristics of corresponding time series. Fractals are geometric objects that exhibit self-similarity at different scales. As we zoom into a fractal, we can see similar structures emerging again and again at different levels of zoom. Due to this property of fractals, measures such as area and length of a fractal are dependent upon the scale of measurement. For example, if we were to measure the length of a curve which is a fractal using a ruler, the measured length of the curve follows an inverse power law with the length of the ruler used for measurement. Alternatively, a log - log plot of the measured length of the curve as a function of the ruler length is a straight line with a negative slope. The power law exponent (the slope of the line in the log - log plot) is termed the fractal dimension D. Euclidean objects have an integer fractal dimension equal to the physical dimension of the object. In contrast, fractals have a non-integer fractal dimension.

A similar concept can be used to characterize a fractal time series, where self-similarity is observed in various timescales. For a fractal time series $v(t)$, $v(ct) = v(t)/c^H$ is also a

signal with same statistics (West *et al.*, 2003). Here, H is the Hurst exponent, a measure of the fractal dimension (D) of the time series (Hurst, 1951). The Hurst exponent H can be related to the fractal dimension D of the time series as $D = 2 - H$. The algorithms that estimate the Hurst exponent from a time series data utilizes this scaling relationship to derive the estimates. In practical situations, the scales present in a system have both upper and lower bounds that are dependent upon the characteristics of the system. Further, the signals might also exhibit complex scaling behavior where the scaling factor is a function of the amplitude of fluctuations. Such time series are called multifractal time series and cannot be described using single Hurst exponent (Mandelbrot, 1999). Hence, we need to define generalized Hurst exponents in order to describe their scaling behavior.

A practical method that can be used to estimate the generalized Hurst exponents called detrended fluctuation analysis (DFA) was introduced by Kantelhatrdt *et al.* (2002). These generalized exponents indicate the scaling behavior for the central moments of the time series appropriately scaled for various orders (both negative and positive). For example, the scaling of the standard deviation with time interval gives the Hurst exponent H_2. For a monofractal signal, the generalized Hurst exponents (H_q) have the same value for different q, whereas for a multifractal signal, the generalized Hurst exponents (H_q) have different values for different q. In DFA, we represent this variation in the generalized Hurst exponents through a Legendre transformation. Under the transformation, the variation in generalized Hurst exponent at different orders is represented as a spectrum of singularities $f(\alpha)$ where α is the conjugate variable corresponding to q. The width of the singularity spectrum gives the degree of multifractality in the signal.

In this work, we use MFDFA to study the multifractal characteristics of the pressure time series. However, the multifractal characteristics of the reconstructed phase space can also be analyzed as shown by Gotoda and coworkers (2012). They were able to identify the capacity dimension of the phase space by analyzing the multifractal spectrum corresponding to the phase space attractor. However, from an online detection and control point of view, MFDFA is superior since the length of the time series and the computational time required for the analysis is much lesser for MFDFA. This is due to the fact that we avoid phase space reconstruction while performing MFDFA. One drawback of using MFDFA is that we will not be able to identify the attractor characteristics (such as capacity dimension of the attractor) using such an analysis. However, this does not hinder our purpose of predicting an impending blowout. The main analysis presented in this chapter is based on MFDFA. Nevertheless, for the completeness of the study, in Appendix A, we compare the multifractal characteristics of phase space attractors representing combustion noise and a state prior to blowout.

Figure 3.3a shows the variation of the Hurst exponent (H_2, estimated from the pressure time series) with equivalence ratio as we approach blowout. The Hurst exponent for this study is estimated from the time series segments ranging from roughly 2 to 4 acoustic cycles. With this choice of range of segment length, we can ensure that we identify the transition of the signal from aperiodic to periodic nature (Nair & Sujith 2014). If we include segments of length less than 1 acoustic cycle, we will be unable to capture the periodicity at the onset of instability. However, for reliable results, guideline says that the lower bound for the segment length should be 2 acoustic cycles (Ihlen 2012, Nair & Sujith 2014). Also, if we were to include segments longer than 4 acoustic cycles, the

fluctuations will be averaged out and we will lose the important information about the scaling characteristics of the signal at faster time scales. From previous studies, it has been observed that a range of scales of 2 to 4 acoustic cycles is optimal for our analysis (Nair & Sujith 2014). The time series used for the analysis is 3s (30000 data points) long. Note that for all the different mass flow rates of fuel, the Hurst exponent approaches zero at the onset of instability and increases to a higher value at blowout. As we approach instability, the pressure signals become intermittent, with the region of periodicity getting longer (Nair *et al.* 2014) and at full blown instability, the pressure signals are sinusoidal in nature (Fig. 3.1). Since sinusoidal signals are not fractal and has an integer fractal dimension ($D = 2$), the Hurst exponent ($H = 2 - D$) for pressure signals during instability is zero (Nair & Sujith 2014).

As the equivalence ratio is reduced further from this point, the pressure fluctuation loses periodicity and as a result, near blow out, the Hurst exponent increases. This loss of periodicity of pressure fluctuations close to blowout could be attributed to the aperiodic flame extinction and reignition events that are present close to lean blowout. Such aperiodic nature of flame extinction and reignition events prior to blow out was observed by Nair (2006) and Muruganandam (2006). They observed that a burst of amplitude in the time series of acoustic pressure coincides with the spatially localized reignition events. Further, as the combustor approached flame blowout, they observed that the frequency of occurrence of aperiodic extinction and reignition events increased. This increase in aperiodic fluctuations near to blowout could be the reason why the Hurst exponent starts to increase close to blowout.

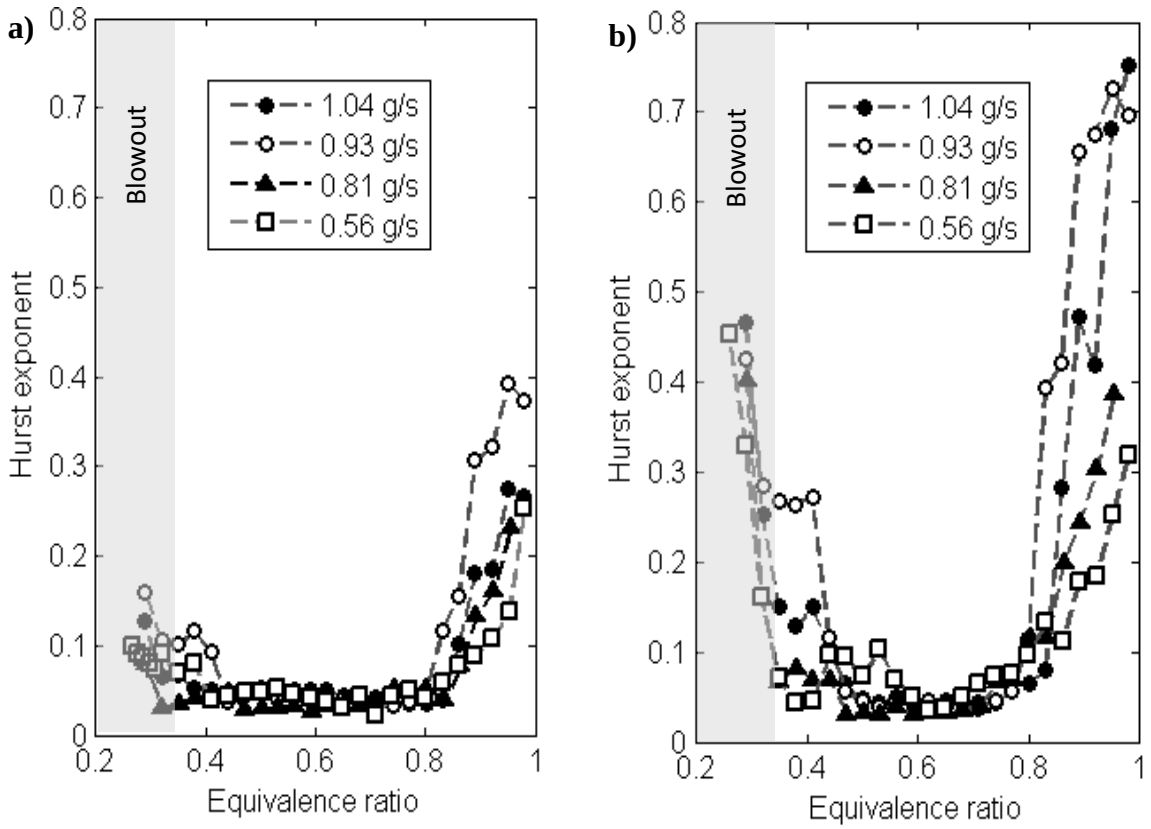

Figure 3.3: a) Variation in Hurst exponent, H_2 estimated based on pressure fluctuations with respect to variation in equivalence ratio. **b)** Variation in Hurst exponent estimated based on chemiluminescence with respect to variation in equivalence ratio. Note that the Hurst exponent reduces its value as we approach the instability and increases as we approach blowout. Hurst exponent for this study is estimated from the time series segments ranging from roughly 2 to 4 acoustic cycles.

In a similar manner, Fig. 3.3.b represents the Hurst exponents calculated from *CH** chemiluminescence intensity measurements measured in sync with the pressure measurements used in Fig. 3.3.a. For chemiluminescence measurements, the variations in the Hurst exponent with equivalence ratio have characteristics similar to that exhibited by the Hurst exponents estimated from unsteady pressure measurements. That is, as we reduce the equivalence ratio from one, initially the Hurst exponent reduces due to

increasing periodicity of the signals. Further, close to blowout, this periodicity is lost due to aperiodic flame fluctuations including extinction and reignition of the flame (Fig. 3.1) and hence the Hurst exponent increases. However, in the case of chemiluminescence measurements, this increase is more pronounced compared to that exhibited by pressure measurements. Close to blowout, the chemiluminescence signals have Hurst exponent approaching a value of 0.5.

However, near the stoichiometric ratio of air fuel mixture, the Hurst exponent obtained from chemiluminescence signal has value greater than 0.5, indicating a persistent nature. A time series is called persistent if a large value is in general followed by a large value and a small value is followed by a small value (Kantelhardt 2011). Persistent signals have slow evolving fluctuations (Ihlen 2012). From Fig. 3.4, we can infer that, near stoichiometric ratio of air fuel mixture ($Eq.\ Ratio = 0.96$), the chemiluminescence signal has fluctuations with longer timescales compared to that of corresponding pressure fluctuations. Here it is evident that the chemiluminescence signal has slow varying fluctuations compared to pressure fluctuations. It has been experimentally observed that flames can drive oscillations at frequencies corresponding to the subharmonics of the acoustic frequency (Bellows 2006). Such low frequency oscillations could be the result of hydrodynamic fluctuations (Nair & Sujith 2015). As a result of this, for a time series segments of length 2-4 acoustic cycles (the highlighted part of Fig. 3.4), the chemiluminescence signal exhibit a persistent behavior. Thus the Hurst exponent estimated based on chemiluminescence fluctuations for this operational condition has a value greater than 0.5.

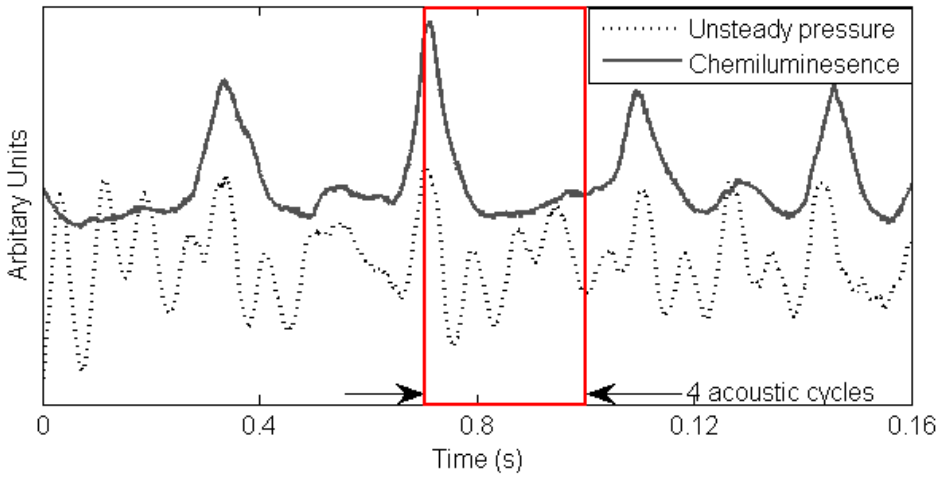

Figure 3.4: Pressure and chemiluminescence fluctuations near stoichiometry ($Eq.Ratio = 0.96$) for a fuel flow rate 1.04 g/s. Note that for 2 to 4 acoustic cycles, the chemiluminescence signal has persistent characteristics. This is because, here the timescales associated with flame fluctuations are longer than acoustic time scales since flame fluctuations have a frequency subharmonic to that of acoustic frequency.

In the previous paragraphs, we looked at the monofractal characteristics of pressure and chemiluminescence time series. Whereas, looking at the previous research (Nair & Sujith 2014), it is highly possible that the signals have multifractal characteristics. Hence, before drawing any conclusions, we need to study the multifractal characteristics of these fluctuations, to obtain a better understanding of the scaling characteristics and the complex nature of the time series. In the following section we will analyze the multifractal characteristics of the unsteady pressure and *CH** chemiluminescence time series.

3.3 Complexity in scaling: Multifractality

The Hurst exponents plotted in Fig. 3.3 indicates the scaling laws corresponding to H_2 (Hurst exponent of order 2). H_2 alone represents only the scaling behavior of the standard deviation of the fluctuations in time series. However, as explained in §3.2, a time series can exhibit multifractal characteristics where the scaling behavior depends upon the amplitude of the fluctuation. In other words, the scaling behavior for central moments of fluctuations varies depending upon the order of the central moment. Already, it is established that turbulent flows have a multifractal scaling behavior (Sreenivasan 1986) arising from the underlying multiplicative process of Richardson's energy cascade (Richardson 1922). Further, we know from recent research that combustion noise is amenable to a multifractal description (Nair & Sujith, 2014). Considering these findings, in this section, we investigate the multifractal nature of pressure and chemiluminescence fluctuations from the bluff body stabilized combustor. In particular, we study the multifractal characteristics of the system close to blowout.

In Fig. 3.5, we can see that when the combustor is operated near stoichiometric air-fuel ratio, the multifractal spectrum is broad. This indicates that the signal is multifractal and that there is an underlying multiplicative process in the system (Sreenivasan 1991, Schertzer & Lovejoy 2011).– As we increase the airflow rate and reach an equivalence ratio of 0.50, the combustor exhibits thermoacoustic instability. During thermoacoustic instability, both pressure and chemiluminescence signals are periodic and sinusoidal in nature. Here, since the fluctuations have sinusoidal nature, the multifractal spectrum collapses and the Hurst exponents becomes near zero for all orders.

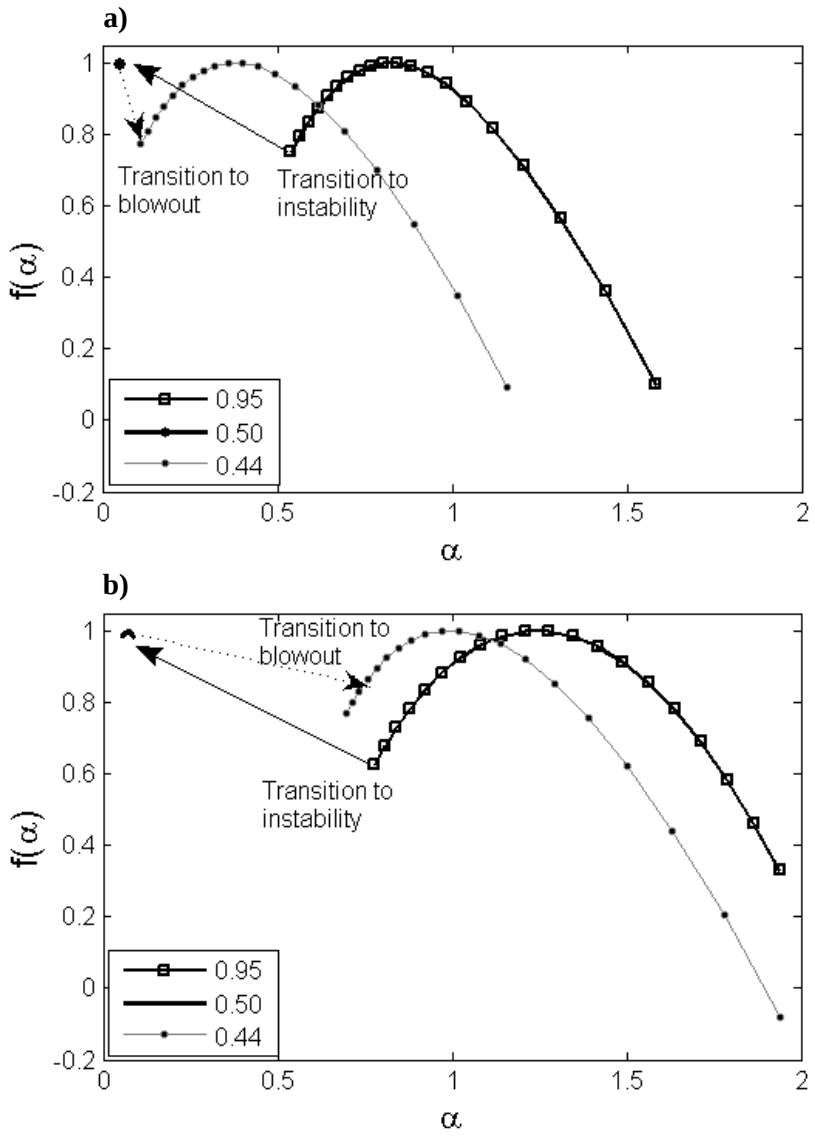

Figure 3.5: The multifractal spectrum for a bluff body combustor for 3 equivalence ratios (0.95, 0.50, 0.44) **a**) estimated based on unsteady pressure time series data, **b)** estimated based on corresponding chemiluminescence time series data. Here, the fuel flow rate is 0.93 g/s. In both cases, initially, the width of the multifractal spectrum decreases as we approach instability and becomes close to zero at instability. At leaner equivalence ratio, we do not have any thermoacoustic instability and we are closer to blowout limit, here the multifractal spectrum width increases. The multifractal spectrum is estimated for *q* ranging from -2 to 2.

However, as we increase the airflow rate further, the equivalence ratio reduces and we approach blowout. Prior to blowout, the multifractal spectrum becomes broader as compared to the multifractal spectra during thermoacoustic oscillations. This is because the signals prior to blowout are intermittent in nature and has a multifractal structure. It is to be noted that the multifractal spectrum is relatively narrower for the pressure signal for all equivalence ratios as compared to that of corresponding chemiluminescence fluctuations. This is due to the preferential amplification of pressure fluctuations close to frequency corresponding to the fundamental acoustic frequency of the combustor due to which the pressure fluctuations always tend to be relatively more periodic compared to the chemiluminescence fluctuation.

3.4 Approach to blowout in the absence of thermoacoustic instability

Till now, we discussed the approach to instability for a combustion system which exhibits thermoacoustic instability at lean equivalence ratios. Thermoacoustic instability can originate when the unsteady heat release rate fluctuations couples with the acoustic field in the combustor, establishing a positive feedback between the acoustic and the heat release fluctuations. Further, limit cycle oscillations are produced only if the acoustic energy added to the system is sufficiently high to balance the losses due to the damping present in the system. Hence a combustor might not exhibit thermoacoustic instability either when a positive feedback is not established, or when the acoustic energy added to the system is not adequate to overcome the acoustic energy lost due to damping in the system. Hence, it is important that we study the blowout behavior for such systems as well.

For this part of the study, we used the same combustor configuration as given in Fig. 2.1. We observe that, this configuration of the combustor does not exhibit thermoacoustic instability at low fuel flow rates (less than 0.4 g/s) due to reduced amplitude of the heat release rate fluctuations. Hence we study the dynamics of pressure and chemiluminescence oscillations at a fuel flow rate of 0.37 g/s. The experiment is performed by varying the airflow rate from a value corresponding to an equivalence ratio of 0.98, in discrete steps, until the flame blowout happens.

As we reduce the equivalence ratio from 0.98 in steps until blowoff, the pressure and *CH** chemiluminescence signals exhibit the following dynamics: Low amplitude aperiodic oscillations → intermittency → low amplitude aperiodic oscillations → blowout. This sequence is illustrated in Fig. 3.6. At equivalence ratio of 0.98, pressure and chemiluminescence signals have low amplitude and are aperiodic in nature. When the equivalence ratio is 0.67, the pressure and chemiluminescence signals exhibit intermittent oscillations where periodic fluctuations alternate with aperiodic fluctuations in an apparently random manner. Further, at an equivalence ratio of 0.38, both chemiluminescence and pressure fluctuations have low amplitude and are aperiodic.

Next, we analyze the multifractal characteristics of these oscillations. Figure 3.7 illustrates the variation of Hurst exponent (H_2) with equivalence ratio for a fixed fuel flow rate of 0.37g/s. We can see that even in this case where the system is not exhibiting instability, the Hurst exponent reduces in value as we approach lean equivalence ratios. At lean equivalence ratio, unsteadiness in the flame causes the heat release rate to fluctuate. As these fluctuations are confined within an acoustic resonator (the combustor), the resonator preferentially amplifies the fluctuations at frequencies close to its natural

frequencies (Chiu & Summerfield 1974, Strahle 1978, Hegde, Reuter & Zinn 1987). However, since the fuel flow rate is low, the unsteady heat release rate is not adequate to drive the system to sustained limit cycle oscillation. Nevertheless, as indicated before, at lean conditions, the signals exhibit intermittency where the signal switches from periodic to aperiodic fluctuations in an apparently random manner (Fig. 3.6b). As a result of intermittent oscillations, there is an increased periodicity in the signals at lean equivalence ratios compared to that near stoichiometric equivalence ratios. However, since the system does not transition to full-blown instability, the Hurst exponent calculated from both pressure and chemiluminescence fluctuations decreases to a value close to 0.2 as opposed to a value near zero in a condition where the system exhibits full-blown instability. Further, near to blowout, the pressure and chemiluminescence fluctuations lose their periodic nature (Fig. 3.7) due to aperiodic flame extinction and reignition resulting in an increase in Hurst exponent.

Another important aspect to be noted here is that the Hurst exponent estimated using both pressure and chemiluminescence time series has a value above 0.5 for equivalence ratios near to stoichiometry and near to blowout. As mentioned before, in this study, Hurst exponent is estimated from the time series segments ranging from roughly 2 to 4 acoustic cycles. This implies that if we have a time series with dominant frequency much less than the acoustic frequency, the signal will largely have persistent characteristics for 2 to 4 acoustic cycles.

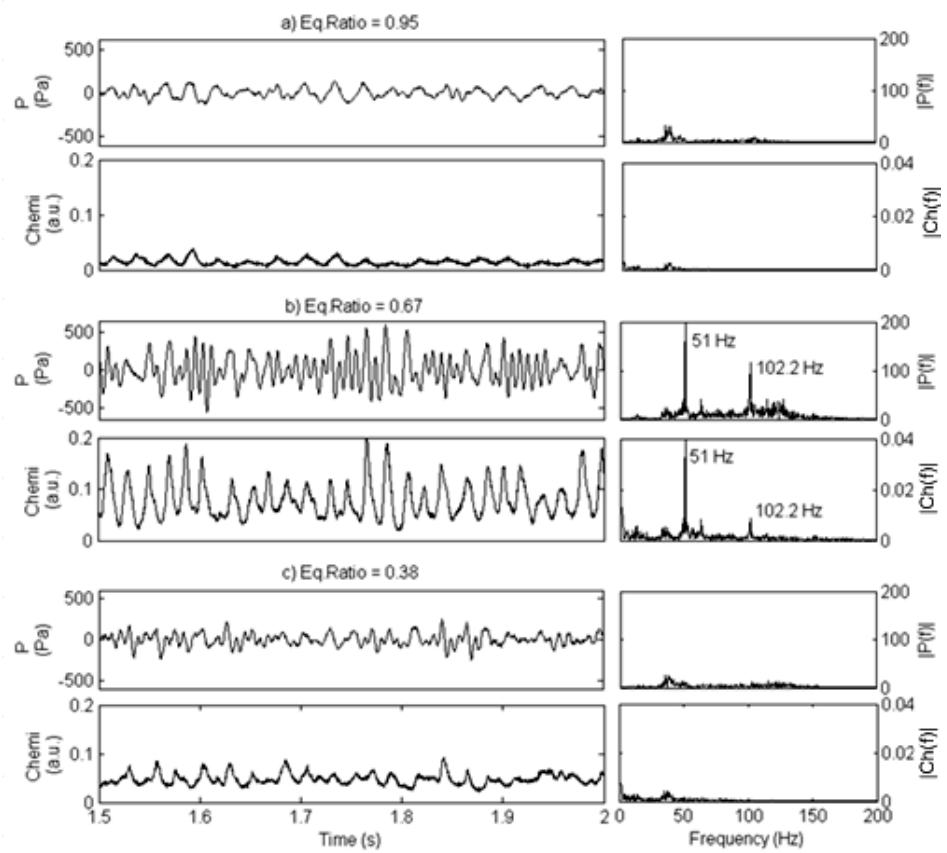

Figure 3.6: The time series and corresponding power spectra for unsteady pressure and *CH** chemiluminescence fluctuations for equivalence ratios of **a)** 0.95 ($Re = 0.44 \times 10^4$) **b)** (0.67 $Re = 0.63 \times 10^4$) and **c)** 0.38 ($Re = 1.10 \times 10^4$). Note that the frequency corresponding to the acoustic mode (fundamental frequency) of the combustor is around 102.2 Hz. Near stoichiometry and near to blowout, both pressure and *CH** chemiluminescence fluctuations does not have a major frequency component near the acoustic mode of the combustor. However, in between, at equivalence ratio of 0.67, the pressure and *CH** chemiluminescence fluctuations have a frequency component at the acoustic mode of the combustor. However, the dominant frequency is a subharmonic (51.0 Hz) of the frequency corresponding to the acoustic mode of the combustor (102.2 Hz). Further, pressure and chemiluminescence signals exhibit intermittency at equivalence ratio of 0.67. The bin size in calculating FFT was 0.3 Hz, and the time series used had 30000 data points.

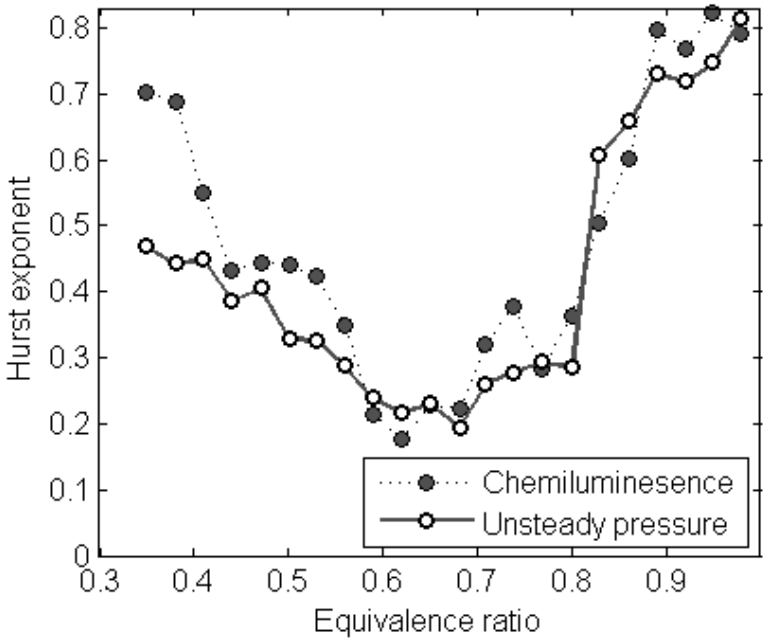

Figure 3.7: Variation of Hurst exponent with equivalence ratio. Here we can notice that even though the system does not transition to instability, the Hurst exponent (H_2, estimated based on both pressure and chemiluminescence signals for time series segments ranging from 2 to 4 acoustic cycles) reduces as we approach lean equivalence ratios and further increases close to blowout. Further, it should be noted that the Hurst exponents have value greater than 0.5 near stoichiometric equivalence ratios indicating that for 2 to 4 acoustic cycles both pressure and chemiluminescence signals have persistent behavior.

The power spectrum corresponding to pressure and *CH** chemiluminescence oscillations measured during near stoichiometric equivalence ratio combustion has a shallow peak at a frequency corresponding to the subharmonic of the acoustic frequency (Fig. 6a). The presence of this dominant low frequency (much lower compared to the acoustic frequency) component in the signal causes the estimated Hurst exponent to have a value greater than 0.5. The physical reason for presence of this subharmonic frequency requires

further understanding of the flow physics and the flame dynamics at this experimental condition and hence is beyond the scope of the present work. At equivalence ratio of 0.67, the oscillations exhibit frequency component corresponding to the acoustic mode of the combustor. However, even in this case, the dominant frequency is the subharmonic (51 Hz) of the frequency of acoustic mode (102.2 Hz) (Bellows 2006, Moeck 2009).

Figure 3.8 illustrates the variation in multifractal characteristics as we approach blowout. Here the multifractal spectrum does not shrink to a point as seen in Fig. 3.5. However, the spectrum width initially decreases as we reduce the equivalence ratio and increases close to blowout. This initial decrease can be attributed to the increase in periodicity of the time series at lean equivalence ratios, due to the appearance of intermittent periodic oscillations at lean conditions (Fig. 3.6b). Further, the preferential amplification of the pressure fluctuations at frequencies close to the natural frequency of the combustor leads to an increased periodicity in the acoustic signals as compared to that of the chemiluminescence signals. As a result, the multifractal spectrum estimated from the acoustic signals are relatively narrower as compared to that estimated from chemiluminescence signals for all equivalence ratios (Fig. 3.8).

From the analysis presented in this section, it is clear that even when the system does not transition to full blown instability, through the presence of intermittency, the system dynamics are affected by the acoustic scales at the lean conditions. Since prior to blowout, we observe intermittency in the time series (Fig. 3.6b), it is advisable to include the acoustic feedback mechanisms in models that predict blowout. Thus, while modeling the dynamics close to blowout, we need to consider the acoustic characteristics of the confinement (the combustor) to be able to capture the intermittent dynamics prior to

blowout. Further, including the acoustic field in the model may be critical for getting accurate estimates for the stability margin for lean blowout.

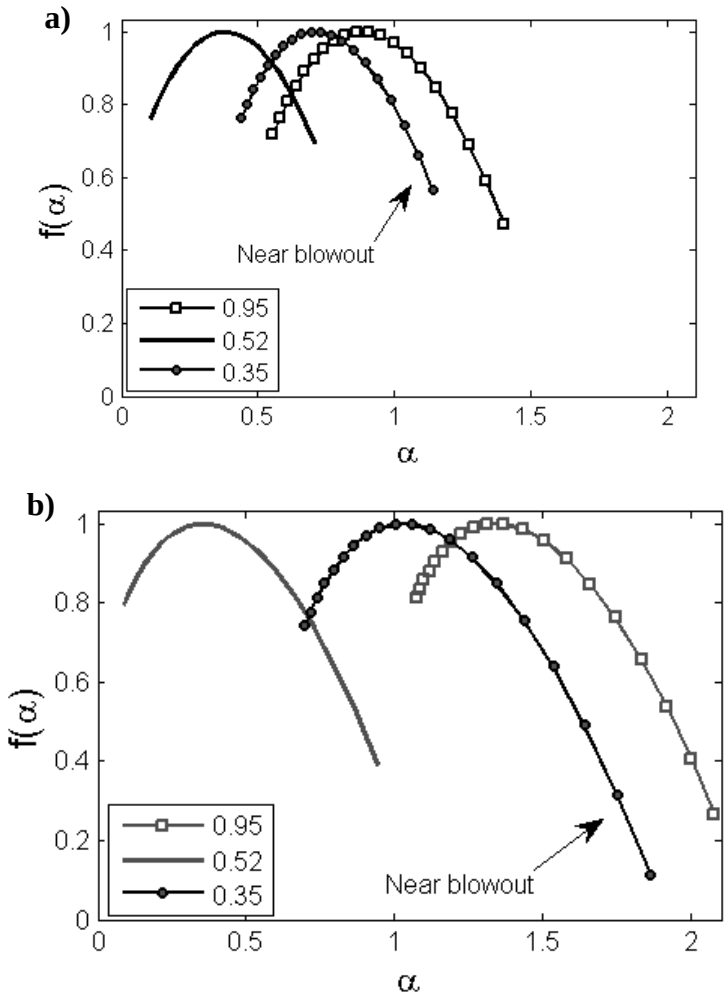

Figure 3.8: The multifractal spectrum for a bluff body combustor for 3 equivalence ratios (0.95, 0.52, 0.35) a) estimated based on unsteady pressure time series data, b) estimated based on corresponding chemiluminescence time series data. Here the fuel flow rate is 0.93 g/s. In both cases, initially, the multifractal spectrum width decreases as the equivalence ratio decreases. However, closer to blowout limit, the multifractal spectrum width increases. The multifractal spectrum is estimated for *q* ranging from -2 to 2.

Further, considering that blowout is indicated by an increase in Hurst exponent (in conjunction with a decrease in equivalence ratio) irrespective of whether or not the combustor exhibits instability, we suggest that the Hurst exponent could be used as a precursor to detect an impending blowout (Unni, Nair & Sujith 2014). Since Nair and Sujith (2014) has already shown that Hurst exponent can be used as a precursor to instability (Hurst exponent approaching a value close to zero is indicative of onset of instability), we conclude that Hurst exponent can be used as the single precursor which could detect both an impending blowout and an impending thermoacoustic instability.

3.5 Multifractal nature of phase space

In previous section, we used Multifractal detrended fluctuation analysis (MFDFA) to analyze the fractal nature of pressure and chemiluminescence fluctuations. However, analyzing the fractal nature of the attractors corresponding to the pressure fluctuations could also give some insights into the structure of phase space attractor corresponding to the dynamics. In this appendix, we will compare the multifractal spectrum corresponding to the phase space attractors reconstructed from a pressure time series obtained prior to blowout (*Eq. Ratio* 0.27, in Fig 3.1) and combustion noise close to stoichiometric combustion (*Eq. Ratio* 0.95, in Fig. 3.1).

We use the method detailed by Harikrishnan *et al.* (2008) to obtain the full multifractal spectrum representing the phase space attractor. We observe that the multifractal spectrum corresponding to either state is similar, suggesting that the multifractal characteristics are similar for both states. Thus this indicates that multifractal spectrum

characteristics alone cannot distinguish between combustion noise and oscillations prior to blowout.

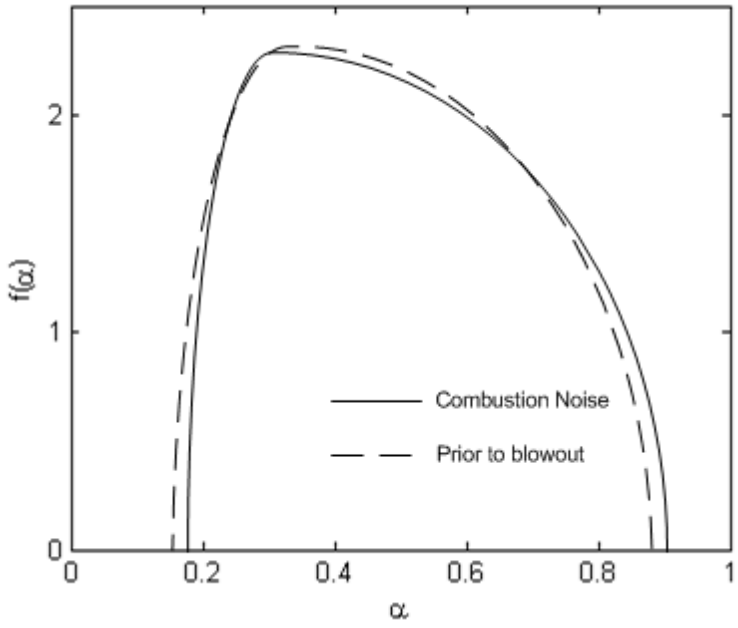

Figure 3.9: The multifractal spectrum for combustion noise (*Eq. Ratio* 0.95, in Fig.3.1) and a state prior to blowout (*Eq. Ratio* 0.27, in Fig. 3.1). We can see that both spectrums are similar indicating that phase space attractor for both combustion noise and the state prior to blowout have similar multifractal characteristics. Here the time series were embedded in 3 dimensional phase space prior to the multifractal analysis.

We chose MFDFA over this method to analyze the multifractal characteristics since MFDFA is faster in terms of computation and can work with much shorter time series (details explained in § 3.2). Further, another aspect that need to be highlighted here is that the phase space corresponding to the attractor has high dimension close to blowout and during combustion instability. Hence, analyzing the multifractality by reconstructing a phase space having lower dimension (3 in this case, also in Gotoda *et al.* (2012)) is disputable. However, embedding the time series in a high dimensional phase space

increases the complexity in computation of the multifractal spectrum and hence makes this method unsuitable for any online precursor detection system.

3.5. Concluding remarks

In this chapter, we investigated the multifractal characteristics of *CH** chemiluminescence fluctuations and pressure fluctuations measured from a turbulent combustor. It was observed that when transition to blowout happens through thermoacoustic instability, the Hurst exponent (estimated both from *CH** chemiluminescence signals and pressure signals) initially approaches close to zero at instability and further increases near blowout. Also, the multifractal spectrum (estimated both from *CH** chemiluminescence signals and pressure signals) that is wide at near-stoichiometric combustion, shrinks to a point at instability and broadens close to blowout. Further, even in an alternative scenario when the transition from stoichiometric combustion to blowout occurred with combustor not exhibiting thermoacoustic instability, we observed that the Hurst exponent (estimated both from *CH** chemiluminescence signals and pressure signals) initially decreases and then increases close to blowout. However, in such a situation, the Hurst exponent does not reduce to a value close to zero. In a similar manner, here the multifractal spectrum width (estimated both from *CH** chemiluminescence signals and pressure signals) reduces initially and then increases close to blowout. However, it does not shrink to a point as in the former case. The presence of intermittency prior to blowout in either case was suggested as the cause for these observed behaviors. The multifractal nature of the pressure and *CH** chemiluminesence signals prior to blowout suggests the complexity in the scaling

behavior of these time series. Considering this complexity in dynamics prior to blowout, we provide a framework based on the multifractal characteristics of pressure and chemiluminescence fluctuations describing blowout as a dynamic instability. Further, within this framework, we saw that when an increase in Hurst exponent is observed in conjunction with a decrease in equivalence ratio, we can identify that we are approaching an impending blowout. Thus, with this study, we were able to suggest a unified framework based on multifractality, within which we can analyze dynamics of both combustion instability and blowout.

CHAPTER 4

Dynamic characteristics of oscillations leading to lean blowout

Pressure and chemiluminesence fluctuations exhibit complex scaling behavior prior to an impending blowout. In previous chapter, we systematically characterized this scaling behavior. In this chapter, we study the various dynamics exhibited by a turbulent combustor as we start from stable combustion at stoichiometric equivalence ratio and approach lean blowout by reducing the equivalence ratio in discrete steps. We use recurrence plots and recurrence quantification analysis to classify different dynamic regimes and thereby characterize the path to blowout. We also show that the parameters used for recurrence quantification can further be used as precursors to blowout. In this chapter, as in chapter 3, we present two different paths to blowout depending upon the power level of the combustor. At higher power levels (high fuel flow rate), as we lower equivalence ratio by increasing the air flow rate, the combustor exhibits thermoacoustic instability prior to flame blowout. In contrast, when the power level is low (low fuel flow rate), as the equivalence ratio is lowered by increasing the air flow rate, the combustor exhibits no thermoacoustic instability prior to flame blowout.

After identifying the path to blowout, we then proceed to identify the type of intermittency present prior to blowout. In the parlance of dynamical system theory, intermittency is a dynamic state where the system switches between a chaotic attractor to a periodic attractor or between two chaotic attractors (Strogatz 2001). In the case of

turbulent combustors, as mentioned before, the observed intermittency is a switch between aperiodic low amplitude fluctuations and periodic high amplitude fluctuations. In general, intermittency is observed in a dynamic system close to a bifurcation point. The type of bifurcation characterizes the nature of intermittent dynamics. In the context of transition from a laminar state to a turbulent state, Pomeau and Manneville (1980) classified intermittency into 3 types based on the underlying bifurcation in the system. In this classification, an intermittent state could be Type I, Type II and Type III, depending upon the corresponding bifurcation being saddle node, subcritical-Hopf or inverse period doubling. They also detailed the characteristic features of each type of intermittency. Identifying these features, one can identify the type of intermittency from a time series obtained from experiments. With the knowledge of the type of intermittency, one can validate models that describe the transition to blowout by comparing the types of intermittency obtained from high fidelity models and that obtained in the experiments. Using the statistics of intermittency, we can determine the proximity the transition. The layout of the rest of the chapter is as follows. In § 4.1 we describe the essential mathematical tools required for recurrence quantification analysis. Section 4.2 details the results obtained from this study. The major conclusions from the study are given in § 4.3.

4.1 Recurrence Quantification Analysis

Time series of state variables measured from combustors exhibit various nonlinear characteristics. Recurrence quantification analysis (RQA) is a powerful tool that can be used to analyze such nonlinear time series. In RQA, we quantify the recurrent behavior of the state of a dynamical system in its phase space (Marwan *et al.*, 2002). By identifying the recurrent behavior, one can analyze the dynamic state of the system.

The first step in RQA is constructing the phase space corresponding to the dynamical state of the system. Phase space is a multidimensional space where all possible states of the system are represented (Takens 1985). The state point, representative of a particular state of the system evolves in the phase space as time progresses. A phase space has n dimensions if n dynamic variables are required to completely describe the state of a system. However, often in our experiments we have access only to one (or a few) state space variables that is measured. In this particular study, we measure the unsteady pressure within the combustor.

For such a situation, Takens (1985) introduced a method of reconstructing the mathematical phase space from a single measured time series, $X(t)$. This method of reconstructing the phase space is known as delay-embedding (Abarbanel *et al.* 1993). In order to reconstruct the phase space, we need to obtain two important parameters: the embedding dimension (d) and an optimal time delay (τ). Optimal time delay (τ) is used to construct d time delayed vectors, $X(t), X(t+\tau), X(t+2\tau) \ldots X(t+(d-1)\tau)$ each representative of one of the state variable of the system. The embedding dimension is representative of the dimension of the phase space corresponding to the dynamics of the system. Using the *d* time delayed vectors, we construct the *d*-dimensional phase space. In this work, we choose the delay corresponding to the first minima of the average mutual information of $X(t)$ as the optimal time delay (Abarbanel *et al.* 1993) and the embedding dimension (d) is obtained using the false nearest neighbor method (Abarbanel *et al.* 1993, Cao 1997). This method of nonlinear time series analysis was introduced in thermoacoustics by Kabiraj *et al.* in their study of route to chaos for a thermoacoustic system (Kabiraj *et al.* 2010).

Once the phase space is reconstructed, we will construct a recurrence plot (RP) corresponding to the dynamics of the system. Recurrence plot is a plot between time (t) and time (t'). It indicates those times (t') for which the state point visits roughly the same volume of the phase space as it was at a particular time (t). Let P_i be the position of the state point in the phase space at i^{th} instant of time; i.e. t_i. Then, we can construct a recurrence matrix (R_{ij}) such that,

$$R_{ij} = \theta\left(\varepsilon - \left\|P_i - P_j\right\|\right) \quad i, j = 1, 2, \dots N \tag{4.1}$$

This implies, if P_j lies inside the d dimensional sphere of radius ε centered around P_i, R_{ij} is one. Otherwise, R_{ij} is zero. Recurrence plot is a graphical representation of the recurrence matrix (R_{ij}) where a value of one is represented in the graph by a black dot and a value of zero is represented by a white dot. Depending upon the recurrent characteristics of the system, a recurrence plot exhibits different spatial patterns. For instance, a periodic signal has an RP with equally separated parallel lines. If the RP has isolated points and short diagonal lines, the corresponding state does not have any long time recurrent behavior and is either a chaotic state or a random state. Once the recurrence plot is constructed, we perform recurrence quantification analysis by defining meaningful statistical measures representative of the distribution of black points in the recurrence plot. In this chapter, we use three different measures to analyze the recurrence characteristics; recurrence rate, entropy of diagonal lines and trapping time. Recurrence rate (RR) measures the density of black points in the recurrence plot and hence is given by,

$$RR = \frac{1}{N^2} \sum_{i,j=1}^{N} R_{ij}$$

Entropy ($ENTR$) represents the Shannon entropy of the distribution of diagonal line lengths ($p(l)$) in the recurrence plot and is given by,

$$ENTR = \sum_{l=l_{min}}^{N} p(l) \ln\big(p(l)\big)$$

Trapping time (τ) is the average length of vertical lines (here, we normalize it with the maximum possible length of a vertical line) and is given by,

$$\tau = \frac{\sum_{v=v_{min}}^{N} vP(v)}{N \sum_{v=v_{min}}^{N} P(v)}$$

We can compare different dynamical states by comparing the recurrence plots or the statistical quantities (*RR*, *ENTR* and τ) estimated from them. However, the characteristics of the recurrence plots and the recurrence quantities would depend upon the manner in which the value of ε is chosen to construct the recurrence plots corresponding to different dynamic states. Here, for recurrence quantification analysis (RQA), the value of ε is chosen to be fixed for different dynamical states and is equal to the size of the phase space attractor corresponding to the aperiodic pressure fluctuations during stoichiometric combustion. The details of the logic behind this choice of ε for RQA is given in §IV. However, with such a choice of ε, during combustion at stoichiometric equivalence ratio, the state points corresponding to all times would be within the d-dimensional sphere of radius ε centered around a state point corresponding to any particular time instant. In other words, in the phase space any state point is within the neighborhood of any other

state points. This implies, the corresponding recurrence plot will be entirely filled with black points. Thus any information about the structure of the attractor is lost. The only information captured is that the entire attractor can be confined within a d-dimensional sphere of radius, ε.

On the other hand, in order to visualize the structure of attractor using RPs, the value of ε is chosen to be equal to 0.1σ, where σ is the standard deviation of all the distances between different state points in the phase space. This ensures that the neighborhood defined by the d-dimensional sphere of radius ε contains only part of the phase space attractor and hence the information about the structure of the attractor is preserved in the corresponding RP.

4.2 Recurrence characteristics of pressure fluctuations

The experiments described in this chapter were conducted at two different fuel flow rates 1.04 g/s (28 SLPM) and 0.56 g/s (10 SLPM). For each fuel flow rate, the air flow rate is varied from a value corresponding to stoichiometric equivalence ratio to leaner equivalence ratios in discrete steps until the flame blows out. At each equivalence ratio, we measured the acoustic pressure within the combustor. As the equivalence ratio is varied, we observed various temporal patterns in the time series of unsteady pressure. In this chapter, we analyze these patterns and the corresponding dynamics using recurrence plots (RP), in order to identify various dynamics of the pressure oscillations as we transition from stoichiometric combustion to blowout in turbulent combustors. We observe that when the fuel flow rate is high, as the equivalence ratio is reduced by increasing the air flow rate, the system exhibits thermoacoustic instability prior to blowout. In contrast, at low fuel flow rate, as we approach lean equivalence ratio, no thermoacoustic instability is encountered prior to flame blowout.

4.2.1 Approach to blowout: High fuel flow rate

In Fig. 4.1 we plot the time series of unsteady pressure acquired at different equivalence ratios for the case of high (1.04 g/s or 28 SLPM) fuel flow rate. Near stoichiometry, the pressure oscillations are aperiodic and have low amplitude (Fig. 4.1.a). The corresponding recurrence plot has a grainy structure (Fig. 4.2.a) indicating that the system does not exhibit any recurrent behavior (recurrence parameters used are $\varepsilon = 0.1\sigma$ and $d = 9$ for Fig. 4.2).

When the equivalence ratio is reduced to 0.77, the oscillations exhibit intermittent behavior where high amplitude periodic oscillations alternate between low amplitude aperiodic oscillations in an apparently random manner (Fig. 4.1.b). The corresponding recurrence plot exhibits rectangular black patches (Fig. 4.2.b) of apparently random dimensions and intervals. These rectangular patches indicate that the state is trapped in a small volume of the phase space for a long period of time, randomly leaves this volume and again comes back to the same part of the attractor. When the state point escapes from this part of the attractor, it reaches a periodic orbit. This is indicated by the lines parallel to the diagonal line of the recurrence plot extending from the black rectangular patches present in the recurrence plot (Fig. 4.2.f). Such a trajectory of the state point is called a homoclinic orbit. On further reduction of equivalence ratio to 0.53, we observe thermoacoustic instability where the unsteady pressure fluctuations have high amplitude and are periodic (Fig. 4.2.c). In the RP, the periodicity of pressure fluctuations during thermoacoustic instability is captured by the lines parallel to the diagonal line of RP (Fig. 4.2.c).

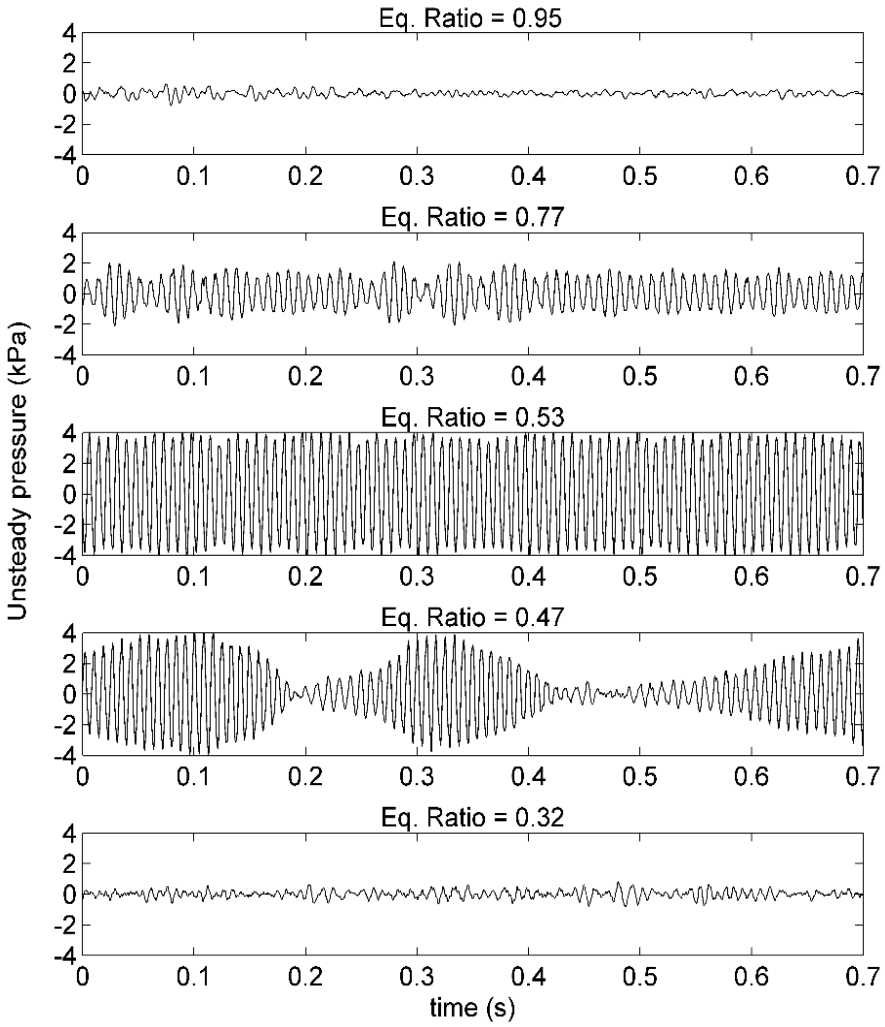

Figure 4.1: Time series of unsteady pressure obtained at different equivalence ratios. a) Near stoichiometric combustion (equivalence ratio of 0.95), the oscillations are aperiodic with low amplitude. b) At an equivalence ratio of 0.77, we observe intermittency prior to instability. c) When the equivalence ratio is 0.53, we observe instability. d) Further, at equivalence ratio of 0.47 we observe intermittency prior to blowout. e) When the equivalence ratio is 0.32, we have low amplitude aperiodic oscillations. On further reduction in equivalence ratio, the flame blows out.

Once the equivalence ratio is reduced to 0.47, the system starts to exhibit intermittency prior to blowout (Fig. 4.1.d). Here, high amplitude periodic fluctuations alternate between

low amplitude aperiodic oscillations. The corresponding recurrence plots exhibit rectangular patches indicating intermittency (Fig. 4.2.d). On further reduction of equivalence ratio, the amplitude of the periodic part of the intermittent oscillations reduces (Fig. 4.1.e). However, the RP still has rectangular black patches (Fig. 4.2.e). On further reduction of equivalence ratio, the flame blows out.

Figure 4.3.a represents the variation of the root mean square of the acoustic pressure (P_{rms}) with equivalence ratio. Here the fuel flow rate is 1.04 g/s. We observe that the P_{rms} increases as we approach thermoacoustic instability and then decreases as we approach blowout. Figures 4.3.b, 4.3.c, 4.3.d represent the variation of different recurrence quantities with equivalence ratio. As explained in § 4.1, in order to perform RQA (ε = 400 Pa, $d = 9$), for all the parameter locations, we have chosen the value of ε to be constant and roughly equal to the size of the phase space attractor corresponding to the aperiodic oscillations during stable combustion at stoichiometric equivalence ratios. By choosing ε in this manner, we will be able to quantify the intermittent oscillations (in other words, the dynamics of the state point in the homoclinic orbit) and hence predict dynamic transitions in the combustor.

The recurrence rate (*RR*), the density of black points in the RP represents the recurrent behavior of the system. During, the occurrence of combustion noise, the amplitude of oscillations is low and hence the phase space is confined to a smaller volume compared to that during thermoacoustic instability. Since the radius of the ε-ball used to construct RP is constant for different parameter locations, during low amplitude aperiodic oscillations, the system is highly recurrent (most of the phase space is covered by the ε-ball). Whereas, during thermoacoustic instability, the trajectory of state point covers a

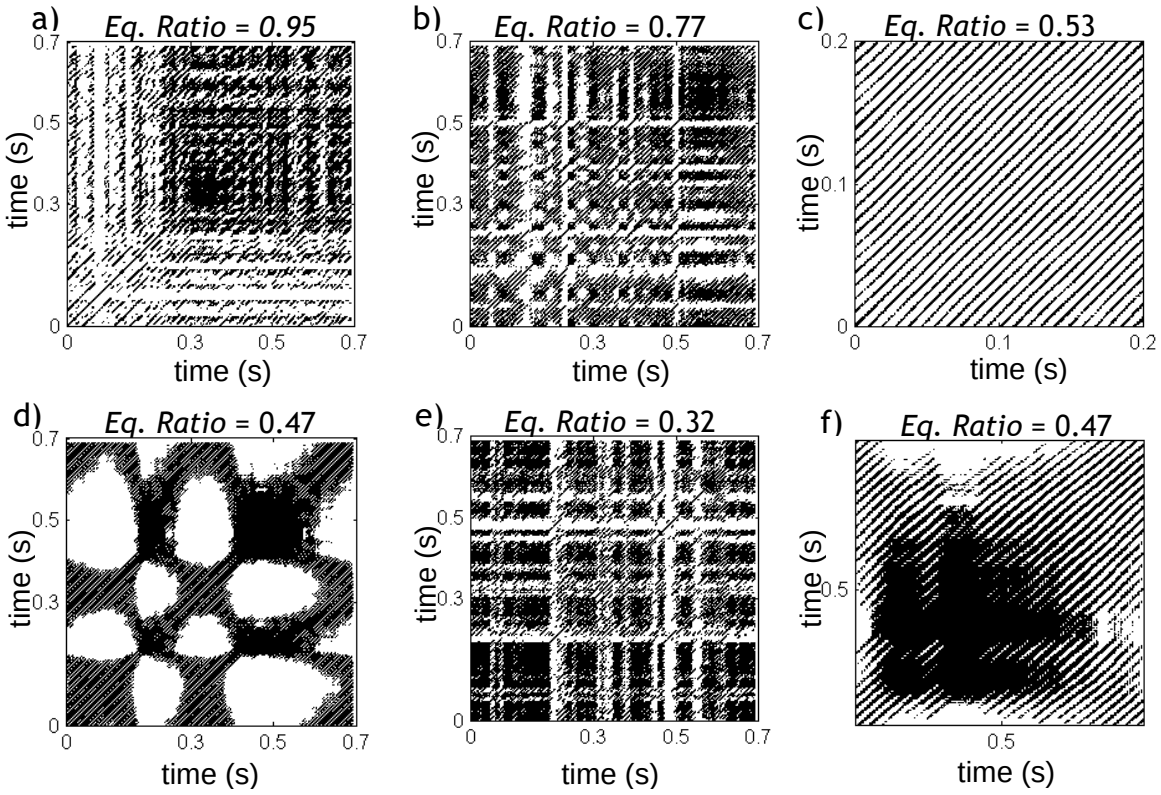

Figure 4.2: Recurrence plots corresponding to pressure fluctuations at different equivalence ratios presented in figure 1. a) When the equivalence ratio is 0.95, the recurrence plot shows grainy structure indicating aperiodic oscillations. b) At an equivalence ratio of 0.77, we observe intermittency where RP shows black rectangular patches. c) The recurrence plot corresponding to periodic oscillations at an equivalence ratio of 0.53. Note that the RP has lines parallel to the main diagonal. d) RP corresponding to intermittency prior to blowout. e) Recurrence plot of aperiodic oscillations prior to blowout. f) Zoomed in image of RP during intermittency (figure 3e). Note that the black patch represent the aperiodic fluctuations and the parallel lines emerging from the black patch represent the periodic motion of state point in the phase space.

larger volume in the phase space and hence is less recurrent. Following the above argument, in Fig. 4.3.b we observe that *RR* reduces as we approach thermoacoustic

instability and increases close to blowout. The increase of *RR* prior to blowout can be attributed to the aperiodicity and low amplitude of the pressure oscillations before blowout causing the corresponding attractor to cover less volume in the phase space.

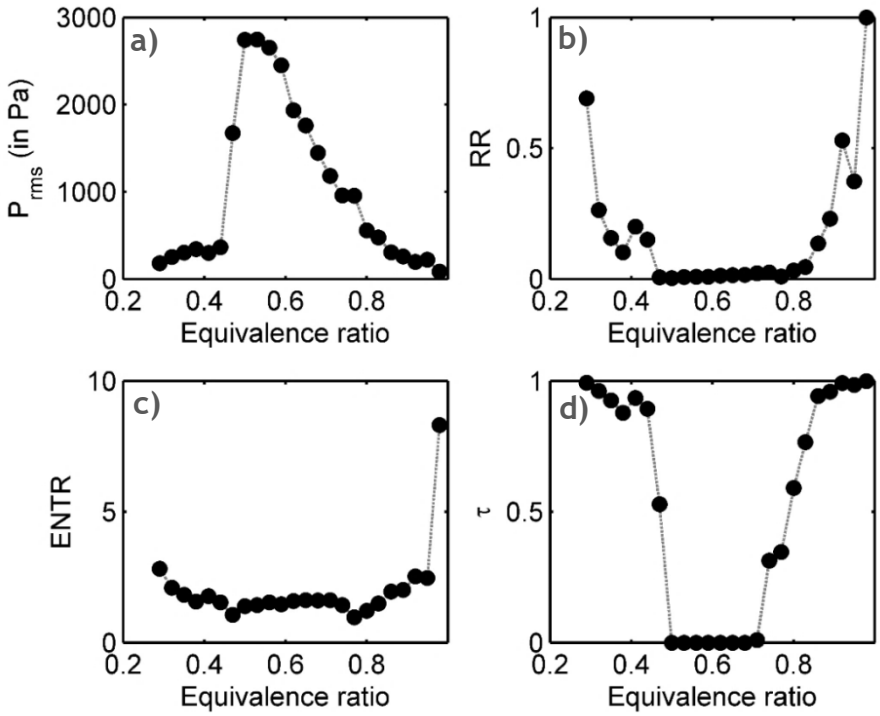

Figure 4.3: Variation in a) Prms, b) recurrence rate (*RR*), c) entropy (*ENTR*) and d) trapping time (τ) as equivalence ratio is varied from stoichiometry to blowout. We can observe that as the system approaches blowout, *ENTR*, *RR* and decreases initially as we approach periodic oscillations towards zero and increases close to blowout.

Entropy is a measure representing the Shannon entropy of lines parallel to the diagonal of an RP. During aperiodic oscillations *ENTR* is high. During periodic oscillations the RP has a regular structure (lines trsaparallel to the diagonal) and hence *ENTR* is low. Thus in Fig. 4c, we can see that *ENTR* decreases as we approach thermoacoustic instability and increases close to blowout. The trapping time (τ) is the average length of vertical lines in

the recurrence plot. A vertical black line in an RP indicates that the state of the system is trapped in a small volume of the phase space for a long time. This happens when the system exhibits low amplitude chaotic oscillations. Since close to blowout, the dynamics is dominated by low amplitude aperiodic oscillations, as the system transits from combustion noise to thermoacoustic instability, τ initially reduces due to the appearance of large amplitude oscillations and increases close to blowout (Fig. 4.3.d) due to the low amplitude oscillations.

4.2.2 Approach to blowout: Low fuel flow rate

When the fuel flow rate is low (0.56 g/s), the combustor is unable to sustain a full blown thermoacoustic instability. In such a case, we do not observe thermoacoustic instability before blowout. In Fig. 4.4, we plot the pressure fluctuations at different equivalence ratios. In Fig. 6, we present the corresponding recurrence plots (here, $\varepsilon = 0.1\sigma$, where σ is the standered deviation for the time series and $d = 9$). Near stoichiometric equivalence ratio, the pressure fluctuations have low amplitude and are aperiodic (Fig. 4.4.a). The corresponding recurrence plot has no specific patterns. When the equivalence ratio is further reduced, the combustor exhibits intermittency in the pressure fluctuations. Here, high amplitude periodic oscillations alternate with low amplitude aperiodic oscillations. The corresponding recurrence plots show rectangular black patches. The black patch in this recurrence plot represents those times during which the trajectory is trapped within the chaotic part of the attractor and the white bands represent the times for which the trajectory leaves the chaotic attractor to follow the trajectory corresponding to the periodic oscillations. On further reduction of equivalence ratio to 0.35, we have low

amplitude aperiodic oscillations. For this case, the corresponding RP is has a grainy structure.

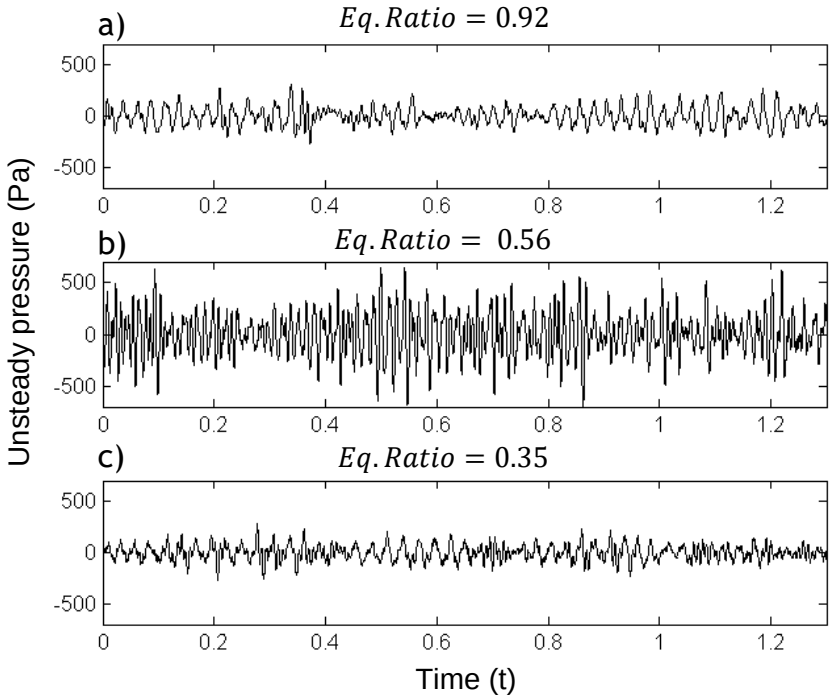

Figure 4.4: Time series of unsteady pressure obtained at different equivalence ratios when the fuel flow rate is 0.56 g/s. a) Near stoichiometric combustion (equivalence ratio of 0.92), the oscillations are aperiodic with low amplitude. b) At an equivalence ratio of 0.56, we observe intermittency. c) Further, when the equivalence ratio is 0.35, we have low amplitude aperiodic oscillations. On further reduction in equivalence ratio, the flame blows out. Note that at this fuel flow rate, the system did not exhibit thermoacoustic instability at fuel lean operating conditions.

On performing recurrence quantification analysis (ε = 150 Pa and $d = 9$), we observe that as the equivalence ratio is varied, even in a case where the system does not encounter thermoacoustic instability at lean equivalence ratios, the recurrence parameters (*RR*, *ENTR*, τ) vary in a similar manner as it varied for the case where the system encounters

thermoacoustic instability at lean conditions. *RR*, *ENTR* and τ decreases initially and increases close to blowout (Fig. 4.6). However, the reduction in the recurrence measures here is less compared to that in Fig. 4.3. In Fig. 4.3.b and 4.3.d, *RR* and τ approach very near to zero during thermoacoustic instability, whereas in Fig. 4.6.b and 4.6.d, the minimum value of *RR* is 0.18 and that of τ is 0.73.

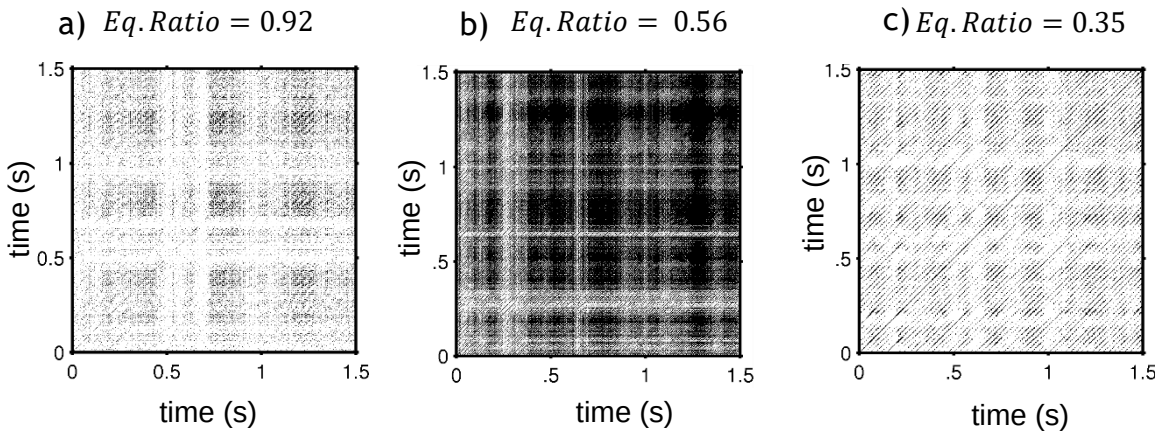

Figure 4.5: Recurrence plots corresponding to pressure fluctuations at different equivalence ratios presented in figure 1. a) When the equivalence ratio is 0.92, the recurrence plot show grainy structure indicating aperiodic oscillations. b) At equivalence ratio of 0.56, we observe intermittency where RP shows black rectangular patches. c) Recurrence plot corresponding to aperiodic oscillations at equivalence ratio 0.35. Note that at this fuel flow rate, the system did not exhibit thermoacoustic instability at fuel lean operating conditions.

Analysis of the recurrence of state point in the phase space helps us identify the dynamic characteristic of the system and further give precursors to impending transitions in the dynamical state. However, since such an analysis involves phase space reconstruction prior to recurrence quantification, and hence is rather computationally intensive. Online prognosis of dynamic transitions in real engine demands methodologies that are

computationally less taxing. Considering this, in next section, we propose adopting a methodology of recurrence quantification analysis that does not involve phase space reconstruction and is nevertheless capable of predicating an impending blowout and thermoacoustic instability.

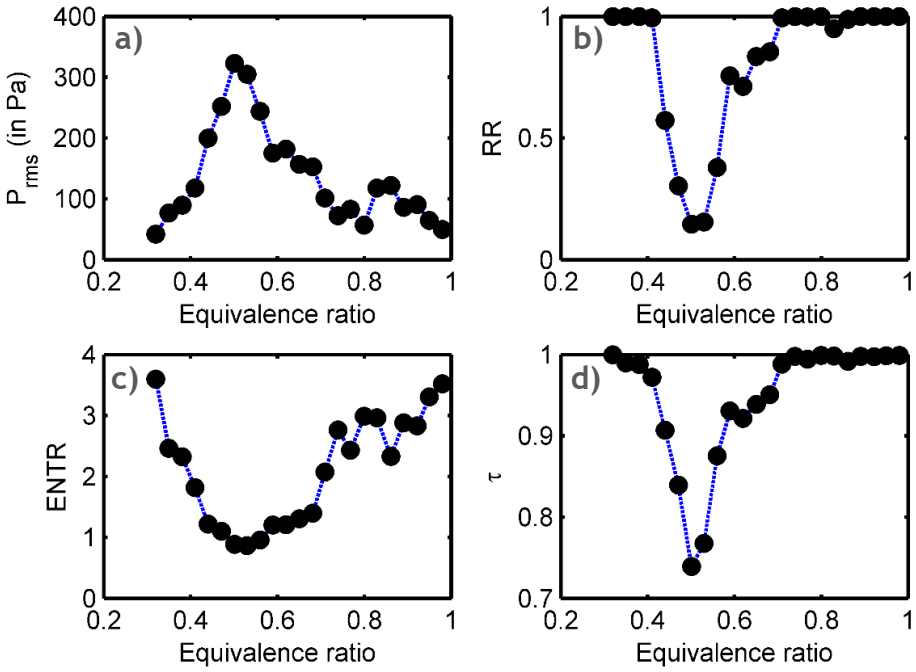

Figure 4.6: Variation in a) Prms, b) recurrence rate (*RR*), c) entropy (*ENTR*) and d) trapping time (τ) as equivalence ratio is varied from stoichiometry to blowout. We can observe that as the system approaches blowout, *ENTR, RR* and decreases initially and increases close to blowout.

4.3 Recurrence analysis with no phase space embedding

The methodology of RQA was first introduced by Iwanski and Bradley (1998). They showed that a recurrence plot that is constructed without embedding the time series in a *d*-dimensional phase space is able to capture the dynamic transitions in a system. In this case, recurrence is considered to have happened at the point (t_i, t_j) in the recurrence

plot, if $X(t_j)$, the value of the time series at time *t*, is within the range $(X(t_i) - \varepsilon, X(t_i) + \varepsilon)$. That is, equitation 2.1 modifies as,

$$R_{ij} = \theta\left(\varepsilon - \left|X_{t_i} - X_{t_j}\right|\right) \quad i, j = 1,2, \dots N \tag{3.1}$$

Here, instead of analyzing the structure of the phase space, we look at the patterns in the time series. Once the recurrence plot is constructed in this manner, recurrence quantification is performed as detailed in §2. The variation of $RR, ENTR$ and τ estimated from recurrence plots constructed without phase space embedding are given Fig. 9 and 10. Figure 9 indicates the variation for the case of high fuel flow rate (1.04 g/s, ε = 400 pa). We can see that trends observed in this case is similar as that of in Fig. 4. As blowout is approached both RR and τ approach 1. Further, $ENTR$ increases close to blowout. We also observe that the increasing trends for the parameters RR, τ and $ENTR$ starts at around same parameter location for both Fig. 4 and 9. We also observe that the method of RQA without embedding is similarly effective even in the case of low fuel flow rate (Fig. 10 where ε = 150 pa).

Similarities in the trends observed in the RQA of the phase space and of the value of the time series is due to the peculiar nature of the phase space attractor during intermittent pressure oscillations. During intermittency, the state point remains near to the center of the d-dimensional phase space during aperiodic oscillations (i.e., when the value of the pressure fluctuations is close to zero) and go away from the center while the pressure time series exhibits high amplitude periodic oscillations. When the amplitude of oscillation is low and the state point is close to the origin, the probability of recurrence is high both in the phase space and in the amplitude of the pressure fluctuations.

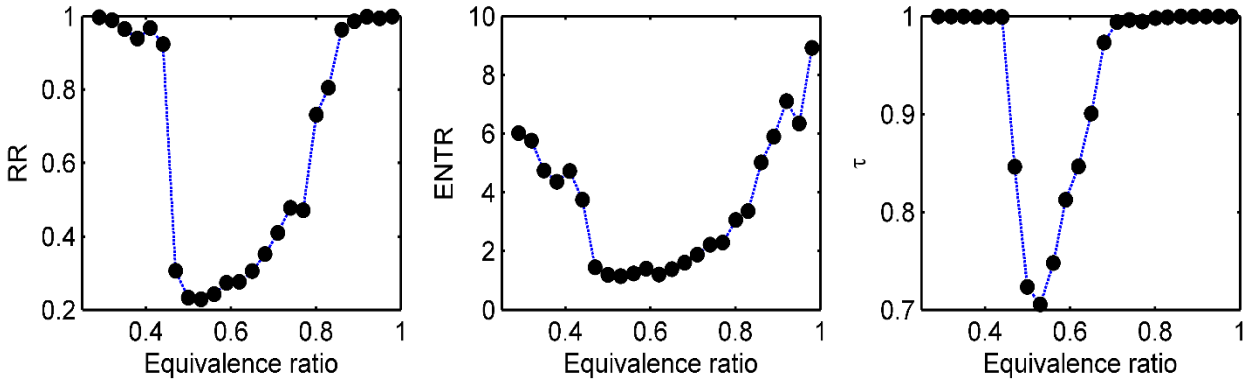

Figure 4.7: Plot of *RR*, *ENTR* and τ for RQA performed without embedding the dynamics in the phase space. The fuel flow rate here is 1.04 g/s. The system encounters thermoacoustic instability at low equivalence ratios as lean blowout is approached. We can observe that as the system approaches blowout, *ENTR*, *RR* and decreases initially as we approach periodic oscillations towards zero and increases close to blowout.

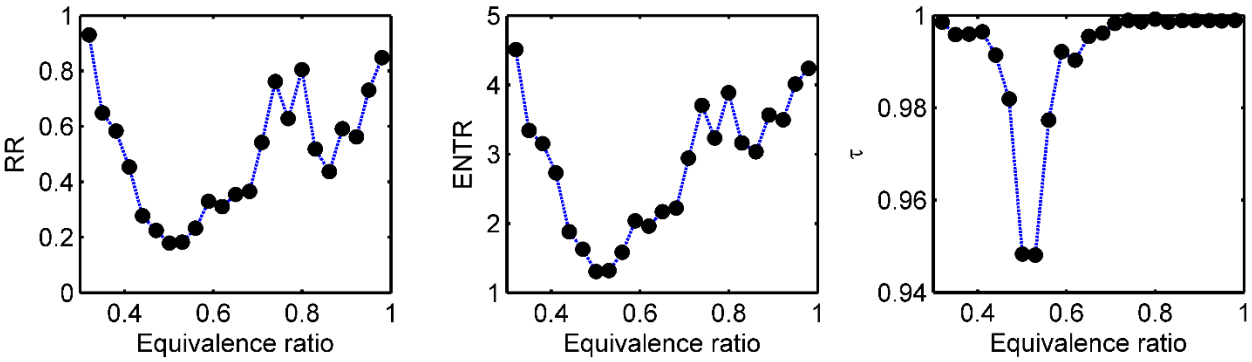

Figure 4.8: RQA performed without embedding the dynamics in the phase space. Here the fuel flow rate is 0.56 g/s. The system do not encounter thermoacoustic instability at low equivalence ratios as lean blowout is approached. We can observe that as the system approaches blowout, *ENTR*, *RR* and decreases initially as we approach periodic oscillations towards zero and increases close to blowout.

On the other hand, when the state point is away from the center of the phase space and the pressure fluctuations have high amplitude, the tendency of recurrence is low both in

phase space and in the amplitude of pressure fluctuations. Thus, recurrence characteristics are similar in both cases.

4.4 Concluding remarks

In this chapter, we showed that recurrence quantification can be utilized to characterize the intermittent pressure oscillations in a turbulent combustor. Various parameters that are estimated from recurrence plots such as trapping time, Shannon entropy of the lines parallel to diagonal and recurrence rate exhibit significant variations as we approach an impending blowout owing to the increased aperiodicity of the oscillations close to blowout and hence can serve as precursors to an impending blowout. We further showed that a method of recurrence quantification analysis that doesn't involve phase space reconstruction and analyzes the recurrence of the value of the state variable in time is effective at prognosis of dynamic transitions in a turbulent combustor. Since such a method is computationally less expensive, it can be adopted for online diagnostics of thermoacoustic instability and blowout in a turbulent combustor.

CHAPTER 5

Flame dynamics during intermittency in a turbulent combustor

Recent studies on combustors with turbulent reactive flow and flame stabilization using swirl (Thampi & Sujith, 2015) or bluff body (Nair *et al.*, 2014) show that on approaching lean equivalence ratios, the reactive flow system exhibits intermittency presaging the onset of thermoacoustic instability. In chapter 3 and 4, it was also seen that as the equivalence ratio was further reduced, the system undergoes another bifurcation and exhibits intermittency post the occurrence of thermoacoustic instability (Unni & Sujith 2015, Nair & Sujith 2015). On further reduction in equivalence ratio, the flame blows out. Further, statistical measures that quantify intermittency were proposed as precursors to impending thermoacoustic instability (Nair *et al.*, 2013). Nevertheless, the similarities and differences between these intermittent states prior to and post thermoacoustic instability has not been systematically investigated. The primary goal of this chapter is to compare and contrast either state both from the perspective of dynamical systems theory, and from the point of view of flame dynamics.

In the context of turbulent flows, intermittency is a well-studied phenomenon that was observed from the early research of Batchelor and Townsend (1949). However, different types of intermittent behaviors are observed in turbulent flows. The interface between the turbulent fluid inside the boundary layer and the irrotational flow outside the boundary layer is found to be intermittent. Further, it is known that the dissipative range of turbulent cascade exhibits intermittency (Frisch, 1995). Additionally, the wall boundary

layer exhibits intermittency caused by the formation of coherent structures that breaks down intermittently, producing bursts of small-scale turbulence (Lumley & Kubo,1985).

In contrast, the intermittency that we focus on in this chapter is the dynamic state of a system with confined turbulent reactive flow that is characterized by bursts of periodic pressure oscillations appearing amidst aperiodic pressure fluctuations in an apparently random manner (Nair *et al.,* 2014, Nair & Sujith 2013). In the context of the onset of thermoacoustic instability, Nair and Sujith (2013) showed that the intermittent dynamics prior to thermoacoustic instability corresponds to dynamics in a homoclinic orbit in the phase space. Further, Nair and Sujith (2015) attributed aperiodic flame extinction and re-ignition events as the cause for the presence of the bifurcation that leads to the occurrence of intermittency after the occurrence of thermoacoustic instability, before eventually reaching blowout. The multifractal characteristics of these oscillations, prior to and post thermoacoustic instability, was detailed in chapter 3. We observed that combustion noise (pressure oscillations during near stoichiometric combustion) and pressure oscillations prior to lean blowout have similar multifractal characteristics. Nevertheless, we did not discuss the characteristics of intermittency before the occurrence of thermoacoustic instability and the intermittency prior to blowout. In this chapter, we provide a detailed comparative analysis of intermittency prior thermoacoustic instability and that prior to blowout.

The presence of intermittency helps us forewarn about the dynamic transitions in a turbulent combustor. Hence, understanding the characteristics of intermittency is important to improve the forewarning capabilities. There are two specific objectives for this study. 1) Compare and contrast the intermittency occurring prior thermoacoustic

instability and prior to blowout using unsteady pressure time series measurements. 2) Study the flame front dynamics during either state using high speed Mie scattering images, acquired simultaneously with unsteady pressure.

The rest of the chapter is laid out as follows. Section 3 talks about the results and discussions. Major conclusions are detailed in §4.

5.1 Comparison of intermittency: analysis of the pressure fluctuations

The unsteady pressure inside the combustor was measured at different global equivalence ratios (details given in §2). Close to stoichiometric combustion, at a global equivalence ratio of 0.98, the pressure oscillation inside the combustor has low amplitude and is aperiodic (Fig. 5.1a). As the global equivalence ratio is reduced, we observe intermittent oscillations (*Eq. Ratio* = 0.86, Fig. 5.1b). At a global equivalence ratio of 0.58, we observe thermoacoustic instability (Fig. 5.1c). The oscillations during thermoacoustic instability has a peak frequency around 248 Hz. On further reduction of global equivalence ratio, the system undergoes another bifurcation and at *Eq. Ratio* = 0.37 and we again observe intermittency (Fig. 5.1d). From these experiments, we can observe that intermittent oscillations appear both before and after the occurrence of thermoacoustic instability. In the rest of this section, we will compare the dynamics of the pressure fluctuations observed during these regimes of intermittency prior to and post the occurrence of thermoacoustic instability.

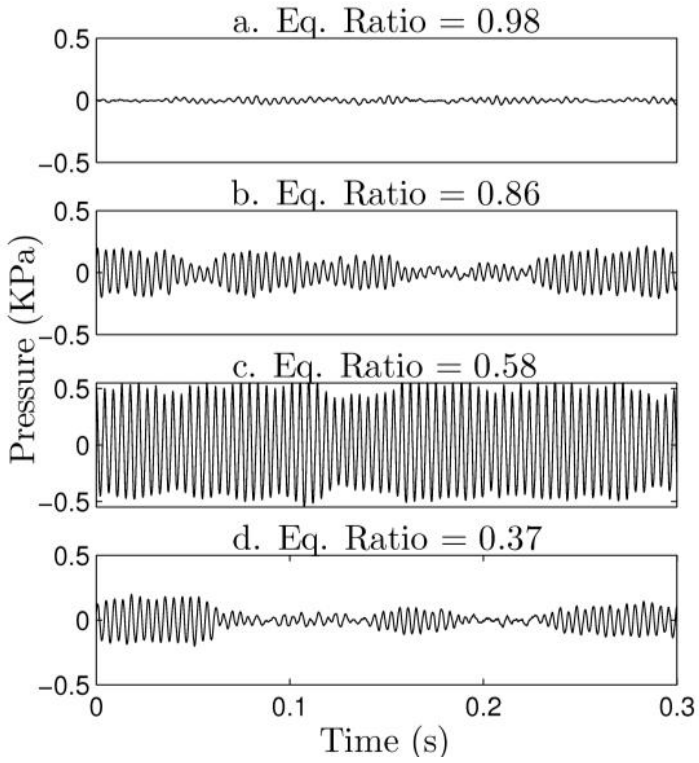

Figure 5.1: Time series of unsteady pressure obtained at different equivalence ratios. a) Near stoichiometric combustion (equivalence ratio of 0.98), the oscillations are aperiodic with low amplitude. b) At an equivalence ratio of 0.86, we observe intermittency prior to instability. c) When the equivalence ratio is 0.58, we observe instability. d) Further, at equivalence ratio of 0.37 we observe intermittency prior to blowout. Length of combustor for this set of experiments is 700 mm.

The pressure time series, spectrogram (window size of 500 data points (0.05 s), overlap 400 (0.04 s) data points) and recurrence plots corresponding to intermittency prior to and after thermoacoustic instability are presented in Fig. 5.2.

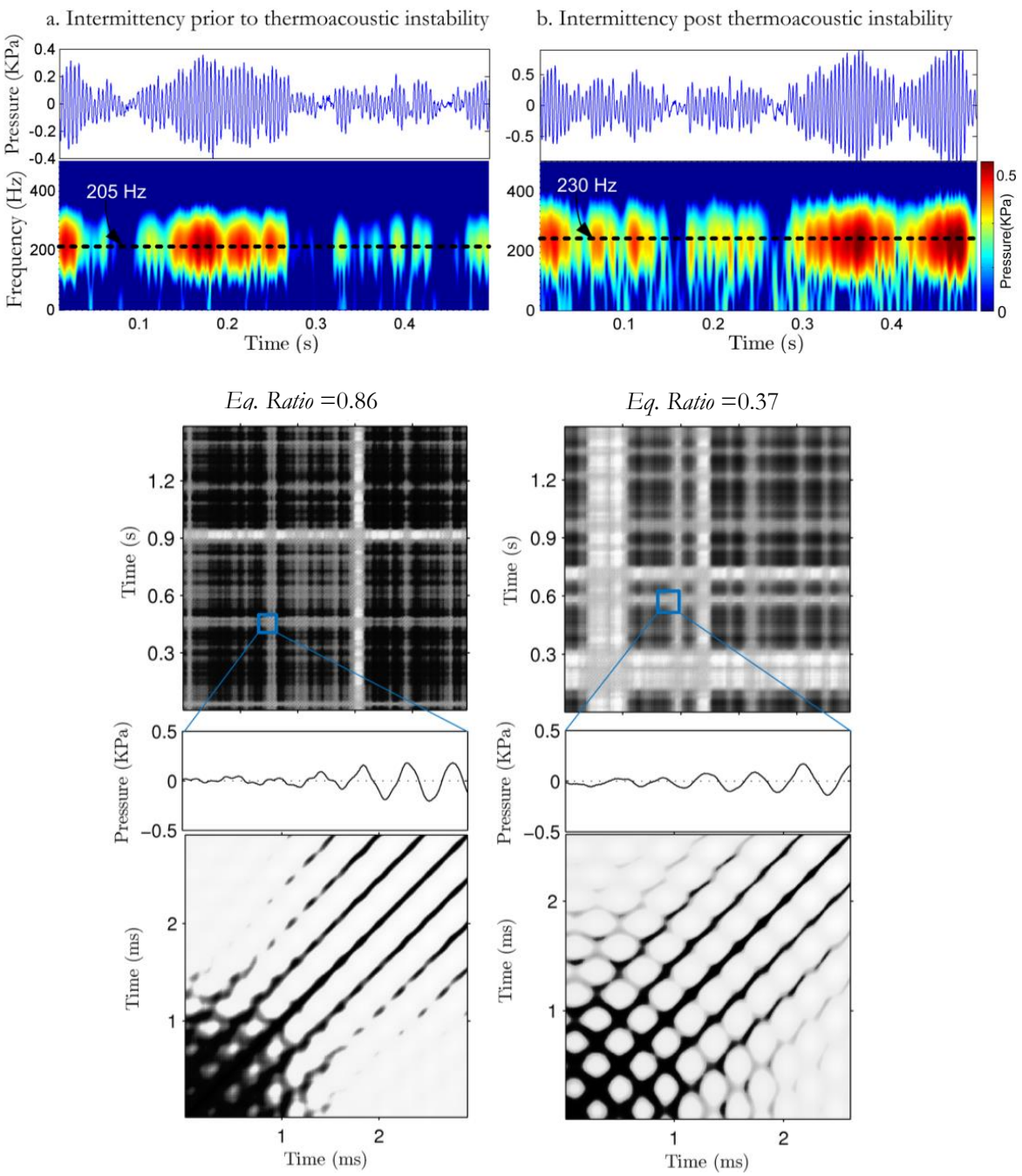

Figure 5.2: Time series, spectrogram and the recurrence plot corresponding to the intermittent pressure oscillations before and after the occurrence of thermoacoustic instability. The recurrence plots with black patches whose corners show perforations indicate that both case of intermittency is Type II and hence dynamically similar. There are no significant differences observed in spectrogram.

From the time series, we can observe that during the occurrence of both intermittent states, in time, bursts of large amplitude periodic oscillations appear in between the aperiodic fluctuations in an apparently random manner. The occurrence of these bursts is reflected as the intermittent peaks observed in the spectrogram. The spectrogram represents the time varying frequency content in a time series. For the duration of the aperiodic fluctuations the spectrogram indicates low amplitude for all the frequencies.

However, as the bursts of periodic oscillations appear, the amplitude of oscillations around 205 Hz increases (peak at 205 Hz, for intermittency prior to thermoacoustic instability). Comparing the spectrograms for the intermittent states, it can be observed that for intermittency after thermoacoustic instability, the peak frequency (230 Hz) is higher than that observed for intermittency prior to thermoacoustic instability.

Next, we investigate the dynamics by analyzing the corresponding recurrence plots. A recurrence plot represents the recurrent behavior of phase space trajectory. A detailed study of the recurrence characteristics of the pressure oscillations in a laminar (Kabiraj & Sujith, 2012) and turbulent (Gotoda *et al.*, 2014) combustor was previously reported. They used recurrence plots to identify different dynamic behaviors exhibited by reactive flow systems. The patterns in recurrence plots indicate the dynamic behavior of the system. For example, the lines parallel to the diagonal in a recurrence plot represent periodic behavior in the phase space. The distance between these parallel lines represents the time period associated with the periodic oscillations. The recurrence plots in Fig. 5.2 have parallel lines interrupted by dark patches. Such a pattern indicates that the oscillations are intermittent in nature; i.e. periodic for some time and aperiodic for the rest. The dark patches reflect the presence of aperiodic oscillations in the time series.

When we zoom in, for both intermittency before and post thermoacoustic instability, we see that the black squares along the diagonal of the recurrence plot have perforated upper and right edges (Fig. 5.2). Such a pattern in a recurrence plot is suggestive of type II intermittency (Klimaszewska & Zebrowski, 2009). Type II intermittency is indicative of the approach of the dynamical system to an underlying subcritical Hopf bifurcation (Pomeau & Manneville, 1980). There could be other types of intermittencies for a dynamical system such as Type I or Type III depending on the underlying bifurcation being either a saddle node bifurcation or an inverse period doubling bifurcation. Here, since the type of the intermittency is the same for both cases, we can possibly conclude that both states exhibit qualitatively similar dynamics. Other than the observed difference in the frequency of the periodic part of intermittent oscillations, the recurrence plot and spectrogram indicate similar qualitative behavior for intermittent state prior to and post thermoacoustic instability, even though the flame dynamics may be different for these two situations. In the next section, we will investigate the flame front dynamics during either states to gain further insights into the similarities and difference in the intermittent dynamics.

5.2. Comparison of intermittency: analysis of flame dynamics

Before comparing the flame dynamics during intermittency preceding and post the occurrence of thermoacoustic instability, we will first analyze the flame stabilization during combustion at *Eq. Ratio*= 0.98 (i.e. global equivalence ratio close to stoichiometric combustion). Fig. 5.3 shows a Mie scattering image that represents a typical flame front imaged along a plane passing through the center of the bluff body. Note that, here the boundary of the illuminated part of the Mie scattering image indicate

the density gradient across the flame and hence represents the flame front (marked by yellow dots in Fig. 5.3). We should note that the flame is stabilized along the outer shear layer (anchored at point Y, stabilized by the recirculation zone at the dump plane) and the inner shear layer (anchored at point X, stabilized by the stagnation point flow behind the dump plane). Through extensive experiments on turbulent flames, Shanbhogue *et al.* (2009) showed that the part of the flame close to its root (anchor point) responded the most to a periodic forcing. They also showed that the dynamics at the tip of the flame contributed mainly to the aperiodicity in the pressure fluctuations. This suggests that, it is the stability of the anchor points that determine the periodic flame dynamics and hence the dynamics of the combustor during thermoacoustic instability.

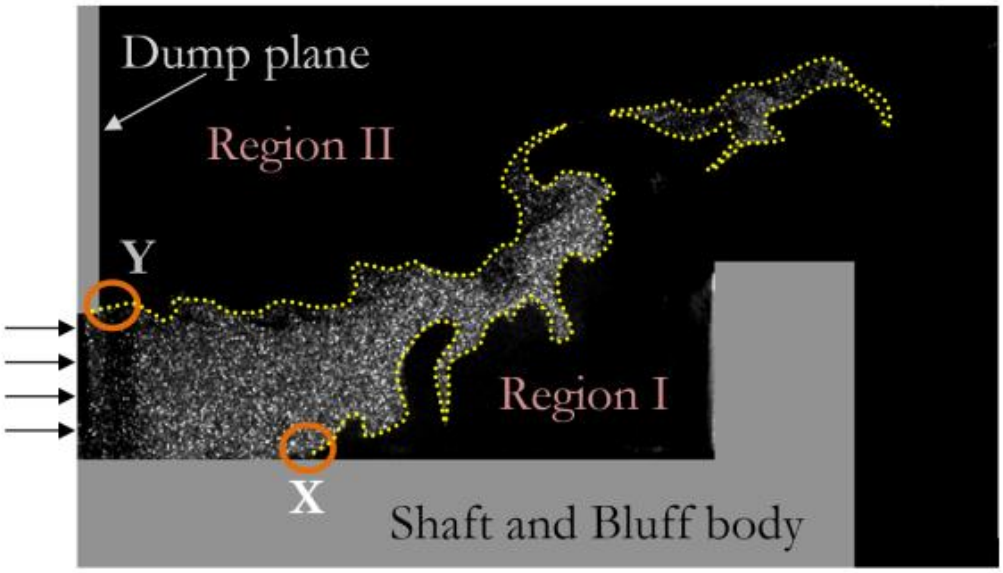

Figure 5.3: Mie scattering image representing the flame front during stable combustion. The flame front is the contour enveloping the illuminated region in the Mie scattering image and is shown here as a dotted yellow line. Here, the $\dot{m_f}$ =1.04 g/s and the *Eq. Ratio* =0.98. The flame is anchored at point X and Y stabilized by the stagnation point flow in the Region I and the recirculation at dump plane (Region II).

During the regime of intermittency prior to the occurrence of thermoacoustic instability, the flame is stabilized as shown in Fig. 5.4. Here, the flame switches between two distinct behaviors.

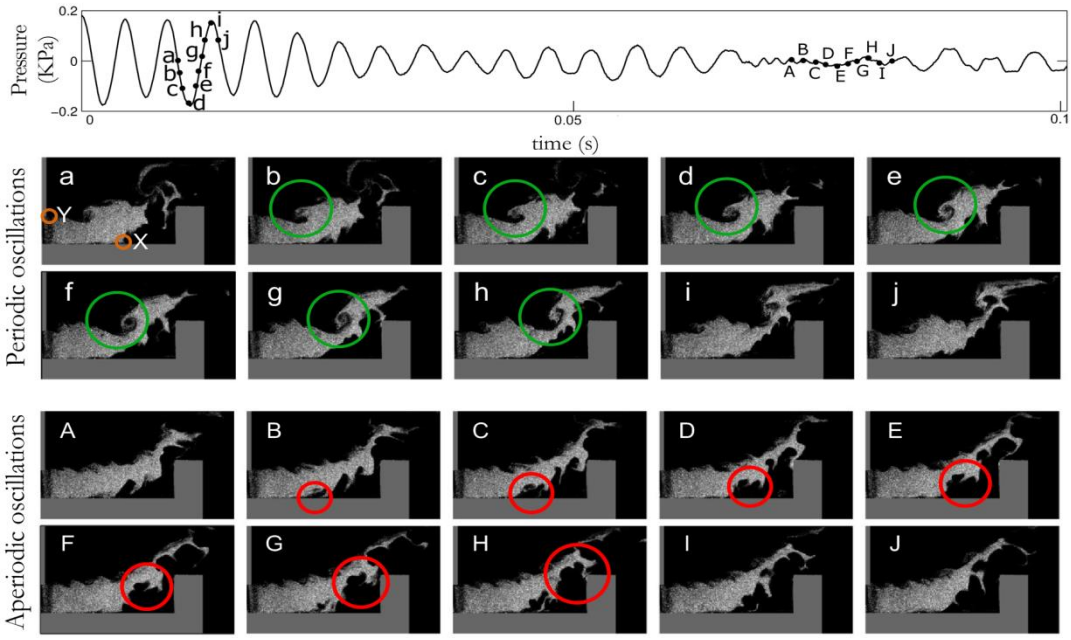

Figure 5.4: Flame images during intermittent oscillations prior to thermoacoustic instability. During periodic part of intermittency, both outer and inner shear layer exhibit periodic fluctuation of the flame front. The green circle marks the flame roll-up due to the vortex that is periodically shed from the dump plane. The red circle marks the flame fluctuation at the inner shear layer that is responsible for the switch from low amplitude aperiodic oscillation to high amplitude periodic oscillation

During the periodic part of pressure oscillations, the part of the flame stabilized along both the inner and outer shear layer oscillates in a periodic fashion. The Mie scattering images show roll-up in the flame front stabilized along the outer shear layer suggesting that ring vortices that emerge from the dump plane perturbs the flame in a periodic manner (Fig. 5.4a-i, the roll-up pattern is marked in Fig. 5.4f with a green circle). The

presence of such ring vortices during thermoacoustic instability has been reported previously (Poinsot *et al.*, 1987). In this study, we observe that such ring vortices are also observed during the periodic part of intermittency. However, this periodic roll-up of the flame front persists only for a small duration and the flame intermittently switches to the alternate flame dynamic configuration that is present during the aperiodic part of the pressure fluctuation (Fig. 5.4A-H).

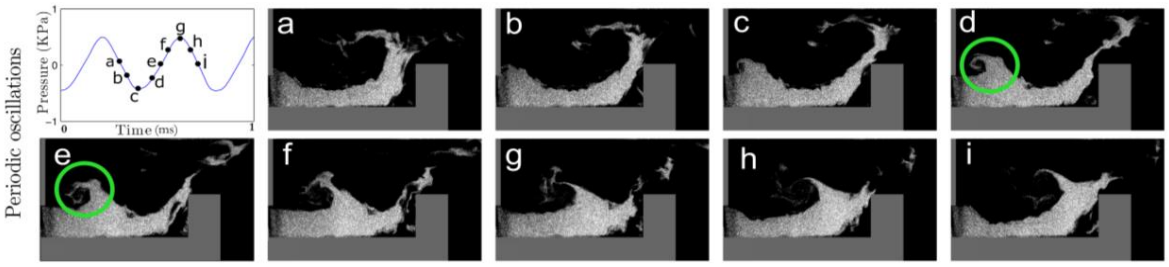

Figure 5.5. Mie scattering images indicating the dynamics of the flame front for different phases of the pressure oscillations during thermoacoustic instability. Figures 5.5**a** to 5.5**i** represent the images corresponding to the specific locations in one cycle of the periodic pressure oscillation as shown in the pressure time series. The green circles mark the rollup of the flame due to the vortex that is shed periodically from the dump plane.

During aperiodic pressure oscillations, the periodic oscillation at the flame root subsides and the tip of the flame oscillates in an aperiodic manner. At the aperiodic part of the intermittent oscillations, we can observe that a wrinkle formed near the anchor point 'X' convects downstream and grows in amplitude causing a fluctuation to the flame front (the wrinkle is marked with red circles in Fig. 5.4) A fluctuation to the flame causes an unsteady heat release rate, which, in turn, causes an acoustic perturbation in the reaction zone. If this acoustic perturbation is significantly high, it could further enhance the fluctuation at the root of the flame by perturbing the shear layer shed from the dump

plane (Yokoyama & Kato, 2009). As the feedback from acoustic field increases, the strength of the periodic fluctuation increases. The sustained high amplitude oscillations of the flame close to the root of the flame during periodic pressure fluctuation can be observed from the Mie scattering images (Fig. 5.4a-j).

During thermoacoustic instability (Fig. 5.5), we can see that a roll-up in the flame front, very similar to that we observed during the periodic part of the intermittent oscillations, imparts much stronger periodic behavior to the flame front. Here, acoustic pressure peaks when the rolled up part of the flame impinges the bluff body (Fig. 5.5g).

The periodic and aperiodic flame fluctuations during intermittency post thermoacoustic instability can be seen in Fig. 5.6. The major difference that needs to be highlighted here is that the stability of the flame along the inner shear layer changes. Note that the anchor point for the flame along the inner shear layer (represented by 'X' in Fig. 5.4a) has moved from the shaft holding the bluff body to the top of the bluff body in Fig. 5.6a. Now, the stagnation point behind the bluff body is no longer able to sustain the flame. Hence the flame along the inner shear layer is attached on top of the bluff body. Further, during the periodic oscillations, the flame along the inner shear layer, anchored on top of the bluff body, no longer exhibits large periodic fluctuations. During the aperiodic part of pressure fluctuations, the flame dynamics is aperiodic and most of the flame fluctuation is near the flame tip. The periodic part has a higher frequency during the intermittency that occurs post of thermoacoustic instability, possibly due to the increased flow velocity resulting in the increased frequency of the vortex shedding from the dump plane.

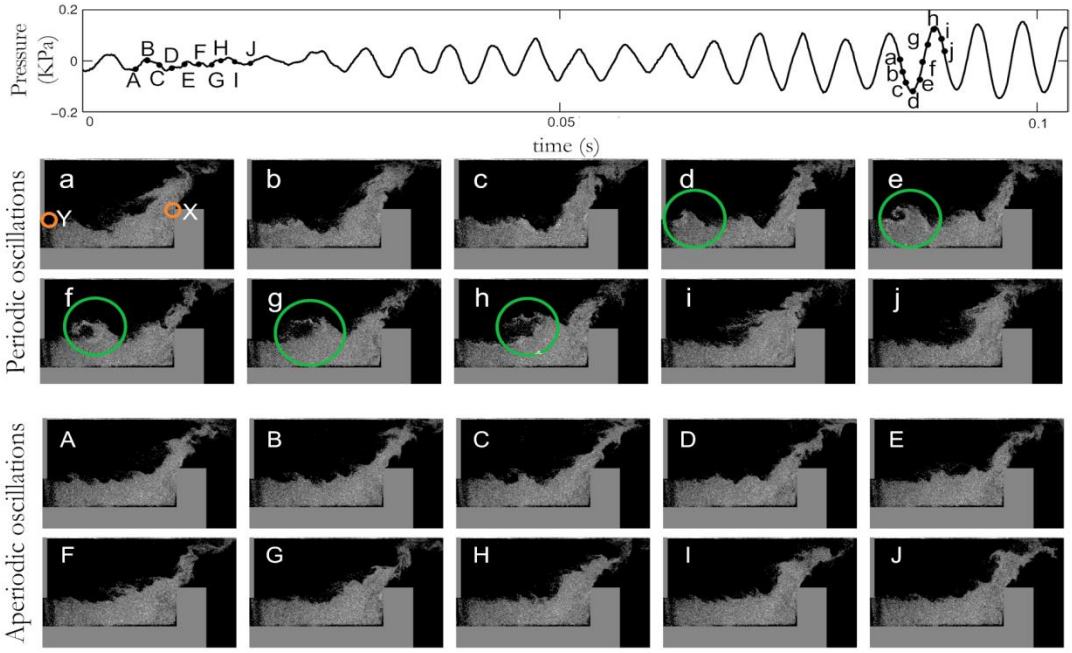

Figure 5.6: Mie scattering images that show flame front fluctuations during intermittent oscillations post thermoacoustic instability. During the periodic part of intermittency, the outer shear layer exhibits periodic fluctuation of the flame front (Fig. 5.6a-j). The green circles mark the rollup of the flame due to the vortex that is shed periodically from the dump plane.

During intermittency prior to thermoacoustic instability, the flame is anchored behind the bluff body on the shaft holding the bluff body (inner shear layer) and at the dump plane (outer shear layer). Here, the flame along the inner shear layer is stabilized due to the stagnation point flow behind the bluff body. Whereas, the flame along the outer shear layer is stabilized by the recirculation zone at the dump plane. During the periodic part of intermittent pressure fluctuations, the flame along the outer and inner shear layer exhibits periodic fluctuations characterized by a rolled-up part of the flame front convecting towards the bluff body, impinging the bluff body and causing an impulse in heat release. We can also observe that during the periodic oscillations, the root of the flame oscillates in a periodic manner.

During intermittency occurring post thermoacoustic instability, the flame is anchored on top of the bluff body (along the inner shear layer) and at the dump plane (outer shear layer). The flame along the inner shear layer is no longer stabilized by the stagnation point flow behind the bluff body, possibly due to the high strain rates due to the increased velocity of the flow at lean equivalence ratios. Similar observations have been made recently by Shanbhogue *et al.* (2016). During periodic part of intermittent pressure fluctuations, the flame along the outer shear layer alone exhibits periodic fluctuations and the inner shear layer no longer exhibit periodic oscillations (Fig. 5.6a-j).

Even though we observe that the system exhibits differences in the flame dynamics during intermittency prior to and after thermoacoustic instability, both intermittent states are of type II and hence have qualitatively similar dynamics, from the perspective of dynamical systems theory.

5.3 Concluding remarks

In this study, we investigated the pressure oscillations and the flame dynamics of intermittency observed prior to and post the occurrence of thermoacoustic instability on reduction of equivalence ratio from stoichiometry to fuel lean conditions. From the analysis of pressure fluctuations, it was observed that both intermittency prior to and post occurrence of thermoacoustic instability are of type II and hence exhibit qualitatively similar dynamics. It may be noted that a stochastically driven oscillator may exhibit similar dynamics (Noiray & Schuermans, 2013) that cannot be conclusively distinguished from a type II intermittency with the proposed method (i.e. recurrence analysis), and further studies are required to conclusively establish the dynamic nature of the

intermittent oscillations. Further, the flame dynamics during either regimes were studied using high speed Mie scattering images acquired simultaneously with the unsteady pressure. We observe that during the periodic part of the intermittency, both prior to and post the occurrence of thermoacoustic instability, the part of the flame anchored along the outer shear layer exhibits periodic roll-up of the flame front, resulting in periodic fluctuation in the heat release rate. However, we observe that the flame stabilized along the inner shear layer exhibits a different behavior during the intermittency prior to and after the occurrence of thermoacoustic instability. During the periodic part of the intermittency prior to thermoacoustic instability, the flame along the inner shear layer exhibits periodic motion along with the flame along the outer shear layer. Also, the flame along the inner shear layer is anchored on top of the shaft holding the bluff body stabilized by the stagnation point flow behind the bluff body. In contrast, during intermittency occurring post thermoacoustic instability, the stagnation point behind the bluff-body loses its ability to stabilize the flame. Hence, the flame is anchored on top of the bluff body and is stabilized by the recirculation zone formed due to the bluff body. During the periodic part of intermittency, the part of flame stabilized along the outer shear layer exhibits periodic fluctuations whereas the part of flame stabilized along the inner shear layer does not exhibit periodic oscillations.

CHAPTER 6

Flame blowout: an absorbing phase transition

In Chapter 5, we discussed the dynamics of the flame during the regime of combustion noise, state of intermittency before the occurrence of thermoacoustic instability, state of intermittency before flame blowout and also during thermoacoustic instability. We did not, however, dwell into the dynamics of flame very close to the flame blowout. Previous studies (detailed in next few paragraphs) indicate that the dynamics of a flame very close to blowout is complex and is largely dominated by the growth of the intermittently formed flame holes. In this chapter, we attempt to develop a low order model that can capture these dynamics. Further, we describe the dynamic transition that this model undergoes as the system encounters a flame blowout.

Historically, there have been various attempts to study lean blowout. Early studies by Longwell, Frost & Weiss (1953) and Spalding (1955) suggest that the Damkhöler number (*Da*), the ratio of the resident time of the reactants and the reaction time scale is an important parameter that determines the LBO margin. It was conjectured that that LBO occurs when *Da* of the reactive flow is lesser than a threshold value. Such a simple description, while befitting for the description of LBO behavior of laminar flames, is seldom true for the case of a turbulent flame. For a turbulent flame, LBO is described as a collective flamelet extinction event (Plee & Mellor 1979; Radhakrishnan, Heywood & Tabaczynski 1981) and the ratio of the flow speed to the flame speed is used to characterize blowout. When this ratio exceeds one, at critical locations inside the combustor, the flame blows out (Chaudhuri *et al.* 2010). However, this description is

highly limited in the practical scenario of near blowoff flames in a highly turbulent flow. Here, the local extinction and reignition events are governed by various other factors such as highly intermittent local strains rates, flame geometry, mixture fraction fluctuations, heat loss from the flames to the wall or to the flow coupled with differential diffusion effects, the local boundary conditions and the detailed chemistry of the reaction. The interaction effects of the above further add to the complexity of the problem

This complex interaction between different processes causes a highly unsteady and aperiodic behavior of the flame prior to blowout. Muruganandam (2006) and Nair (2006) observed that both chemiluminescence and pressure fluctuations close to flame blowout exhibits burst like behavior. Gotoda *et al.* (2012) further observed that these oscillations also exhibit multifractal characteristics. The flame dynamics close to blowout was investigated by De Zilwa, Uhm & Whitelaw (2000) using high-speed flame images and simultaneous pressure fluctuations. They observed that the flame exhibited highly unsteady behavior prior to lean blowout. Nair and Lieuwen (2007) showed that the approach to blowout is through increased appearance of flame holes in the reactive flow field in a random manner. Later, Chaudhari *et al.* (2010) investigated the interaction between flame-fronts and shear layer vortices by performing time-resolved chemiluminescence imaging along with simultaneous particle image velocimetry (PIV) and OH planar laser-induced fluorescence (PLIF). This study suggested that close to blowout, it is the interaction between the shear layer vortices and flame fronts that causes the local stretch rates along the flame to exceed the extinction stretch rates leading to the local extinction of the flame and thus the production of a flame hole. The flame dynamics

in specific combustor configurations and a more general review of the work on blowout of bluff body stabilized flames are given by Shanbhogue, Husain & Lieuwen (2009).

There have been numerous efforts to capture the flame dynamics close to blowout using direct numerical simulations (DNS) and large eddy simulations (LES) (Gokulakrishnan *et al.* 2006, Kim *et al.*, 2006.). Similar to many experimental studies (Zhang et al, 2007, Driscoll & Rasmussen, 2005), the primary goal for most of these studies were to obtain semi-empirical correlations that could identify the LBO margins for specific configurations of combustors. While they were largely successful in their pursuit of predicting stability margins, few models tried to capture the unsteady dynamics of the flame close to blowout. However, till date there are no lower order models that exist that tried to capture the complex dynamics of the flame close to blowout. In this work, we try to bridge that gap and introduce a low-order phenomenological model that captures the flame dynamics of a turbulent combustor at lean limit. The model considers the flame confined in the combustor as a collection of flamelets interacting with each other. This interaction between flamelets leads to emergence of various dynamics at different dynamic conditions. Thus, this model preserves the main philosophy of this thesis and treats the combustor as a complex system where the individual subunits of the system interact with each other resulting in complex emerging dynamics.

6.1 The population dynamics model for flame blowout

Inside a combustor, the flame exists at those locations in the reactive flow field where reactants react to form products. When reactants burn (assuming the fuel is a hydrocarbon), they produce hot radicals such as OH which participate in the key chain

branching combustion reaction: $H + O_2 \longrightarrow OH + O$. The flame inside a combustor is sustained when the hot radicals formed at a particular instant interact with the unreacted air-fuel mixture that enters the combustor at the next instant thus making sure that a chain reaction is established inside the combustor. Thus, during stable combustion, there is always some amount of hot free radicals inside the combustor. The locations where these free radicals are present mark the spatial distribution of the flame inside the combustor. The concentration of the free radicals indicates the rate of reaction and hence the heat release rate. The experimental techniques (e.g. planar laser induced florescence - PLIF) that are used to capture the flame dynamics essentially map the concentration of CH or OH free radicals within the flow field. Thus, the flame dynamics in a combustor is in essence equivalent to the dynamics of the concentration the free radicals in the reactive flow field. In the model, for simplicity, we consider that the flame is comprised of multiple flamelet. A gas parcel that contains free radicals or flame is called a flamelet. The flame dynamics is the result of the local interaction between these multiple flamelets that compose the reaction field. In this narrative of flame dynamics, lean blowout is a scenario where the inability of the reactive flow to sustain the chain reaction results in the extinction of the population of flamelets in the flow field. Inspired from this connection between the flame dynamics and the population dynamics of the flamelets, in this chapter, we introduce a population dynamics model that captures the complex dynamics that the flame exhibits close to lean blowout.

The effort to comprehend the dynamics of populations has been underway for more than two centuries beginning with the seminal work of Malthus (1798) that suggested that population of a society undergoes an exponential growth in time eventually inducing a

demand and supply mismatch of resources in the society. This model did not consider the effect of finiteness of resources and was soon replaced by the famous logistic model that considered population growth to be limited by the carrying capacity of the environment (Verhulst, 1838). With further advent of mathematical biology, over the years, more sophisticated models started to emerge that would model the spatiotemporal aspects of population growth under various constraints imposed by its environment and the rules of interaction among the population. Today, population dynamics models are widely used to study the dynamics of various natural phenomena such as spread of epidemics (Anderson & May, 1981), desertification of forests, extinction of species (Woodroffe & Ginsberg, 1998), population dynamics of fisheries (Kapur, Troy & Oris, 1997), societal and cultural collapse (Russell & Russell, 2000) etc.

While in each situation, the details of the model vary, the commonality is that, in every model, there is interplay between the birth and death process that control the emergent global dynamics of the population. When we try to describe the population dynamics in a spatially extended system, the effect of spatial distribution in the interaction among the population becomes a decisive factor in the birth and death process and hence the population dynamics (Karaiva 1990). For example, the spread of an epidemics is at times controlled by minimizing the interaction between the infected population with the healthy population by spatially quarantining the infected population (Arino *et al.* 2005).

In adapting a population dynamics model for describing the dynamics of flame, we consider the process of ignition of the reactants as the birth process of a flamelet and the process of extinction of a flamelet as equivalent to the death of the flamelet. The ignition of an unburned gas parcel in a reactive flow is the result of its interaction with

neighboring gas parcels which contain hot free radicals (flamelets). Hence, the spatial distribution of the flamelets determines the flame propagation within the reactive field and hence controls the combustion dynamics. Considering these aspects, we define a cellular automaton (CA) for the population dynamics of flamelets that would mimic the flame dynamics inside a combustor. A cellular automaton is a discrete computational system that is useful in modeling a complex system. A generic cellular automaton consists of regular array of cells (in most cases formed by a regular grid). At each time instant of the cellular automaton, each cell can assume any one of the finite number of states that are allowed. The states of the cells evolve in parallel at discrete time steps according to state update functions or dynamic transition rules. The update rules are a function of the state of the cell and its neighborhood. The characteristic feature of cellular automata is their ability to display emergent dynamic behavior as the result of the local interaction between the states of the multiple cells that they are comprised of. Thus, they form an ideal basis for studying complex system behavior. In this chapter we define a cellular automaton that mimics the flame dynamics inside a combustor. In defining the cellular automaton, we treat the combustor as a complex system in which the emergent dynamics of the flame is the result of local interaction between multiple flamelets, the unburned reactants and the products of combustion.

Our primary objective is to model the flame dynamics close to flame blowout. First, a few simplifying assumptions are made. We consider the blowout characteristics of two different configurations of combustor. A combustor with a simple premixed conical flame (Fig. 6.1a) and a combustor with a bluff body stabilized premixed flame (Fig. 6.1b). The geometries of combustors are shown in the Fig. 6.1. A two-dimensional

reaction field is considered for simplicity. It is assumed that the premixed air-fuel mixture enters the combustor with a uniform velocity *2U* across the inlet for both combustors. Both combustors have a width of W_c. The inlet for the conical flame combustor (Fig. 6.1a) has a width of $W_c/2$. The bluff body in Fig. 6.1b has a width of $W_c/2$.

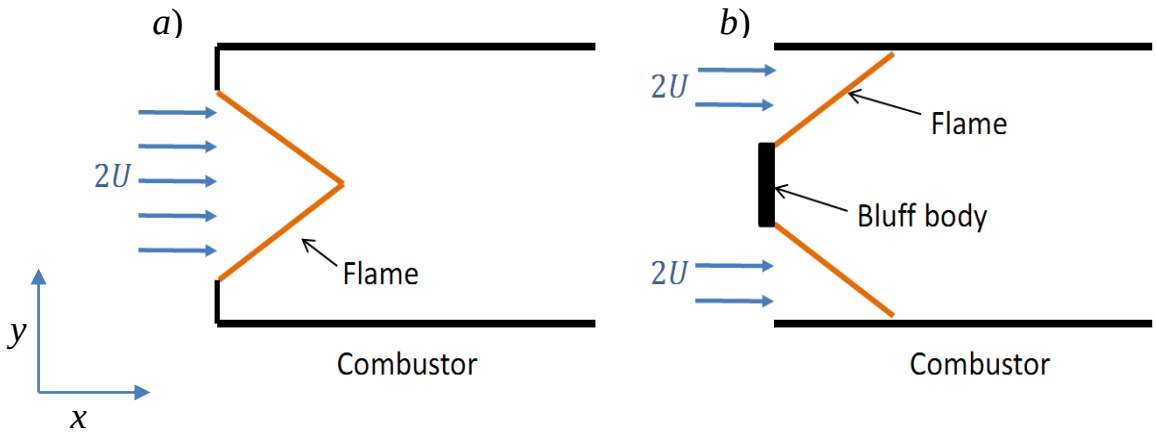

Figure 6.1: The schematic of the combustor configuration that is modeled using a cellular automata. a) Conical flame. b) Buff body stabilized flame. For simplicity, we assume that the premixed air-fuel mixture enters the combustor with a uniform velocity *2U* across the inlet for both combustors. Both combustors have a width of W_c. The inlet for the conical flame combustor (Fig. 6.1a) has a width of $W_c/2$. The bluff body in Fig. 6.1b has a width of $W_c/2$.

To construct cellular automata, first, we divide the reaction field inside the combustors into a uniform square grid. Each vertex of the grid represents the state of the flow in that spatial location. The states can be, unburned (0), burning (1) or burned (2). In each step of cellular automata, the fluid elements at each vertex interact with each other following a set of rules. This local interaction between the flowing gas parcels which are unburned, burning, or burned leads to the propagation of flame in the flow field. The specific characteristics of the interaction between the fluid elements that we need to capture in

this model are the localness and the effect of the underlying turbulent flow in the system. The rules of cellular automata that define flame propagation are given in Fig. 6.2. In each step, a burned site would remain burned and a burning site will become burned. An unburned site would burn with a probability P, if there is at least one site in its Moore neighborhood (i.e., the eight sites which surround it) which is burning. Here, *P* is the probability of flame propagation. When the probability of flame propagation *P* reduces, the average flame speed reduces. At lean equivalence ratios close to blowout, the flame velocity reduces when the equivalence ratio of combustible mixture reduces. Thus, reducing P is equivalent to reducing the equivalence ratio of the combustion and approaching blowout.

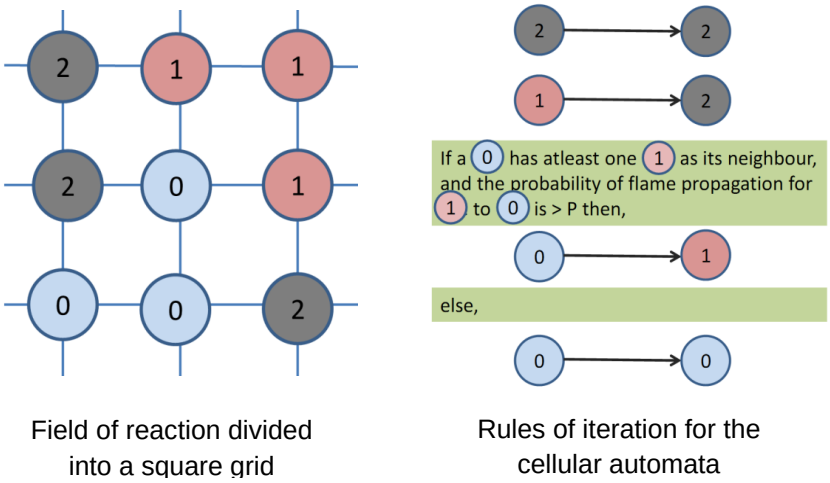

Figure 6.2: a) Rules of iteration for the cellular automata (CA) model. The state of the fluid at each vertex can be, unburned (0), burning (1) or burned (2). In each step, a burned site would remain burned, and a burning site will become burned. An unburned site would burn with a probability P, if there is at least one site in its Moore neighborhood (i.e., the eight sites which surround it) which is burning. Here, *P* is the probability of flame propagation.

The probability of flame propagation *P*, can be related to the varying strain rates in a turbulent flow. It is known that a flamelet propagates into a neighboring unburned fluid parcel, only if the strain rates corresponding to the unburned fluid parcel is less than the ignition strain rate (S_{ign}) and the strain rate along the flamelet is less than the extinction strain rates (S_{ext}) (Law, 2010). Hence, a flame needn't always propagate into a surrounding unburned gas parcel. The probability of propagation depends upon the strain rates of the flamelet and the surrounding unburned gas parcel. In a combustor, there is a non-uniform, turbulent field of strain rate for the reactive flow. In cellular automaton, we incorporate the turbulence in the reactive flow field by assuming that there is a time varying random field of strain rate in the flow field. For simplicity, we assume the random strain rate along the grid points in the field to have the characteristics of white noise. The probability associated with flame propagation will depend on the strain rates of the unburned fluid parcels surrounding a burning fluid parcel and the strain rate of the burning fluid parcel. For premixed combustion, as equivalence ratio is reduced, S_{ign} and S_{ext} reduces. This implies, as equivalence ratio is reduced the probability of flame propagation, *P* reduces. S_{ign} and S_{ext} With this definition *P*, is also related to the flame speed. As *P* reduces, the flame speed reduces.

The mean flow of the unreacted mixture is simulated by removing two columns of vertices from the right side of the grid representing the reactive field and adding two columns of vertices with unburned sites to the right of the grid in each step. This essentially, moves the grid representing the reaction field towards left by two columns. The mean flow of the unreacted mixture is simulated by removing two columns of vertices from the right side of the grid representing the reactive field and adding two

columns of vertices with unburned sites to the right of the grid in each step. This mimics the outflow of fluid parcels (burned, burning or unburned) from the combustor and the influx of the unburned fluid parcels into the combustor. In order to initiate burning and to keep the flame anchored at the exit of the burner, burning fluid parcels are added at point A and B in every iteration of the cellular automata s. This mimics the outflow of fluid parcels (burned, burning or unburned) from the combustor and the influx of the unburned fluid parcels into the combustor. In order to initiate burning and to keep the flame anchored at the exit of the burner, burning fluid parcels are added at point A and B in every iteration of the cellular automata with a probability P (for reducing complexity of the model, we take this as equal to the probability of flame propagation) provided; there be at least N number of burning parcels in the reactive field. If the number of burning fluid parcels in the reactive field goes below N, then the flame is no longer anchored at the burner. This corresponds to a situation when the flamelets fail to sustain the chain reaction eventually leading to flame blowout. In this work, N is taken to be 3. This happens when there is at least one extra burning fluid parcel other than the two added at the inlet during every iteration of cellular automata. The value of N determines the value of P at which blowout happens. In experiments, this would correspond to the minimum reaction rate in the reaction field to ensure the chain reaction.

The 2D reaction field is divided into a regular square grid where the side of each grid is one unit long. In every iteration of the cellular automata, the grid is moved by two columns (a distance of 2 units) of vertices towards left. We consider the corresponding flow velocity to be $2U$. Whereas, in every iteration, the flame can propagate to its immediate Moore neighborhood. In the Moore neighborhood, the neighbors along x and y

axis are one unit distance away from the central site, and the neighbors along the diagonals are $\sqrt{2}$ unit distance away from the central site. This means, in every iteration, the flame travels $\sqrt{2}$ unit along the diagonal of the square grid and one unit along the *x* and *y* directions. As a result, the flame velocity is *U* along the *x* and *y* directions of the square grid of the cellular automata. Whereas, along the direction parallel to the diagonals of the grid, the flame propagates with a velocity of $\sqrt{2}U$. As a result, at equilibrium, when $P = 1$, for CA's corresponding to both combustor I and combustor II, flame is stabilized at an angle of 45^0 to the mean flow (Fig. 6.1). The component of mean flow velocity along the diagonals of the square grid is balanced by the flame velocity in the same direction. As *P* reduces, the average flame velocity reduces. Making the flame more and more parallel to the flow.

6.2 The flame dynamics close to lean blowout

The typical flame configuration observed at various values of *P* for combustor-I is shown in Fig. 6.3 and for combustor-II is shown in Fig. 6.4. Both combustor configurations exhibit similar flame dynamics. Reducing the value of *P* is equivalent to reducing the value of equivalence ratio. Here we observe that at lower values of *P*, flame holes are generated. Flame holes are the gaps in the flame front where the flamelets gets extinguished. The processes of initiation and recovery of flame holes create unsteadiness in the heat release rate. Nair and Lieuwen (2007) observed this phenomena in experiments with bluff-body stabilized flames and called it the first stage of blowout. They reported that during this stage, even though the flame is unsteady due to the formation and recovery of flame holes, the overall position and the qualitative behavior

of the flame remains the same. Chaudhuri *et al.* (2010) showed that during the 1st stage of blowout, the flame holes are formed due to the interaction of shear layer vortices with the flame front. However, during this stage, the recovery time for a flame hole is small enough that it ensures that the flame still remains in varicose mode (symmetrically distorted flame). A similar behavior is seen for the flame dynamics observed for P = 0.70, P = 0. 50, and P = 0.45 in Fig. 6.3 and Fig. 6.4. Here, the flame is distorted due to the formation of flame holes. Nevertheless, the flame holes recover fast enough, ensuring that the flame dynamics remain largely symmetric.

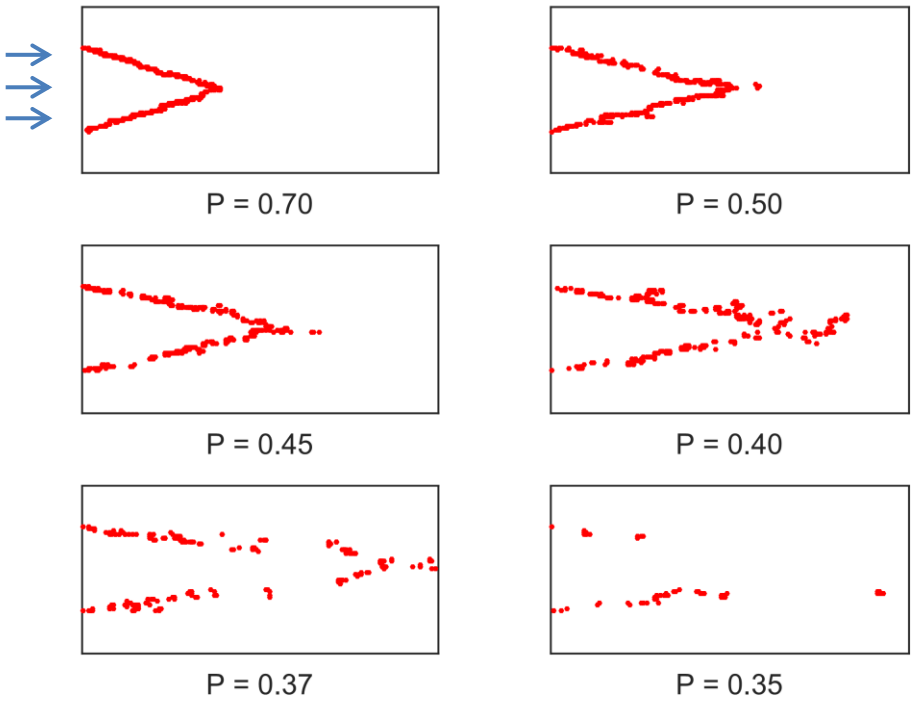

Figure 6.3: The typical snapshot of the conical flame for different values of probabilities of reignition (P). Note that the length of the flame reduces as value of P is reduced. There is growth of flame holes at lower values of P.

At lower values of P, we see asymmetric behavior for the flame dynamics (cases of P = 0.40 and P = 0.37 in Fig. 6.3). This is because the reduced value of P results in larger flame holes that take longer time periods to recover. Energy released per unit time reduces with formation of flame holes. However, when the recovery of flame holes happens, there is a burst of energy that is released. Since the formation of flame holes does not happen in a symmetric manner about the axis of the combustor, the bursts of energy also happen in an asymmetric manner. Similar asymmetrical behavior of flame is also observed in the experiments (Nair, 2006; Chaudhuri *et al.* 2010). However, in experiments, this asymmetry is enhanced by the formation of vortices along the shear layer at locations where the flame hole is formed due to the increased predominance of Kelvin-Helmholtz instability at these places. This results in the dominance of absolute instability at the locations of flame holes eventually leading to a sinus mode oscillation for the flame. This is also seen as the flapping of the flame.

Very close to blowout, at the final stage, the variation of the chemiluminescence fluctuation reduces. In figure 6.3 when P = 0.35, the flame is highly asymmetrical and flamelets are scattered along the flow field. The flame becomes columnar and parallel to the flow. This is indicative of the strain rates along the flame being close to extinction strain rates. In experiments, the formation of columnar flames before blowout was observed by Chaudhuri *et al.* (2010). In the model, as the probability to flame propagation reduces, the unburned parcel travels much more distance in the flow field before it starts to burn. This causes the average length of the flame to increase and the flame to be more and more parallel to the flow as we approach blowout.

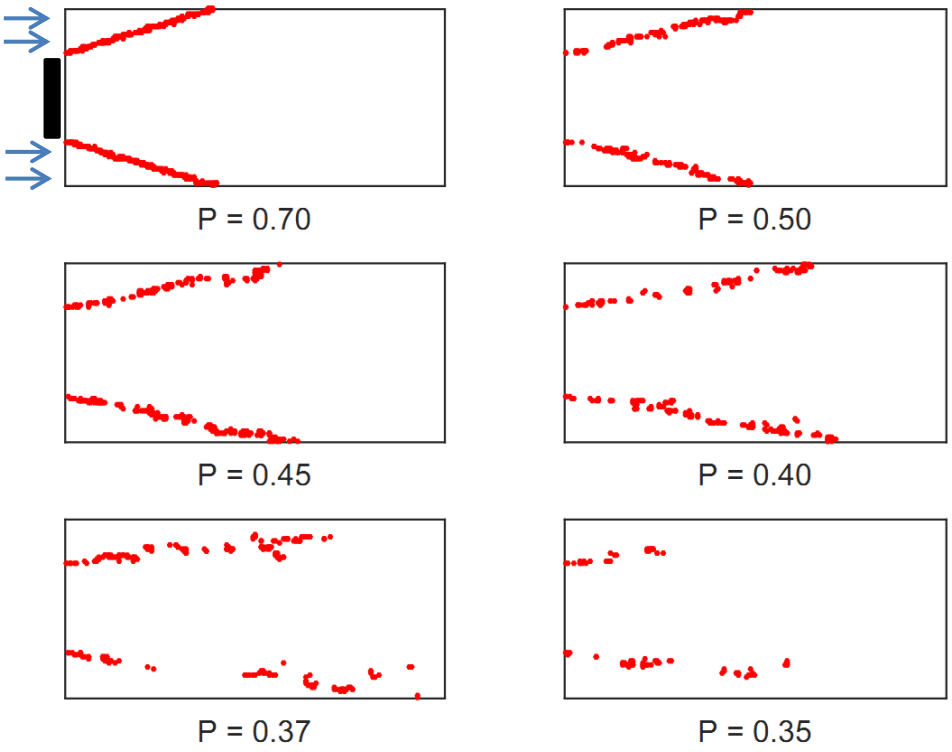

Figure 6.4: The typical snapshot of the flame for different values of probabilities of reignition (*P*) for a bluffbody stabilized flame. Note that the length of the flame reduces as value of *P* is reduced. There is growth of flame holes at lower values of *P*.

The total *CH** chemiluminescence intensity inside a bluff-body stabilized combustor was measured using a photomultiplier tube for different equivalence ratios. This measurement gives an indication of the unsteady reaction rate and hence the heat release rate inside the combustor. We compare this measured chemiluminescence intensity fluctuations at different equivalence ratios to the fluctuation of the population of flamelets inside the reaction field in the cellular automata model. Population of flamelets gives an estimate of heat release rate inside the combustor.

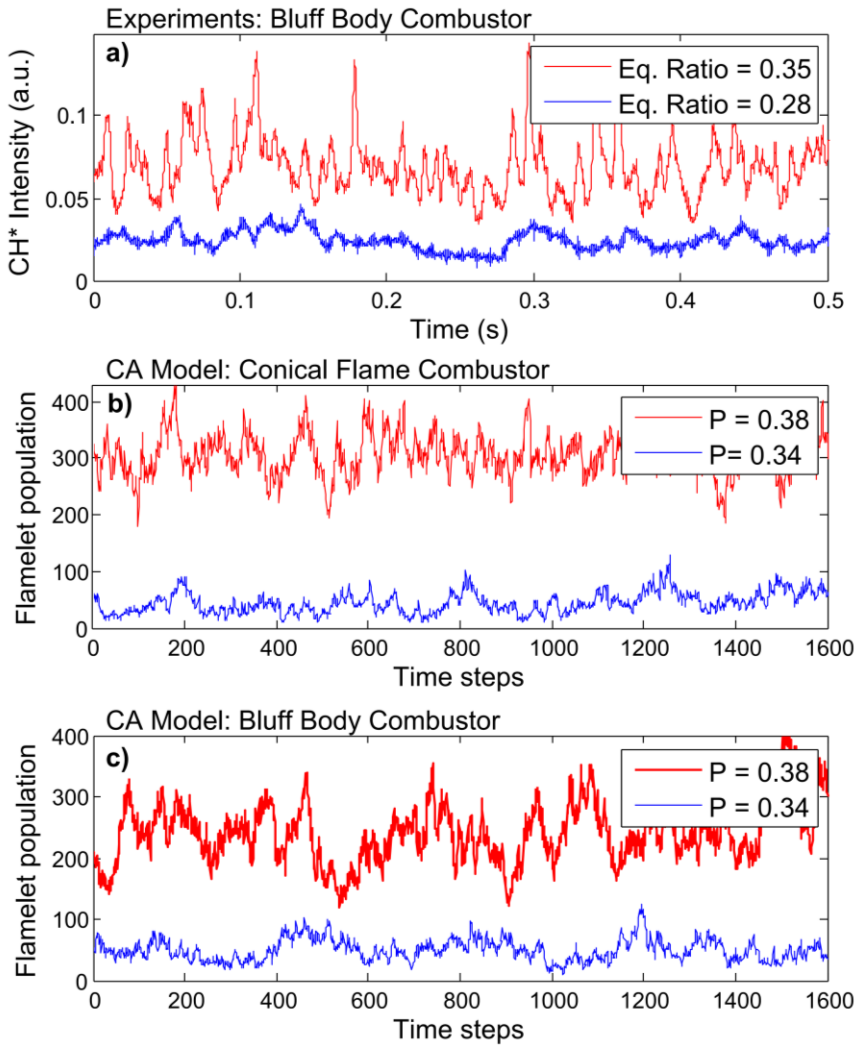

Figure 6.5: a) Variation of *CH** chemiluminescence intensity for different values of equivalence ratio away and near lean blowout from experiment. **b**) Variation of flamelet population obtained from model (conical flame) for different values of *P* as we approach blowout. **c**) Variation of flamelet population obtained from model (bluff body combustor) for different values of *P* as we approach blowout. As the combustor approaches blowout (i.e. when *Eq. Ratio* is reduced), the variations in the heat release rate reduces. Similarly, as *P* reduces, for the models of both combustors, the variation in flamelet population reduces.

We observe that there is a striking resemblance between the behavior of the model and the experiment. In both case, away from blowout, the variation of *CH** is higher compared to that close to blowout. In experiments, the increased variance of chemiluminescence fluctuations away from blowout (stage 2) is the result of vigorous flame flapping that is caused due to the growing tendency of the reactive flow to exhibit absolute instability (Chaudhuri 2010).

We also observe that close to the blowout, the oscillations have increased low-frequency content which can be attributed to the longer recovery times for the flame holes as we approach blowout. In experiments, the increase in low-frequency content for oscillations prior to blowout is reported previously by Nair & Lieuwen (2005).

6.3 Similarities of blowout with an absorbing phase transition

Population dynamics models can either be mean field based (MF) models such as a logistic model or models based on contact process (Marro and Dickman 1999, Hinrichsen 2000a). In mean field models, the dispersion effect of the population does not affect the population growth rate. For example, in the logistic model, the growth rate depends on the carrying capacity of the environment and the total population at any moment both of which are mean field measures. Whereas, in a contact process the population growth is dispersion limited and the spatial distribution of the existing population influences the growth of population. That is birth and death process at any spatial location is influenced not only by the mean field measures but the local characteristics of the population distribution. Our model that describes the population of flamelets in a reactive flow field is a type of contact process. In the model, the birth of flamelet at any spatial location is

influenced by the characteristics of the fluid parcel at that place and the states of the fluid parcels in its neighborhood with which the fluid parcel is in contact with (and hence a contact process).

In a contact process, the characteristics of extinction of population depend upon the dispersion characteristics of the system. Close to population extinction, the distribution of population becomes highly fragmented. This fragmentation further reduces the stability of the population. In Fig. 6.3 and Fig. 6.4, we can observe that at low values of *P*, the flame becomes more and more fragmented. This dispersion limited nature of population dynamics warrants that for a contact process, the population extinction is a threshold like process and is analogous to a critical phase transition (Obornay *et al.* 2005). In Fig. 6.6 we see that as *P* reduces, the average density of population of flamelets reduces. We see that the reduction in population density is nonlinear with *P*. Furthermore, beyond a threshold value of *P*, the density of population goes to zero indicating an extinction of flamelets in the reactive field. Similar observations are made in our experiments when the average *CH** chemiluminescence intensity from a bluff body stabilized combustor was measured using a photomultiplier tube. We observe that the average *CH** intensity reduces as equivalence ratio is reduced and goes to zero beyond a threshold value of equivalence ratio. We further note that the variation in average *CH** intensity with equivalence ratio or flamelet population with *P* are nonlinear. Thus, population extinction of flamelets that corresponds to flame blowout in a combustor seems to have the characteristics of a threshold like process analogous to a critical phase transition.

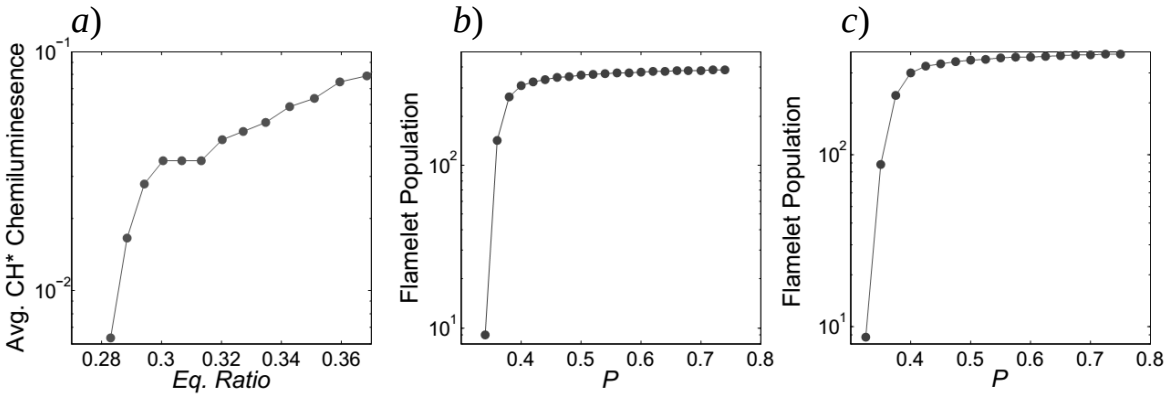

Figure 6.6: **a**) Variation of average *CH** intensity for different values of equivalence ratio obtained from the experiment. **b**) Variation of flamelet population for different values of P obtained from the population dynamics model for a conical flame. **c**) Variation of flamelet population for different values of P obtained from the population dynamics model for a bluff body stabilized flame.

In the cellular automata model, the flame oscillation prior to blowout exhibit a metastable state during the intermittent formation of large flame holes followed by rapid transition to a reactive state which is short lived and produces a burst of energy in the system. This can also be observed in the behavior of *CH** chemiluminescence intensity obtained from experiments just prior to flame blowout (Fig. 6.4a, *Eq. Ratio* = 0.28). Further, as the equivalence ratio is varied, the flame blows out. This flame blowout corresponds to the population extinction of flamelets in the CA model up on the reduction of *P*. In the context of population dynamics the extinct phase is called an absorbing state. Once reached, an absorbing state cannot be escaped by a mere dynamic transition (Hinrichsen, 2000). Transition to absorbing state is ubiquitous in problems of non-equilibrium phase transitions that fall under the universality class of directed percolations. The CA model that we use to describe flame blowout transitions to an extinct phase. Upon reaching

extinction, the system is frozen or trapped in the extinct phase. Thus, suggesting that reduction of probability of flame propagation P, beyond a threshold value cause the system to undergo a phase transition into an absorbing state.

6.5 Concluding remarks

Considering that a turbulent flame can be viewed as a collection of flamelets, we were able to recast the problem of flame stabilization in a turbulent combustor as a problem of population dynamics of flamelets. In this context, the birth process of a flamelet was considered to be equivalent to the process of ignition of the reactants and the process of extinction of flame equivalent to the death of a flamelet. Further, lean blowout corresponds to a scenario where the inability of the reactive flow to sustain the chain reaction results in the extinction of the population of flamelets in the flow field. A cellular automata model was constructed to capture the population dynamics of flamelets close to a flame blowout. We observed that the model can capture various dynamic characteristics of the flame close to lean blowout such as the stretching of the flame, the increase in the number of flame holes in the flame, reduction of average intensity of the flame, etc. Further, we observe that the cellular automata model that represent the dynamics of the turbulent combustor undergoes a phase transition to an absorbing state (the extinct phase) imitating flame blowout in the turbulent combustor.

CHAPTER 7

Conclusions and Outlook

The main focus of the present thesis was on characterizing the complex dynamics that a dump combustor with a bluff-body stabilized turbulent flame exhibits during transition from stable combustion to lean blowout. Using Multifractal Detrended Fluctuation Analysis (MFDFA), we were able to study the scaling characteristics of the pressure and chemiluminesence fluctuation. We observed that while we approach thermoacoustic instability, the multifractal spectrum width reduces to zero and as blowout is approached, the multifractal spectrum width increases. Thus we were able to propose a unifying description based on multifractality to both blowout and thermoacoustic instability where the onset of thermoacoustic instability can be considered as loss of multifractality and the approach to blowout as an increase in multifractal spectrum width. Further, we also show that Hurst exponent, in conjunction with equivalence ratio, can be used as a precursor to an impending blowout.

The dynamic characteristics of the pressure oscillations at different equivalence ratios were studied using recurrence quantification analysis (RQA). We showed that various recurrence parameters such as trapping time, Shannon entropy of the lines parallel to the diagonal and recurrence rate increase as we approach an impending blowout due to the increased aperiodicity of the oscillations close to blowout and hence can serve as precursors to blowout. We also showed that a method of recurrence quantification analysis that doesn't involve phase space reconstruction and instead analyzes the recurrence of the value of the state variable in time is effective at prognosis of dynamic

transitions in a turbulent combustor. Since such a method is computationally less expensive, it can be adopted for online diagnostics of thermoacoustic instability and blowout in turbulent combustors.

We observe that the turbulent combustor exhibits intermittency both prior to thermoacoustic instability and prior to lean blowout. Studying the characteristics of the corresponding recurrence plots, we observed that both intermittencies are possibly of Type II and are hence dynamically very similar. However, the high speed Mie scattering experiments showed that the flame dynamics corresponding to either intermittency is different due to the difference in the flame stabilization during both dynamic regimes. We also noted that the flame dynamics very close to blowout is largely affected by the intermittent formation of flame holes making the pressure oscillations just before blowout to be highly aperiodic. Even though we were successful in quantitatively characterizing the dynamics prior to blowout using recurrence quantification analysis, we were not able to systematically assert particular dynamical nature to the unsteady pressure or chemiluminesence fluctuations corresponding to the different flame dynamics observed very close to blowout (the 3 stages of blowout as described by Shanbhogue 2009). This should be the focus of a later study that intends to characterize the spatio-temporal dynamics of combustor close to lean blowout.

Finally, we were able to provide a low order model that could capture the complex dynamics. In the model, the problem of flame stabilization in a turbulent combustor is recast as a problem of population dynamics of flamelets. In this context, the birth process of a flamelet is equivalent to the process of ignition of the reactants and the process of extinction of a flamelet is equivalent to the death of the flamelet. Also, lean blowout is a

scenario where the inability of the reactive flow to sustain the chain reaction results in the extinction of the population of flamelets in the flow field. A cellular automata model was constructed to capture the population dynamics of free radicals close to flame blowout. The model is able to qualitatively mimic various dynamic characteristics of a turbulent flame close to lean blowout such as the stretching of the flame, the increase in the number of flame holes in the flame, reduction of average concentration of free radicals etc. Further, we observe that the cellular automata model that represents the dynamics of the turbulent combustor undergoes a phase transition to an extinct phase, imitating flame blowout in the turbulent combustor. The system is then trapped in this extinct phase from which the system cannot escape merely through a dynamic transition. Such a dynamic state is called an absorbing state and thus the transition to blowout can be considered as an absorbing phase transition.

In summary, we were able to characterize the complex scaling behavior of acoustic oscillations prior to blowout. We characterized the intermittency in acoustic pressure fluctuations from stable combustion to blowout. Through these analyses, we were able to obtain precursors to an impending blowout. We were able to suggest a low order model that mimics the complex dynamics prior to lean blowout based on the population dynamics of flamelets. We observed that transition to blowout in the context of this model can be considered as an absorbing phase transition.

The future work would involve identifying the specific dynamic states prior to blowout, characterizing the spatio-temporal behavior of the combustor at different dynamic states and thus identifying possible strategies to control both thermoacoustic oscillations and lean blowout.

APPENDIX A

Online detection of thermoacoustic instability using tools from symbolic time series analysis

In Chapter 3 and Chapter 4 of this thesis, we identified precursors to lean blowout based on RQA and multifractal analysis. These nonlinear techniques were first used to characterize oscillations leading to thermoacoustic instability. We extended those approaches to detecting an impending blowout. Previously, a nonlinear time series analysis technique, symbolic time series analysis was used to detect an impending blowout. However, the ability of this method to detect onset of thermoacoustic instability was never tested. In this Appendix, we show how symbolic time series analysis can be used to detect an impending thermoacoustic instability.

In the past, various techniques were introduced in order to detect and control instabilities in combustion systems. Poinsot *et al.* (1992), introduced a technique to control instabilities in gas turbine engines. In this technique, the pressure fluctuation in the combustion chamber is measured and a delayed signal (control signal) is generated based on the pressure fluctuation signal, which in turn is used to modulate the fuel pressure inside the fuel line. By selecting an appropriate delay for the control signal, they were able to actively control the instability. Hobson *et al.* (2000) analyzed the stability of industrial gas turbine engines by monitoring the casing vibration and the pressure fluctuations inside the combustion chamber. They analyzed the stability of the engine in terms of frequency and bandwidth of the principal peak in the vibration and pressure

spectra. It was observed that as the system approached the stability limit, the bandwidth of the principal peak decreased. This was an indication for damping approaching zero near the stability limit. In a similar way, Lieuwen (2005) used autocorrelation of the pressure signals inside the combustor to characterize the damping of the system and thereby predict the stability margin. The techniques used above rely on detecting the characteristics of the instability to detect it. In our work we were interested in understanding the dynamics of the transition regime from combustion noise to combustion instability in order to come up with a precursor which can forewarn the operators about an impending instability.

In the past, there have been a few studies that focused on the dynamics of the regime transition from stable to unstable operation of a combustor. Chakravarthy *et al.* (2007) in an experimental study suggested that a lock on mechanism between vortex shedding and duct acoustics was responsible for the transition. When the vortex shedding and the acoustic modes are not locked on, the system has low amplitude broadband noise and once the lock-on happens, the system has high amplitude tonal oscillations. Further, Gotoda *et al.* (2011) reported that in a turbulent combustor, as the equivalence ratio is varied from stoichiometric to lean limits, transition from stochastic fluctuations(combustion noise) to periodic oscillation happened through a state of low dimensional chaos.

Recently, Nair *et al.* (2013) studied the characteristics of the transition region using tools from dynamical system theory. They established that combustion noise resulting from combustion of a turbulent flow in a confined enviornment is not stochastic and is in fact chaos of moderately high dimension (of the order of 8 to 10). Further, it was shown that

the onset of instability is essentially a transition from chaos to order. They used a test for chaos, known as 0–1 test for chaos (Gottwald & Melbourne 2004), as a measure of the proximity of the combustor to an impending instability. Nair *et al.* (2013) also indicated that the transition from chaos to order happened through intermittency (Nair & Sujith 2013). In this context, they introduced recurrence parameters as precursors to the impending instability in a practical gas turbine combustor (Nair *et al.*, 2012). In this appendix, we introduce a method based on symbolic time series analysis in order to detect the proximity of a particular dynamic state of the combustor to that of instability by analyzing the peculiar patterns in time series data of unsteady pressure fluctuations born out of the dynamics in the transition regime.

Symbolic time series analysis provides a simpler way to analyze the dynamics of nonlinear systems (Ray, 2004). A symbolic time series can be generated from a time series obtained from experiments or simulations in various ways. The different approaches to construct a symbolic time series is described by Daw *et al.* (2003). Rajagopalan & Ray (2006) and Subbu & Ray (2008) describe different methods used to generate a symbolic time series. Further they also describe a procedure for early detection of anomalous behaviors in dynamical systems based on symbolic dynamic filtering (SDF).Application of anomaly detection using SDF was carried out successfully in various physical systems (Gupta *et al.*, 2007, Bhambare *et al.*, 2008). Gupta *et al.* (2006), Chakraborty *et al.* (2008) and Datta *et al.* (2006) used SDF to detect the extinction events in a mathematical model describing a pulse combustor. Dynamics of a spark ignition engine was characterized by Daw *et al.* (1998) using symbolic time series analysis.

Mukhopadhyay *et al.* (2013) used symbolic time series analysis for prediction of lean blow out in laboratory-scale gas turbine combustors.

In this chapter, we describe a methodology to detect the proximity of the dynamic state of a combustor to an impending instability (Unni *et al.* 2013). This methodology uses symbolic time series analysis for identifying the precursor to the impending instability. A detailed description of symbolic time series analysis is given in the following section.

A.1 Symbolic time series analysis

Symbolic time series analysis is a technique used in order to encode the complex dynamics of a system embedded in a time series signal $\{T[k]|k = 0 \dots N-1\}$ into a set of finite number of variables. The particular analysis technique used in here involves a three-step process. The first step is the generation of the symbolic time series $\{ST[k]\}$ from the actual time series. The second step is the construction of a state vector SVp corresponding to the symbolic time series, representing the dynamics of the state that is responsible for the generation of the actual time series $\{T[k]|k = 0 \dots N-1\}$. In the third step, an anomaly measure M is defined which serves as an indicator of the proximity of a dynamical state to the stability margin. Detailed explanations for these processes are given in the following subsections.

A.1.a. Construction of a symbolic time series

Consider the time series signal $\{T[k]|\ k = 0 \dots N-1\}$. This signal is a discrete function in time represented by the N data points, N being the length of the time series signal. The data point at the k^{th} instant is $T[k]$. Each of the data point has a particular value$T[k]$ and

a particular time stamp 'k' associated with it. Now in order to construct the symbolic time series from the time series signal $\{T[k] | \, k = 0 \ldots N-1\}$, the N data points constituting the time series signal are partitioned into a mutually exclusive and exhaustive set of finitely many segments. Here, the partitioning is performed by dividing the points into different sets based on the range of the instantaneous value ($T[k]$) in which they lie (illustrated in Fig. A.1a, the details on how the upper and lower limit of value of $T[k]$ for each partition is selected and how the number of partitions is decided are described later). This technique of directly partitioning the time series is called 'simple partitioning'. Further descriptions of partitioning techniques are described by Ray (2004) and Mukherjee & Ray (2014). Here, the number of segments for partition is fixed to be 10.

Once the data points are partitioned, each partition is represented by a particular symbol (For the purpose of illustration, assume that we are partitioning the data points into 4 segments,α, β, γ and δ).Now, the value of the time series data at each instant $k$is replaced by the symbol corresponding to the partition to which that particular data point belongs. Thus a symbolic time series is generated (Fig. A.1.b).

A.1.b. Construction of Probabilistic Finite State Automata (PFSA)

Once the symbolic time series $\{ST[k]\}$is generated, a probabilistic finite time automata is constructed to represent the dynamic state that generated the time series $\{T[k] | k = 0 \ldots N-1\}$. The main assumption in construction of PFSA is that the symbolic process (represented by the symbolic series) under all conditions can be approximated as a Markov chain of order D (D- Markov machine) representing a quasi- stationary stochastic process. For a D- Markov machine, probability of occurrence of a new symbol depends

only on the last *D* symbols, implying that the memory of the system is only extended up to *D* past observational instances. With this assumption, the states of the *D*- Markov machine are essentially represented by a word of length *D* in the symbol string of the symbolic time series. Hence, for a symbolic series represented by *P* symbols, the number of possible states in a *D*- Markov machine is P^D. With increase in the word size *D*, the memory embedded in the Markov states of the PFSA increases.

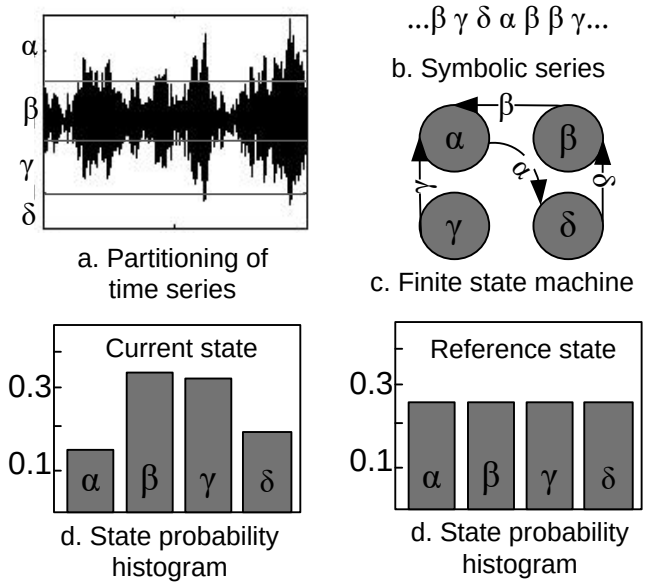

Figure. A.1. Construction of symbolic state probability histogram from a finite time - time series data (here, we use the unsteady pressure time series data from a combustor). Note that the different steps involved are a) Simple partitioning, b) generation of a 'symbolic sequence', c) construction of a 'finite state machine', and d) developing a 'state probability histogram'(representative of state probability vector).

However, as *D* increases, the total number of possible states for PFSA increases and hence the computational expenses needed to construct the PFSA also increases. Keeping

this in mind, we have restricted the word size D to 1. Hence, the number of states possible for the PFSA constructed in this work is P.

It is seen from the experiments that with a word size of 1 itself, the predictability of the control system for the instability analysis is quite impressive although D>1 is expected to produce more accurate results at the expense of significant increase in computational effort.

A.1.c. Construction of the Anomaly measure

First step in constructing an anomaly measure is identifying a reference state. The anomaly measure in this particular work is expected to indicate the proximity of the current state to the onset of instability (here, the current state is the state for which the anomaly measure is estimated). Hence, it is only natural to select the dynamical state corresponding to the onset of instability as the reference state. Once the reference state is identified (in the context of this work, a method for identifying the appropriate reference state, i.e. the state that is considered as the onset of instability or stability margin is described in Section 4), then the data points in the pressure time series corresponding to the reference state is partitioned into P mutually exclusive and exhaustive segments in such a way that each of the segment contains approximately equal number of data points. The partition technique used here is equiprobable partitioning, which is based on maximization of information entropy, as seen in Fig. A.1.The implication is that when PFSA is constructed using this partition, the reference state will have a uniform probability for all symbolic states (P^0 is the state probability vector for the reference state). Once the partitioning of reference state is performed, same partition is used in order to construct the symbolic time series corresponding to the other dynamical states.

Hence, when PFSA is constructed for dynamical states other than the reference dynamical state, the probabilities associated with symbolic states have a non-uniform distribution (P^k is the state probability vector for the current state). Thus, an anomaly measure, which is an indicator of proximity of a dynamical state to the reference state, is defined as follows,

$$M = Cos^{-1}\left(\frac{< P^k P^0 >}{\|P^k\|\|P^0\|}\right)$$

Here, $< P^k P^0 >$ is the inner product of the state probability vectors $P^k$and $P^0$and $\|P\|$denotes the Euclidian norm of the vector P. More details of anomaly detection using symbolic logic have been described by Ray (2004).

A.2 Results and discussions.

In this study, the experiments were conducted as follows. For a given value of fuel flow rate (for example, 28 SLPM), the air flow rate was varied in a quasi-steady manner. The initial airflow rate was chosen in such a way that it corresponded to an equivalence ratio of one. Subsequently air flow rate was increased, thereby reducing the equivalence ratio. At each equivalence ratio, the dynamics of the pressure fluctuations inside the combustor was recorded by acquiring the unsteady pressure time trace using a piezoelectric transducer. The time series data of these pressure fluctuations at various air flow rates are then used to perform symbolic time series analysis for anomaly detection. As described in Section 2c, the first step in the analysis is identifying an appropriate reference dynamical state. In order to identify that, we adopt the following procedure. Henceforth, we refer to this procedure as the training drill for online anomaly detection.

The aim of the training drill is to identify that particular pattern of oscillations in the combustor, which is to be considered as the appropriate margin for the operational regime of the combustor such that instability can be avoided. In order to identify such a margin, we apply anomaly detection technique to the normalized time series data taking a unit amplitude sinusoidal wave with a frequency approximately equal to the instability frequency(in this context, the instability frequency corresponds to the natural frequency of the combustor at which an instability is expected)as the reference state. On doing so, we essentially are comparing the pattern of the normalized time series representing a particular dynamical state to that of a state of instability. Hence, an anomaly measure defined in this context as described in the § A.1 will approach zero as we approach a state of instability (Fig. A.2a and Fig. A.3a). Due to the particular nature of the partitioning performed in this work (simple equiprobable partitioning), this decrease in anomaly measure is rather rapid and very close to the onset of instability (note that the anomaly ratio is almost constant prior to the first drop). Nevertheless, this decrease in anomaly measure is an indicator for the dynamics of the state being close to that of a limit cycle behavior. Hence, from this training drill, we select the time series corresponding to point 'A' (marked in both Fig. A.2a and Fig. A.3a) as the representative time series for the reference dynamical state to be used in the online anomaly detection for the respective cases. However, depending up on the discretion of the operator and the design of a particular combustor, dynamic states further close to instability can also be used as the reference state. Further, it is to be noted that a rise is pressure amplitude is not necessarily suggestive of presence of instability. The rise in the amplitude of pressure signals could even correspond to an increase in the intensity of combustion noise. Whereas, with the

aforementioned technique, we can clearly identify whether we are approaching an impending instability since a decrease in the anomaly measure is a sure indicator of the increased presence of sinusoidal component in the time series.

Once the reference state for online anomaly detection is fixed, the anomaly measure for online detection of an impending instability is defined as described in § A.1. Examining the variation of anomaly measure with airflow rate, we see that (Fig. A.2b and Fig. A.3b)as the system approaches the reference state, the anomaly measure starts to reduce; i.e., the angle between the PFSA of the reference state and the current state approaches zero as the current state approaches the reference state. Furthermore, unlike in the case of anomaly measure defined for the training drill, the anomaly measure for online detection starts reducing towards zero much before the reference dynamical state. These behaviors are explained in the following paragraphs.

At low airflow rates (i.e., near stoichiometric equivalence ratios), the pressure fluctuation inside the combustor is mainly due to combustion and flow noise. These oscillations have amplitudes of the order of 200 Pa (Fig. A.4a). Further, it has been already shown that these oscillations are chaos of moderately high dimension (8 to 10 dimensions) (Nair *et al.*, 2013). Hence when the PFSA is formed for the time series corresponding to combustion and flow noise, using the partition corresponding to the time series representing the reference state (A), most of the data points fall in those symbolic segments which correspond to low values of $|P|$. Hence, the corresponding PFSA has a probability distribution as seen in the Fig. A.4e.

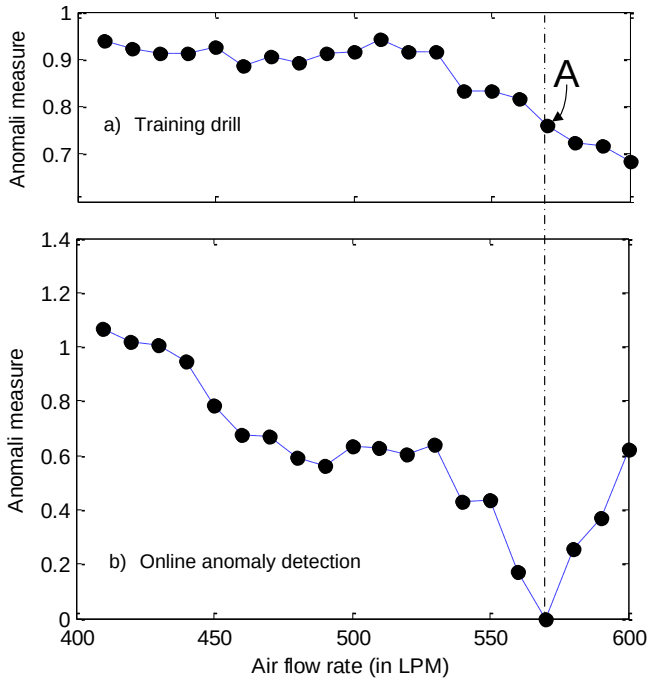

Figure A.2: Variation of anomaly measure for combustor with a swirl stabilized flame. a) Represent the training drill and b) represent the online anomaly detection drill. The reduction of anomaly measure as we approach the reference state (*A*) is the precursor to instability.

Now as we increase the airflow rate (i.e., move towards lean equivalence ratios), the pressure oscillations start to become intermittent. This intermittent behavior of the pressure signals arise from the fact that the state point corresponding to the dynamical state responsible for these oscillations follow a homoclinic orbit in the phase space (Nair & Sujith, 2013).In this homoclinic orbit, the state point alternates between a chaotic attractor corresponding to the low amplitude fluctuations to an attractor corresponding to the high amplitude limit cycle oscillations in an apparently random fashion. As the equivalence ratio decreases away from the stoichiometric equivalence ratio, the time spent by the state point in the chaotic attractors reduces and the time spent in the attractor

corresponding to the limit cycle increases. In the time series, the effect of this dynamical behavior is reflected.

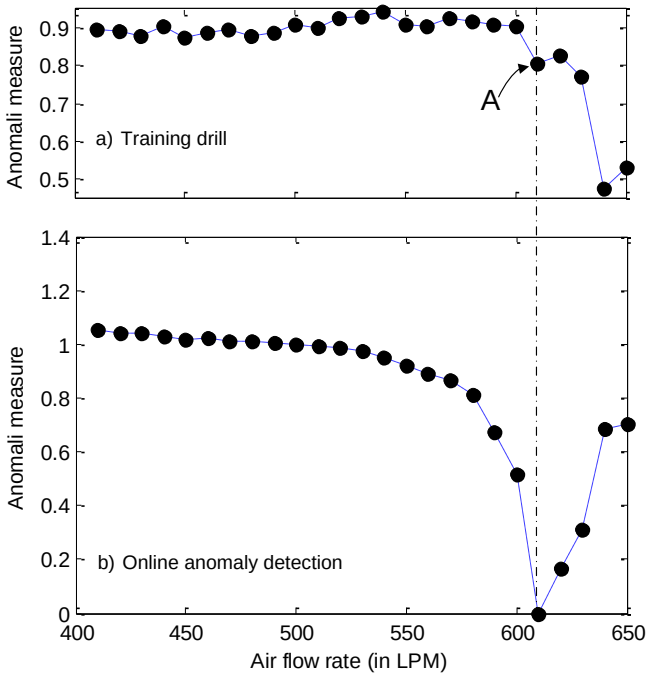

Figure A.3: Application of anomaly detection technique to a combustor with bluff body stabilized flame. a) Represent the training drill and b) represent the online anomaly detection drill. The reduction of anomaly measure as we approach the reference state (*A*) is the precursor to instability.

During intermittency, the time series is characterized by alternating low amplitude chaotic oscillations and high amplitude limit cycle oscillations. As we approach closer to instability, in the time series, the duration for which the limit cycle oscillations are observed increases and the duration of chaotic oscillation decreases. This implies the probability associated with the symbols corresponding to the high amplitude oscillations increases as we approach the instability. Also, the symbol sequence increasingly matches to that of the reference state (a near limit cycle state).Ultimately at the reference state all

the symbols have an equal probability associated with it (Fig. A.4g). If we move beyond reference state, the amplitude of the time series increases due to increased proximity to the instability and hence the symbols corresponding to the higher amplitudes have a higher occurrence probability (Fig. A.4h). This leads to an increase in the anomaly measure beyond the reference state. From Fig. A.2b and Fig. A.3b it can be observed that a state before and beyond the reference state can have the same value of anomaly measure.

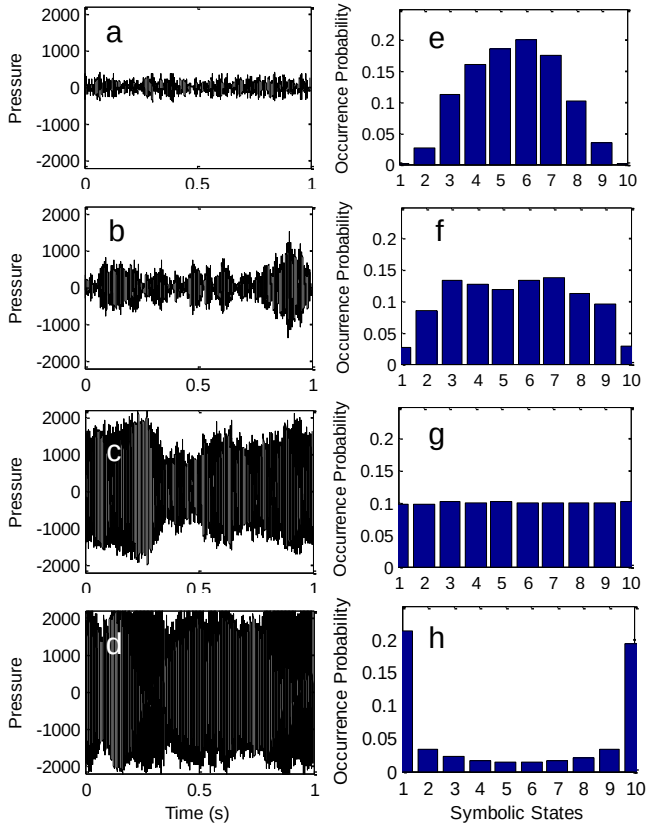

Figure A.4: The variation of signal characteristics and corresponding PSFAs as the system approaches instability. a) and e) represent combustion noise at equivalence ratio 1. b) and f) represent an intermediate state, c) and g) represent the reference state and d) and h) represent a state beyond the reference state.

However, in such a case, they can be distinguished by comparing the probability distribution of the symbolic states. For example, Fig. A.4b and Fig. A.4d represent two time series with similar value for anomaly measure. However, comparing the corresponding occurrence probability distribution, it is clear that Fig. A.4d represents a dynamical state beyond the reference state. From the above discussions, it is clear that the anomaly measure approaching zero is a precursor to the onset of instability.

In essence, using symbolic time series analysis, we are able to compare the patterns present in the time series corresponding to any dynamical state to that of the reference state by defining a vector measure (state probability vector, Fig. A.3) corresponding to each pattern. We see that the occurrence probability distribution of symbolic state varies continuously as we approach the reference state (Fig. A.3). We exploit this behavior of state probability vectors to define the anomaly measure which indicates the proximity of any state to the reference state. Since the particular patterns found in the pressure time series arises due to intermittency and intermittency is a dynamic behavior, time series corresponding to other measurements (such as heat release rate fluctuations, temperature fluctuations etc.) from the combustion system must also exhibit similar patterns close to instability. Hence, such measurements also could be used in a similar fashion to predict the onset of instability.

A.3 Concluding remarks

Anomaly detection technique, a novel strategy of online prediction of an impending instability is developed based on symbolic time series analysis. A precursor for an impending instability, i.e. the anomaly measure, was identified from unsteady pressure

measurements for two types of combustors (a swirl stabilized combustor and a bluff body stabilized combustor). Using anomaly detection technique, we were able to compare the pattern of a time series at any instant to that of a reference pattern and thereby quantify the proximity of the instantaneous dynamical state to a reference dynamical state (a dynamical state close to onset of instability). In this context, a novel method of identifying an appropriate reference state for online instability detection, i.e. the training drill, was introduced. The current technique of anomaly detection uses a simple method for partition of time series data known as simple equiprobable partition. More research has to be performed in order to identify the optimal partitioning technique to be used for predicting an impending instability in a combustor. Further, the effects of increasing the word size D for the formation of PFSA on the predictive capabilities of anomaly measure also have to be studied. However, anomaly measure thus identified was able to indicate the proximity of the combustion system to regimes of instability for both the combustors.

APPENDIX B

Multifractal detrended fluctuation analysis (MFDFA)

Detrended fluctuation analysis (DFA) can be used to characterize the multifractal charecteristics of a time series, *P*(*t*). First, the time series is mean adjusted to get a cumulative deviate series $y_k$as,

$$y_k = \sum_{t=1}^{k}(P(t) - m) \quad \text{where, } m \text{ is the mean of time series } P(t).$$

The deviate series is then separated into an integer number n_w of non-overlapping segments of equal width w $(y(i), i = 1\ to\ n_w)$. A local polynomial fit $\bar{y}_i$ is made to the deviate series y_i, and the fluctuations about the fit are obtained by subtracting the polynomial fit from the deviate series. Now, we define a structure function F_w^q, of order q and span *w* as,

$$F_w^q = \left(\frac{1}{n_w} \sum_{i=1}^{n_w} \left(\sqrt{\frac{1}{w} \sum_{t=1}^{w} (y_i(t) - \bar{y}_i)^2} \right)^q \right)^{\frac{1}{q}}$$

Structure function represents the divergence rate of non-stationary, detrended fluctuations. F_w^q is a function of both the order q and span *w*. The generalized Hurst exponent of the order q, H_q, is the slope of the linear regime in a log-log plot of F_w^q, for a range of span sizes w. For mono fractal and non-fractal signals, is constant with q. H_q varies with q for multifractal signals. That is, the scaling of fluctuation is depended up on

the amplitude of the fluctuation. The variation of H_q with q can alternatively be represented as a spectrum of singularities $f(\alpha)$ through a Legendre transformation.

$$\tau_q = qH_q - 1\,; \qquad \alpha = \frac{\partial \tau_q}{\partial q}\ ;\ \text{and}\ \ f(\alpha) = q\alpha - \tau_q$$

The curve between $f(\alpha)$ and α is called the multifractal spectrum which gives the information about the varying fractal nature of the signal.

REFERENCES

Abarbanel, H. D. I., Brown, R., Sidorowich, J. J. and Tsimring, L. (1993). The analysis of observed chaotic data in physical systems. *Rev. Mod. Phys*., **65**, 1331–1392.

Anderson, R. M., and May, R. M. (1981). The population dynamics of microparasites and their invertebrate hosts. *Philosophical Transactions of the Royal Society of London B: Biological Sciences* **291(1054)**, 451-524.

Arino, J., Davis, J. R., Hartley, D., Jordan, R., Miller, J. M., and Van Den Driessche, P. (2005). A multi-species epidemic model with spatial dynamics. *Mathematical Medicine and Biology* **22(2)**, 129-142.

Bake, F., Richter, C., Mühlbauer, B., Kings, N., Röhle, I., Thiele, F., and Noll, B. (2009). The entropy wave generator (EWG): a reference case on entropy noise. *Journal of Sound and Vibration* **326(3)**, 574-598.

Batchelor, G. K., and Townsend, A. A. (1949). The nature of turbulent motion at large wave-numbers. *In Proceedings of the Royal Society of London A: Mathematical, Physical and Engineering Sciences* **199**, 238-255.

Bellows, B. D., Neumeier, Y. and Lieuwen, T. (2006). Flame transfer function saturation mechanisms in a swirl-stabilized combustor, *J. Propul. Power* **22 (5)**. 1075–1084.

Bhambare, K. S., Gupta S., Mench, M. M., Ray, A. (2008). A Carbon Monoxide Sensor in Polymer Electrolyte Fuel Cells based on Symbolic Dynamic Filtering, *Sensors and Actuators B: Chemical*, **134 (2)**, 803–815.

Chakraborty, S., Gupta, S., Ray, A. and Mukhopadhyay, A. (2008) Data-Driven Fault Detection and Estimation in Thermal Pulse Combustors, *Proceedings of the Institute of Mechanical Engineers, Part G: J. Aerospace Eng.* **222 (8)**, 1097–1108.

Chakravarthy, S. R., Sivakumar, R. and Shreenivasan, **O. J.** (2007). Vortex-acoustic lockon in bluff-body and backward-facing step combustors, *Sadhana* **32**, 145–154.

Chaudhuri, S., Kostka, S., Renfro, M. W. and Cetegen, B. M. (2010). Blowoff dynamics of bluff body stabilized conical premixed flames. *Combust. Flame* **157**, Issue 4, 790-802.

Cheng, S. I. and Kovitz, A. A. (1958). Theory of Flame stabilization by a Bluff body, *Proc. Comb. Inst.* **7**, 681-691.

Chiu, H. H. and Summerfield, M. (1974). Theory of combustion noise. *Acta Astronautica* **1(7-8)**, 967–984.

Culick, F. E. C. (1970). Stability of longitudinal oscillations with pressure and velocity couping in a solid propellant rocket. *Combustion Science and Technology*, **2**, 179–201.

Culick, F. E. C. (1976a). Nonlinear behavior of acoustic waves in combustion chambers-i. *ACTA Astronautica*, **3**, 715–734.

Culick, F. E. C. (1976b). Nonlinear behavior of acoustic waves in combustion chambers-ii. *ACTA Astronautica*, **3**, 735–757.

Culick, F. E. C. (1994). Some recent results for nonlinear acoustics in combustion chambers. *AIAA Journal*, **34**, 146–169.

Culick, F. E. C. (1988). Combustion instabilities in liquid-fueled propulsion systems: an overview. In AGARD Conference for Combustion Instabilities in Liquid Propulsion Systems, NATO. Seuille-Sur-Seine, France.

Culick, F. E. C. (2006). Unsteady motions in combustion chambers for propulsion systems.,volume AG-AVT-039. RTOAGARDograph.

Datta, S., Mukhopadhyay, A. and Sanyal, D. (2006). Use of temporal irreversibility of symbolic time series for early detection of extinction in thermal pulse combustors, *Proceedings of IMECE – ASME*, IMECE2006-16249.

Daw, C. S., Finney, C. E. A. and Tracy, E. R. (2003) A review of symbolic analysis of experimental data, *Review of Scientific Instruments,*, **74 (2)**, 915–930.

Daw, C. S., M. B. Kennel, C. E. A. Finney, F. T. (1998). Connolly, Observing and modeling nonlinear dynamics in an internal combustion engine, *Phy. Rev.* E., **57 (3)** 2811–2819.

De Zilwa, S. R. N., Uhm, J. H., and Whitelaw, J. H. (2000). Combustion Oscillations Close to the Lean flammability Limit, *Combust. Sci. Technol.* **160**, 231–258.

Domen, S., Gotoda, H., Kuriyama, T., Okuno, Y., and Tachibana, S. (2015). Detection and prevention of blowout in a lean premixed gas-turbine model combustor using dynamical system theory. *Proc. Combust. Institute* **35**, 3245-3253.

Dowling, A. P. (1997). Nonlinear self-excited oscillations of a ducted flame. *Journal of Fluid Mechanics*, **346**, 271–290.

Fichera, A., Losenno, C. and Pagano A. (2001). Experimental analysis of thermo-acoustic combustion instability. *Applied Energy*, **70**, 179–191.

Frisch, U., *Turbulence: The legacy of A. N. Kolmogorov*. Cambridge University Press, Cambridge, UK, 1995.

Glassman, I., (1996) *Combustion*, 3rd Edition, Academic Press, San Diego.

Goh, C. S., and Morgans, A. S. (2013). The influence of entropy waves on the thermoacoustic stability of a model combustor. *Combustion Science and Technology*, 185(2), 249-268.

Gokulakrishnan, P., Pal, S., Klassen, M., Hamer, A., Roby, R., Kozaka, O., and Menon, S. (2006). Supersonic combustion simulation of cavity-stabilized hydrocarbon flames using ethylene reduced kinetic mechanism. In Proceedings of the AIAA/ASME/SAE 42nd Joint Propulsion Conference, Sacramento, CA, July (pp. 9-12).

Gopalakrishnan, E. A. and Sujith, R. I. (2015). Effect of external noise on the hysteresis characteristics of a thermoacoustic system, *Journal of Fluid Mechanics*, **776**, 334-353.

Gotoda, H., Amano, M., Miyano, T., Ikawa, T., Maki, K. and Tachibana, S. (2012). Characterization of complexities in combustion instability in a lean premixed gasturbine model combustor. *Chaos* **22**, 043128.

Gotoda, H., Nikimoto, H., Miyano, T., and Tachibana, S. (2011). Dynamic properties of combustion instability in a lean premixed gas-turbine combustor. *Chaos* **21**, 013124.

Gotoda, H., Shinoda, Y., Kobayashi M., Okuno, Y. and Tachibana S. (2014). Detection and control of combustion instability based on the concept of dynamical system theory. *Physical Review* E **89**, 022910

Gottwald, G. A., Melbourne, I., (2004). A new test for chaos in deterministic systems, *Proc. R. Soc. Lond.* A, **406**, 603–611.

Gupta, S., Ray, A., Keller, E. (2007). Symbolic Time Series Analysis of Ultrasonic Data for Early Detection of Fatigue Damage, *Mechanical Systems and Signal Processing*, **21 (2)**, 866–884.

Gupta, S., A. Ray, Mukhopadhyay, A. (2006). Anomaly Detection in Thermal Pulse Combustors, *Proceedings of the Institution of Mechanical Engineers, Part I: J. Systems and Control Eng.*, **220 (5)**, 339–351.

Harikrishnan, K. P., Misra R., Ambika G. and Amritkar, R. E. (2010). Computing the multifractal spectrum from time series: An algorithmic approach, *Chaos*, **19**, 143129

Hegde, U. G., Reuter, D., Daniel, B. R. and Zinn, B. T. (1987). Flame Driving of Longitudinal Instabilities in Dump Type Ramjet Combustors. *Combustion Scence and Technology*. **55**. 125-138.

Hinrichsen, H. (2000). Non-equilibrium critical phenomena and phase transitions into absorbing states. Advances in physics, 49(7), 815-958.

Hobson, D. E., Fackrell, J. E. and Hewitt, G. (2000). Combustion instabilities in industrial gas turbines: Measurements on operating plant and thermoacoustic modeling, *J. Eng. Gas Turbines Power*; 122, 420–428.

Hosseini, S. M. R. and C. J. Lawn, Nonlinearities in the thermo-acoustic response of a v premixed swirl burner. In 12th International Congress on Sound and Vibration. Lisbon, Portugal, 2005.

Huber, A. and Polifke, W. (2009a). Dynamics of practical premix flames, part i: Model structure and identification. *International Journal of Spray and Combustion Dynamics*, **1(2)**, 199–229.

Huber, A. and Polifke, W. (2009b). Dynamics of practical premix flames, part ii: Identification and interpretation of cfd data. *International Journal of Spray and Combustion Dynamics*, **1(2)**, 229–250.

Hurst, H. E. (1951). Long-term storage capacity of reservoirs. *Trans. Am. Soc. Civil Eng.* **116**, 770–799.

Ihlen, E. A. (2012). Introduction to multifractal detrended fluctuation analysis in Matlab. *Frontiers in physiology* **3**. 00141.

Iwanski, J. S., and Bradley, E. (1998). Recurrence plots of experimental data: To embed or not to embed?. *Chaos: An Interdisciplinary Journal of Nonlinear Science*, **8(4)**, 861-871.

Jahnke, C. C., and Culick, F. E. (1994). Application of dynamical systems theory to nonlinear combustion instabilities. *Journal of Propulsion and Power*, **10(4)**, 508-517.

Jegadeesan, V. and Sujith, R. I. (2013). Experimental investigation of noise induced triggering in thermoacoustic systems. *Proceedings of the Combustion Institute*, **34(2)**, pp.3175-3183.

Juniper, M. P. (2011). Triggering in the horizontal Rijke tube: non-normality, transient growth and bypass transition. *Journal of Fluid Mechanics*, **667**, 272–308.

Juniper, M. P. (2012). Triggering in thermoacoustics. *International Journal of Spray and Combustion Dynamics*, 4(3), 217-238.

Kabiraj, L. and Sujith, R. I. (2012). Nonlinear self-excited thermoacoustic oscillations: intermittency and flame blowout, *Journal of Fluid Mechanics*, **713**, 376-397.

Kabiraj, L. and Sujith, R. I. (2012). Nonlinear self-excited thermoacoustic oscillations: intermittency and flame blowout. *J. Fluid Mech.* **713**, 376–397.

Kabiraj, L. and Sujith, R. I., (2011). Investigation of subcritical instability in ducted premixed flames. In ASME 2011 Turbo Expo: Turbine Technical Conference and Exposition. American Society of Mechanical Engineers. 969-977.

Kabiraj, L., Wahi, P., and Sujith, R. I. (2012a). Bifurcations of Self-Excited Ducted Laminar Premixed Flames, *Journal of Engineering for Gas Turbine and Power*, **134**, Article Number 031502.

Kabiraj, L., Wahi, P. and Sujith, R. I. (2012b). Investigating Dynamics of Combustion Driven Oscillations Leading to Lean Blowout, Fluid Dynamics Research, **44**, 031408.

Kabiraj, L., Wahi, P. and Sujith, R. I. (2012c). Route to chaos for combustion instability in ducted laminar premixed flames, *Chaos*, **22**, 023129.

Kantelhardt, J. W. (2011). Fractal and multifractal time series. In R. A. Meyers (ed.), *Mathematics of Complexity and Dynamical Systems*. Springer 463–487.

Kantelhardt, J. W., Zschiegner, S. A., E. Koscielny-Bunde, S. Havlin, A. Bunde, and Stanley, H. E. (2002). Multifractal detrended fluctuation analysis of non-stationary time series. *Physica A* **316**, 87–114.

Kapur, V., Troy, D., and Oris, J. (1997). A sustainable fishing simulation using mathematical modeling and database access through the World Wide Web. Crossroads, **4(1)**, 9-12.

Kareiva, P., Mullen, A., and Southwood, R. (1990). Population dynamics in spatially complex environments: theory and data [and discussion]. *Philosophical Transactions of the Royal Society of London B: Biological Sciences*, **330(1257)**, 175-190.

Kashinath, K. (2013). *Nonlinear thermoacoustic oscillations of a ducted premixed laminar flame.* Ph.D. thesis, University of Cambridge, Cambridge, UK.

Kashinath, K., Waugh, I. C., and Juniper, M. P. (2014). Nonlinear self-excited thermoacoustic oscillations of a ducted premixed flame: bifurcations and routes to chaos. *Journal of Fluid Mechanics*, **761**, 399-430.

Khanna, V. K. (2001). *A Study of the Dynamics of Laminar and Turbulent Fully and Partially Premixed Flames.* PhD diss., Virginia Polytechnic Institute and State University.

Kim, W. W., Lienau, J. J., Van Slooten, P. R., Colket, M. B., Malecki, R. E., and Syed, S. (2006). Towards modeling lean blow out in gas turbine flameholder applications. *Journal of engineering for gas turbines and power*, 128(1), 40-48.

Klimaszewska, K., and Żebrowski, J. J. (2009). Detection of the type of intermittency using characteristic patterns in recurrence plots. *Physical review E*, 80(2), 026214.

Komarek, T. and Polifke, W. (2012). Impact of swirl fluctuations on the flame response of a perfectly premixed swirl burner. *J. Eng. Gas Turb. Power*, **132**, 061503.

Lei, S. and Turan, A. (2009). Nonlinear/chaotic behaviour in thermoacoustic instability. *Combustion Theory and Modeling*, 13, 541–557.

Lewis, B. and von Elbe, G. (1987). *Combustion, flames and explosions of gases*, 3rd edition, New York, Academic Press.

Lieuwen, T. (2001). Theoretical investigation of unsteady flow interactions with a premixed planar flame. Journal of Fluid Mechanics, 435(1), 289-303.

Lieuwen, T. (2007). Static and Dynamic Combustion Instability. *Gas Turbine Handbook U.S. Department of Energy*, DOE/NETL-2006/1230, 197-203.

Lieuwen, T. (2002). Experimental investigation of limit-cycle oscillations in an unstable gas turbine combustor. Journal of Propulsion and Power, 18(1).

Lieuwen, T., (2005). Online Combustor Stability Margin Assessment Using Dynamic Pressure Data, *J. Eng. Gas Turbines Power*, **127**, 478–482.

Lind, D., M. Marcus, *An Introduction to Symbolic Dynamics and Coding*, Cambridge University Press, 1995.

Longwell, J. P. (1953). Flame stabilization by bluff bodies and turbulent flames in ducts. International Symposium on Combustion, **4**, No. 1, 90-97.

Longwell, J., Frost, E. and Weiss, M. (1953). Flame stability in bluff body recirculation zones, *Ind. Eng. Chem.* **45**. 1629–1633.

Malthus, T. R. (1798). An essay on the theory of population.

Mandelbrot, B. B. (1999). *Multifractals and 1/f Noise*. Vol. **14**. New York: Springer-Verlag.

Marble, F. E., and Candel, S. M. (1977). Acoustic disturbance from gas non-uniformities convected through a nozzle. Journal of Sound and Vibration, 55(2), 225-243.

Mariappan, S. and Sujith, R. I. (2010) "Thermoacoustic Instability in Solid Rocket Motor: Non-normality and Nonlinear Instabilities", Journal of Fluid Mechanics, 653, 1-33.

Mariappan, S., Schmid P and Sujith R. I. (2010). Role of Transient Growth in Subcritical Transition to Thermoacoustic Instability in Rijke Tube

Marro, J., and Dickman, R. (2005). Nonequilibrium phase transitions in lattice models. Cambridge University Press.

Marwan, N., Romano, M. C., Thiel, M. and Kurths J. (2007). Recurrence plots for the analysis of complex systems. Phys. Reports, 438, 237–329.

Marwan, N., Wessel, N., Meyerfeldt, U., Schirdewan, A. and Kurths, J. (2002). Recurrence-plot-based measures of complexity and their application to heart-rate-variability data. Phys. Rev. E, 66, 026702.

Matveev, K. and Culick, F. E. C. (2003). A model for combustion instability involving vortex shedding. *Combust. Sci. Tech.*, **175**, 1059–1083.

McManus, K. R., Poinsot, T. and Candel, **S. M.** (1993). A review of active control of combustion instabilities, *Prog. Energy Combust. Sci. Tech.*, **16**, 1–29.

Moeck, J. P., Oevermann, M., Klein, R., Paschereit, C. O. and Schmidt, H. (2009). A two-way coupling for modeling thermoacoustic instabilities in a flat flame Rijke tube, *Proc. Combust. Insti.*, **32**, 1199-1207.

Mukherjee K., and Ray, A. (2014). State Splitting & Merging in Probabilistic Finite State Automata for Signal Representation and Analysis, *Signal Processing*, **104**, 105-119.

Mukhopadhyay, A., Chaudhari, R. R, Paul, T., Sen S. and Ray, A. (2013). Lean Blow-Out Prediction in Gas Turbine Combustors Using Symbolic Time Series Analysis. *Journal of Propulsion and Power*, **29**, 950-960.

Muruganandam, T. (2006) *Sensing and dynamics of lean blowout in a swirl dump combustor*. PhD diss., Georgia Institute of Technology.

Murugesan, M., Sujith, R. I. (2015). Combustion noise is scale-free: transition from scale-free to order at the onset of thermoacoustic instability. Journal of Fluid Mechanics, **772**, 225-245.

Nagaraja, S., Kedia, K. and Sujith, R. I. (2009). Characterizing Energy Growth During Thermoacoustic Instabilities: Eigenvalues or Singular Values?, *Proceedings of the Combustion Institute*, **32 (2)**, 2933-2940.

Nair, S. and Lieuwen, T. C., (2007). Near-Blowoff Dynamics of a Bluff-Body Stabilized Flame, *Journal of Propulsion and Power* **23**, 421-427.

Nair, S., (2006). *Acoustic characterization of flame blowout phenomena*. PhD diss., Georgia Institute of Technology.

Nair, V. and Sujith, R. I. (2014). Multifractality in combustion noise: predicting an impending combustion instability. *J. Fluid Mech* **747**, 635-655.

Nair, V. and Sujith, R. I. (2013). Identifying homoclinic orbits in the dynamics of intermittent signals through recurrence quantification. *Chaos* **23**, 033136.

Nair, V. and Sujith, R. I., (2015). A reduced-order model for the onset of combustion instability: Physical mechanisms for intermittency and precursors, *Proc. Combust. Insti.* **35,** 3193-3200.

Nair, V., Thampi, G., Sulochana, K., Saravanan, G. and Sujith, R. I. System and method for predetermining the onset of impending oscillatory instabilities in practical devices, Provisional patent, filed Oct. 1 2012.

Nair, V., Thampi G. and Sujith, R. I. (2014). Intermittency route to thermoacoustic instability in turbulent combustors. *Journal of Fluid Mechanics* **756**, 470-487.

Nair, V., Thampi, G., Karuppusamy, S., Gopalan, S. and Sujith, R. I. (2013). Loss of chaos in combustion noise as a precursor of impending combustion instability. *International J. of Spray and Combust. Dynamics* **5**, 273-290.

Noiray, N. and Schuermans B. (2013). Deterministic quantities characterizing noise driven hopf bifurcations in gas turbine combustors. *Int. J. Non-Lin. Mech.*, **50**, 152–163.

Oborny, G. M., and György Szabó, B. (2005). Dynamics of populations on the verge of extinction. Oikos, 109(2), 291-296.

Orchini, A., Illingworth, S. J., and Juniper, M. P. (2015). Frequency domain and time domain analysis of thermoacoustic oscillations with wave-based acoustics. *Journal of Fluid Mechanics*, **775**, 387-414.

Pan, J. C., Vangsness, M. D., and Ballal, D. R. (1991). Aerodynamics of bluff body stabilized confined turbulent premixed flames. In *ASME 1991 International Gas Turbine and Aeroengine Congress and Exposition* (pp. V003T06A019-V003T06A019). American Society of Mechanical Engineers.

Pawar, S. A., Vishnu, R., M. Vadivukkarasan, M. V. Panchagnula, and R. I. Sujith (2016). Intermittency Route to Combustion Instability in a Laboratory Spray Combustor, *Journal of Engineering for Gas Turbines and Power*, **138**, 041505-1 - 041505-8.

Peracchio, A. A. and Proscia, W. M. (1999). Nonlinear heat-release/acoustic model for thermo-acoustic instability in lean premixed combustors. *Journal of Engineering for Gas Turbines and Power-Transactions of the ASME*, **121**, 415–421.

Peters N. and Williams F. A., (1983). Lift-off Characteristics of Turbulent Jet Diffusion Flames, *AIAA Journal*, Vol.21 (3), 423-429.

Plee, S. and Mellor, A., (1979). Characteristic time correlation for lean blowoff of bluff-body-stabilized flames *Combust. Flame* **35**, 61–80.

Poinsot, T., F. Lacas, J. Chambon, D. Veynante, and A. Trouve, Apparatus for active monitoring of combustion instability, US patent (US 5145355 A) filed on September 8, 1992.

Polifke, W. (2004). Combustion instabilities. *Advances in Aeroacoustics and Applications*, 2004-05.

Pomeau, Y. and P. Manneville (1980). Intermittent transition to turbulence in dissipative dynamical systems. *Commun. Math. Phys.*, 74, 189–197.

Preetham, S. H. and T. C. Lieuwen, Nonlinear flame-flow transfer function calculations: Flow disturbance celerity effects - part 2. In AIAA Paper Number 2005-0543, 43rd AIAA Aerospace Sciences Meeting and Exhibit. Reno, Nevada, 2005.

Preetham, S. H. and T. C. Lieuwen, Nonlinear flame-flow transfer function calculations: Flow disturbance celerity effects -part 1. In AIAA Paper Number 2004-4035, 40th AIAA / ASME / SAE / ASEE Joint Propulsion Conference and Exhibit. Fort Lauderdale, Florida, 2004.

Radhakrishnan, K., Heywood J. and Tabaczynski R. (1981). Premixed turbulent flame blowoff velocity correlation based on coherent structures in turbulent flows. *Combust. Flame*, **42**, 19–33.

Rajagopalan, V., Ray, A., (2006). Symbolic time series analysis via wavelet-based partitioning. *Signal Processing*, 86 (11), 3309–3320.

Rasmussen, C. C., Driscoll, J. F., Carter, C. D., and Hsu, K. Y. (2005). Characteristics of cavity-stabilized flames in a supersonic flow. *Journal of Propulsion and Power*, 21(4), 765-768.

Ray, A., (2004). Symbolic Dynamic Analysis of Complex Systems for Anomaly Detection, *Signal Processing*, 84(7), 1115–1130.

Rayleigh, L. (1878). The explanation of certain acoustical phenomenon. *Nature*, 18, 319–321

Richardson, L. F., *Weather Prediction by Numerical Proces*s. Cambridge University Press, Cambridge, UK, 1922.

Russell, C., and Russell, W. M. S. (2000). Population crises and population cycles. *Medicine, Conflict and Survival* **16(4)**, 383-410.

Sarkar S., Mukherjee K., Sarkar S. and Ray A., (2012). Symbolic transient time-series analysis for fault detection in aircraft gas turbine engines, *American Control Conference*, Montreal, 5132 - 5137.

Sarkar, S., A. Ray, A. Mukhopadhyay, R.R. Chaudhari, and S. Sen, (2014). Early detection of lean blow out (LBO) via generalized D-Markov machine construction, *American Control Conference*, 3041-3046.

Schertzer D. and Lovejoy S. (2011). Multifractals, generalized scale invariance and complexity in geophysics. *International Journal of Bifurcation and Chaos* **21**, No. 12, 3417–3456.

Shanbhogue S. J., Husain S. and Lieuwen T. C., (2009). Lean blowoff of bluff body stabilized flames: Scaling and dynamics, *Prog. Energy Combust. Sci.* **35**, 98-120.

Shanbhogue, S. J., Sanusi, Y. S., Taamallah, S., Habib, M. A., Mokheimer, E. M. A., and Ghoniem, A. F. (2016). Flame macrostructures, combustion instability and extinction strain scaling in swirl-stabilized premixed CH 4/H 2 combustion. *Combustion and Flame*, **163**, 494-507.

Spalding, D. B. (1955). *Some Fundamentals of Combustion.* Butterworth Press: London, U.K.

Spalding, D. B. (1953). Theoretical aspects of flame stabilization: an approximate graphical method for the flame speed of mixed gases. *Aircraft Engineering and Aerospace Technology*, *25*(9), 264-276.

Sreenivasan, K. R. and C. Meneveau (1986). The fractal facets of turbulence. *Journal of Fluid Mechanics*., 173, 357–386.

Sterling, J. D. (1993). Nonlinear analysis and modeling of combustion instabilities in a laboratory combustor. *Combustion Science and Technology*, **89**, 167–179.

Stöhr, M., Boxx, I., Carter, C., and Meier, W. (2011). Dynamics of lean blowout of a swirl-stabilized flame in a gas turbine model combustor. *Proceedings of the Combustion Institute*, **33(2)**, 2953-2960.

Stöhr, M., Boxx, I., Carter, C., and Meier, W. (2011). Dynamics of lean blowout of a swirl-stabilized flame in a gas turbine model combustor. *Proceedings of the Combustion Institute*, **33(2)**, 2953-2960.

Strahle, W. C. (1978) *Combustion noise*. *Prog*. *Energy Combust*. *Sci*., **4**,157–176.

Strogatz, S. H., (2001). *Nonlinear Dynamics And Chaos: With Applications To Physics, Biol-ogy, Chemistry, And Engineering (Studies in Nonlinearity).*Westview Press.

Subbu, A., Ray, A. (2008). Space partitioning via Hilbert transform for symbolic time series analysis, *Applied Phys. Letters*, 92 (8), 084107.

Subramanian, P. (2011). *Dynamical systems approach to the investigation of thermoacoustic instabilities*. Ph.D. thesis, Indian Institute of Technology Madras, Chennai, India.

Subramanian, P., and Sujith, R. I. (2011). Non-normality and internal flame dynamics in premixed flame–acoustic interaction. *Journal of fluid mechanics*, **679**, 315-342.

Thampi, G., and Sujith, R. I. (2015). Intermittent Burst Oscillations: Signature Prior to Flame Blowout in a Turbulent Swirl-Stabilized Combustor. *Journal of Propulsion and Power*, **31(6)**, 1661-1671.

Tony, J., Gopalakrishnan, E. A., Sreelekha, E. and Sujith, R. I. (2015). Detecting deterministic nature of pressure measurements from a turbulent combustor, *Physical Review E*, **92 (6)**, 062902.

Unni, V. R., and Sujith, R. I. (2015). Multifractal characteristics of combustor dynamics close to lean blowout. *Journal of Fluid Mechanics*, **784**, 30-50.

Unni, V. R., Nair, V. and Sujith, R. I. (2014). System and method to control blowout in combustion systems, Patent, PCT Filed on 7th Nov.

Unni, V. R., V. Nair, A. Mukhopadhyay, R. I. Sujith, System and method for controlling oscillatory instabilities in a device, Provisional patent, filed on Dec. 4, 2013.

Verhulst, P. F. (1838). Notice sur la loi que la population suit dans son accroissement. *Correspondance mathématique et physique publiée par a. Quetelet*, **10**, 113-121.

Waugh, I. C. and Juniper, M. P. (2011). Triggering in a thermoacoustic system with stochastic noise. *International Journal of Spray and Combustion Dynamics* **3**, 225–242.

West B. J., Latka, M., Glaubic-Latka M. and Latkam, D. (2003). Multifractality of cerebral blood flow. *Physica A* **318**, 453–460.

Williams, G., Hottel, H., and Scurlock, A., (1951). Flame Stabilization and Propagation in High Velocity Gas Streams, *Proc. Comb. Inst.*, Vol. 3, 1951, pp. 21-40.

Woodroffe, R., and Ginsberg, J. R. (1998). Edge effects and the extinction of populations inside protected areas. *Science*, 280(5372), 2126-2128.

Yamaguchi, S., Ohiwa, N., and Hasegawa, T. (1985). Structure and blow-off mechanism of rod-stabilized premixed flame. *Combustion and flame*, *62*(1), 31-41.

Zhang, Q., Noble, D. R., and Lieuwen, T. (2007). Characterization of Fuel Composition Effects in H2/ CO/ CH4 Mixtures Upon Lean Blowout. *Journal of engineering for gas turbines and power*, **129(3)**, 688-694.

Zinn, B. T. and Lieuwen, **T. C.** (2005). Chapter 1: Combustion instabilities: Basic concepts. In T. C. Lieuwen and V. Yang (eds.), Combustion Instabilities in Gas Turbine En-gines: Operational Experience, Fundamental Mechanisms, and Modeling., volume 210. *Progress in Astronautics and Aeronautics*, AIAA Inc.

Zukoski, E. E. and Marble, F. E. (1954). The Role of Wake Transition in the Process of Flame Stabilization in the Bluff Bodies. AGARD Combustion Researches and Reviews, Butterworth Scientific Publishers, London, 167-180.

Zukoski, E. E., and Marble, F. E. (1956). Experiments concerning the mechanism of flame blowoff from bluff bodies. In *Proceedings of the Gas Dynamics Symposium on Aerothermochemistry* (pp. 205-210).

LIST OF PAPERS BASED ON THESIS

Refereed Journals

1. **Unni V. R.** & Sujith R. I. (2015), Multifractal characteristics of combustor dynamics close to lean blowout, *Journal of fluid mechanics*, 784, 30- 50.

2. **Unni, V. R.**, Mukhopadhyay, A., & Sujith, R. I. (2015). Online detection of impending instability in a combustion system using tools from symbolic time series analysis. *International Journal of Spray and Combustion Dynamics*, 7(3), 243-256.

3. **Unni, V. R.** & Sujith, R. I. (2016). Flame dynamics during intermittency in a turbulent combustor. *Proceedings of Combustion Institute*, ISSN 1540-7489, http://dx.doi.org/10.1016/j.proci.2016.08.030.

4. **Unni, V. R.** & Sujith R. I. Precursors to blowout in a turbulent combustor based on recurrence quantification, *Journal of Propulsion and Power* (Under review)

Peer-reviewed conferences

1. **Unni, V. R.** & Sujith R. I. (2015), A unified framework to describe dynamics of thermoacoustic instability and blowout in a turbulent combustor. ICSV 22, Florence, Italy, July 12-16.

2. **Unni, V. R.** & Sujith R. I. (2015), Multifractal characteristics of combustion dynamics, 51st AIAA/SAE/ASEE Joint Propulsion Conference, Orlando, Florida, USA, July 27-29.

3. **Unni, V. R.** & Sujith R. I. (2016), 52nd AIAA/SAE/ASEE, Precursors to blowout in a turbulent combustor based on recurrence quantification, Joint Propulsion Conference, Saltlake city, USA, July 25-28.

4. **Unni, V. R.** & Sujith R. I. (2016), Flame dynamics during intermittency in a turbulent combustor. 36th International symposium on combustion, Seoul, Korea, July 31- Aug 5.